Evaluating thymocyte negative selection within the polyclonal population

A DISSERTATION
SUBMITTED TO THE FACULTY OF THE
UNIVERSITY OF MINNESOTA
BY

Elise Ristig Breed

IN PARTIAL FULFILLMENT OF THE REQUIREMENTS
FOR THE DEGREE OF
DOCTOR OF PHILOSOPHY

Advisor: Kristin Ann Hogquist, Ph.D.

AUGUST 2019

Acknowledgements

This thesis and my graduate work are the result of a collective effort put forth by my family, friends, and mentors. I will be forever grateful to those who not only encouraged and challenged me scientifically, but to those who helped me take a step away at the most necessary moments to breathe.

I am often told that good mentors are essential for laying the groundwork for success. The mentors that I gained over the last ten years helped mold me as a scientist and encouraged my creativity. Importantly, I would never have known about my selected career path as a physician scientist without my mentor, Craig Coopersmith M.D., at Emory University. After an interview in which we bonded over our shared passion for music (I had noted that Craig had literally hundreds of CDs stacked on his office shelves), Craig hired me as the second member of his newly formed lab after transitioning from Washington University in St. Louis. He took time each week to teach me his scientific and personal philosophies, and through these meetings I learned the importance of good mentorship. Craig treated me like an adult, he allowed me to explore my ideas, and most importantly, he let me flounder, even as a research assistant. Craig was also uniquely equipped to show me what a career as a physician scientist looked like and, with his encouragement, I decided that that was the career path that I would like to follow.

I met Kris Hogquist, Ph.D. while interviewing for the MSTP at the University of Minnesota. At the time, I was still interested in studying host responses to pathogens. However, her excitement and passion for her research and her trainees was pronounced. I met with her again during my revisit and decided that I would like to rotate

in her lab. During that rotation, when others in the center for immunology would ask who I was working with, I would always get the same excited response, “Oh, Kris is the best!” I knew based not only on my personal experience, but by the comments of others, that Kris’ mentorship would be invaluable. Kris is extraordinarily thoughtful, encouraging, and her excitement about data and new experiments is contagious. I feel so fortunate to be able to call her my mentor and I will always treasure our Friday morning meetings. Whenever anyone asks me about the lab, I can honestly say that Kris is, in fact, the best.

I am fortunate to have a number of physician scientist mentors at the University of Minnesota as well. Erik Peterson, M.D. is not only an outstanding clinical mentor, but always asks thoughtful questions about my research. Bryce Binstadt, M.D., Ph.D. has been the fulcrum of my graduate phase work. He was the Chair of my preliminary examination committee and is the Chair of my thesis committee. He is also an exceptional clinical mentor, who helped me hone my skills when interacting with patients and think about the importance of understanding the basic science that underlies many of the pathologies we saw together. He simultaneously encourages and challenges. Most importantly, he takes the time to give thoughtful and insightful feedback, both clinically and scientifically, which while important for a mentor, is incredibly rare.

The Center for Immunology (CFI) is filled with remarkable mentors and is surely one of the greatest training environments. Through our semi-weekly tea times and weekly supergroups, I have gleaned helpful insight and even mentorship from nearly every member of the CFI. I am thankful to Marc Jenkins, Ph.D. for encouraging such a collaborative, passionate, and robust environment. The additional members of my thesis committee, Dave Masopust, Ph.D., Brian Fife, Ph.D., and Dan Mueller, M.D., are both

the products and producers of this incredible environment. Each of them fulfills the philosophy of the CFI by providing helpful and challenging feedback to my thesis work.

My adoration for Kris should already be evident, however it is clear, that through her incredible mentorship that she has shaped a lab with similarly passionate and thoughtful members. Obviously, this was not without the help of Steve Jameson, Ph.D., who is equally considerate and insightful. The Jamequist lab constitutes a remarkable training environment, with diverse ideas and unique skillsets. Gretta Stritesky, Ph.D. (a former post-doc in Kris' lab) and Sara Hamilton, Ph.D. first showed me what a wonderful training environment the Jamequist lab is during my first summer rotation. Since then, a number of former and present members of the lab have been incredible allies and have provided support in more ways than I can count. Thank you to Roland Ruscher, Ph.D., Haiguang Wang, Ph.D., Thera Lee, and my partner in crime, Oscar Salgado, for helping me through the trials and tribulations of studying thymocyte development. A special thank you to Katie Block, Ph.D. and Matt Huggins, Ph.D. who provided both moral support during happy hours and game nights and scientific feedback by coming up with some of the most ridiculous experiments.

In addition to the outstanding support provided by the CFI, the MICaB graduate program has also helped facilitate my growth as a scientist and provided a generous environment in which to thrive. I am generally oblivious to all things administrative and absolutely would not have successfully navigated my way through graduate school without the help of Louise, Meg, and the DGSs (Steve and Wade). The moral support provided by my MICaB classmates– particularly from Sarah Lucas, Mark Daniel, and Dylan White during our weekly happy hours was immeasurable. These happy hours

served as a constant in the great void that is graduate school and were something that genuinely kept me pushing.

The MSTP is sincerely responsible for all of the mentorship, opportunities, and personal and professional growth listed above. Most importantly, Yoji Shimizu, Ph.D., is the bedrock of this incredible program. He is tireless in his passion for improving the program and encouraging a diverse, inclusive, and thriving student body. Nick Berg and Susan Shurson, continue to help me navigate the numerous bureaucratic challenges that I encounter. Peter Bitterman, M.D., Lisa Schimmenti, M.D., Linda McLoon, Ph.D., Bryce Binstadt, M.D., Ph.D., and Elizabeth Seaquist, M.D. have further shaped this program into its current, outstanding form. Of course, this program would not be what it is without such a considerate group of trainees. Importantly, my fellow classmates, Amanda Barks, Adam Cheng Ph.D., Ethan Leng, Lee Meier Ph.D., Rebecca Speltz, and Germán Vélez Reyes Ph.D. have been outstanding allies throughout this seemingly endless journey.

Of course, my friends outside of the lab have been equally important in helping me through my graduate studies. My friends from medical school, Felicia Hansell M.D., Holly Belgum M.D., Brook Cole M.D., Susan Sun M.D., and Dorothy Curran M.D. have been great sources of emotional support. In addition, my college friends, Kristen Psaty J.D. and Kelly Harris D.D.S. helped me navigate applying for a professional degree. My friends from home, Catherine Meredith, Michelle Kleiman M.D., Becca Davidson, Allie Vostrejs, and Daniel Boyle are always an incredible source of support and fun when I go home.

Notably, my family, through weekly phone calls and text messages has been invaluable. My mom and dad encouraged my scientific creativity from a young age and

prompted me to pursue this career path without any hesitation. I credit my dad with teaching me how to write. My mom is a constant source of emotional comfort. My sister has also been unequivocally compassionate throughout the past four years, even with a 7-hour time difference.

Charlie, my dog, has provided me with unwavering and unconditional love, without which I would likely not have made it through this process. Quinn has been steadfast in his patience and support for me. He challenges me intellectually, is the ultimate companion, and I am so excited to see what adventures the future holds for us.

Dedication

To everyone who provided me with emotional and intellectual support over the past four years.

Abstract

The development of a self-tolerant and effective T cell receptor repertoire is dependent on interactions coordinated by various antigen presenting cells (APC) within the thymus. T cell receptor–self-peptide–MHC interactions are essential for determining T cell fate, where high affinity interactions can result in clonal deletion or regulatory T (Treg) cell differentiation of potentially autoreactive T cells. The APCs that provide these signals have distinct localization, different antigen processing features, and can provide different co-stimulatory signals that are also critical to these selection processes and may distinguish the ultimate fate of a T cell. Clonal deletion and Treg differentation of T cells specific for self-antigens in the thymus have been widely studied, primarily by approaches that focus on a single receptor (using TCR transgenes) or a single specificity (using pMHC tetramers). However, little is known about how distinct APCs coordinate clonal deletion and Treg cell development at the population level.

Here, we report an assay that measures cleaved caspase 3 to define clonal deletion at the population level. This assay distinguishes clonal deletion from apoptotic events caused by neglect and approximates the anatomic site of deletion using CCR7. This approach showed that 78% of clonal deletion events occur in the cortex in mice. Medullary deletion events were detected at both the semi-mature and mature developmental stages, although mature events were associated with failed Treg cell induction. Using this assay, we showed that bone marrow derived APC drive approximately half of deletion events at both stages. We also found that both cortical and medullary deletion rely heavily on CD28 co-stimulation.

We further assessed the contribution of distinct APC subsets to clonal deletion and Treg cell selection using cell type ablation or deficiency. We found that total deletion and nascent Treg cell events were not altered in the absence of B cells, pDC, or XCR1$^+$ cDC1. In an effort to eliminate SIRPα^+ cDC2, we discovered that a fraction of thymic SIRPα^+ cDC2 express the lectin CD301b. These cells resemble the type 2 immune response-promoting CD301b$^+$ DC that are present in skin draining LN. CD301b expression was localized primarily within the thymus medulla and depended on IL-4R. Deficiency of these IL-4 and IL-13 signaled cDC2 caused a measurable reduction in clonal deletion events, suggesting a non-redundant role for tolerance induction.

These findings demonstrate useful strategies for studying clonal deletion and nascent Treg cell development within the polyclonal population. Additionally, they provide valuable insight into how and when thymocytes undergo clonal deletion as they traverse through the thymus and interact with distinct APC during development.

Table of Contents

List of Figures

Chapter 1

Introduction

1.1 Thymocyte selection

Random rearrangement of the T cell receptor (TCR) α and β genes in the thymus enables the T cell repertoire to broadly react to a universe of potential antigens derived from pathogens. However, many TCRs will not be able to bind to those antigens when presented by the host's limited set of major histocompatibility complex (MHC) molecules. Thus, a positive selection step that ensures that TCRs recognize antigens in the context of the host's own MHC molecules is needed to guarantee that T cells are well equipped to respond when these pathogens are encountered. In addition, the ability to distinguish self-peptides from foreign peptides is essential to prevent the pathogenesis of autoimmune disease. Therefore, as T cells develop in the thymus, tolerance to self-peptides is acquired, in which autoreactive clones are pruned from the repertoire (clonal deletion) or directed to a regulatory lineage (Treg differentiation).

Antigen presenting cells (APC) orchestrate these selection events in the thymus. The strength of the interaction between the TCR and the self-peptide–MHC complexes presented by thymic APCs is crucial in determining the fate of a T cell. Weak interactions facilitated by cortical thymic epithelial cells (cTEC) promote positive selection, whereas stronger interactions drive both clonal deletion and Treg differentiation. But in addition to the strength of the TCR interaction, the specific peptides presented and the cytokine/costimulatory context of that recognition plays a critical role in the outcome of selection. Here, we discuss the diverse thymic APCs and how they facilitate the generation of a safe and effective T cell repertoire.

1.2 Cortical Thymic Epithelial Cells

Double positive $CD4^+CD8^+$ (DP) thymocytes first express a surface αβ TCR in the cortex of the thymus. Weak TCR interactions with peptide-MHC complexes in this environment mediate positive selection and CD4 and CD8 lineage commitment (1). Cortical thymic epithelial cells (cTEC) play an essential role in this process (Figure 1.1). In fact, cTECs are uniquely primed to drive positive selection, in part due to their ability to process and present antigens via machinery distinct from other antigen presenting cells.

1.2.1 Cortical Thymic Epithelial Cells and Antigen Processing

Proteasomes degrade cytosolic proteins, resulting in peptide fragments that can be loaded onto MHC I molecules in the endoplasmic reticulum (ER). The catalytic core of the proteasome includes the three β-subunits: β1, β2, and β5 (2). While other cell types express either the β5- or β5i- subunits, cTECs have a specialized proteasome subunit that is critical for positive selection: β5t (3, 4). The 'thymoproteasome', unique to cTECs, is specifically composed of β1i (*Psmb9*), β2i (*Psmb10*), and β5t (*Psmb11*) subunits. Mice that lack β5t, and therefore, the thymoproteasome, have a substantial defect in positive selection of CD8 T cells (3). The number of CD8 T cells in β5t deficient mice is approximately 20% that of their wild type counterparts (5, 6). In addition, the ensuing T cell pool has diminished responsiveness to infection, demonstrating that the thymoproteasome is critical for shaping the T cell repertoire (5, 6).

Since the proteasome plays a key role in producing peptides that are loaded onto MHC I molecules, it is reasonable to hypothesize that the β5t-containing thymoproteasomes may have proteolytic capabilities that lead to a unique peptide–MHC repertoire. Indeed, β5t promotes decreased chymotrypsin-like activity compared to

proteasomes that use either β5 or β5i (3). Therefore, it was hypothesized that β5t-containing thymoproteasomes would produce peptides that are enriched for basic residues at the C-terminus. Since a substantial portion of the binding energy of MHC to peptides is through the hydrophobic C-terminus of the peptide, the thymoproteasome could generate peptides that bind to MHC molecules more weakly. However, it has been recently shown that while the thymoproteasome does produce unique peptides compared to the β5i-containing immunoproteasome; both generate peptides with hydrophobic residues at the C-terminus (7).

The question then becomes whether cTECs promote positive selection merely because their peptides are different from those presented by other APCs during negative selection, or if the cTEC-exclusive peptides themselves are somehow specialized for inducing positive selection. Experimental results are mixed. When both the immunoproteasome and thymoproteasome subunits were removed, leaving just the constitutive proteasome in all thymic APCs, only 10% of mature $CD8^+$ thymocytes developed (8). This decrease in CD8 T cells was rescued in Bim-deficient mice, suggesting that negative selection was responsible for the death of most $CD8^+$ thymocytes (8). The authors concluded that the peptidome therefore needs to be distinct between cTEC and other thymic APC in order to generate a normal sized repertoire, and the role of β5t is to generate a distinct peptidome in cTEC. However, in another study, mice were engineered to express different peptidomes in cTEC versus other thymic APC, but without using β5t. In these mice, positive selection of CD8 T cells was still diminished (9), suggesting that the β5t generated peptidome is specialized for inducing positive selection. It is possible that both concepts are accurate, that thymoproteasome-dependent peptides are both distinct from other thymic APC and specialized for positive

selection. Although the mechanism of this specialization is unclear, it may relate to preferentially producing low-affinity TCR ligands (7).

Another interesting possibility that has not yet been explored experimentally is that the thymoproteasome may change the extent to which the peptide repertoire consists of “spliced peptides.” CD8 T cells have been shown to recognize peptides formed from two noncontiguous fragments of a protein that have been spliced together (10). This splicing is proteasome dependent; for example an immunoproteasome is not always capable of generating the same spliced peptide as a constitutive proteasome (11). It was recently suggested that in humans, approximately one-third of the peptides presented by HLA I molecules may be spliced peptides (12), indicating that this subset is a non-trivial proportion of the overall peptide repertoire. As the catalytic mechanism proposed in peptide splicing includes the function of the β-subunit of the proteasome (11), this leads to the appealing question of whether cTECs present unique spliced peptides that somehow facilitate positive selection of an even more diverse T cell repertoire.

In an analogous fashion to the thymoproteasome, genes involved in the proteolysis of endosomal proteins are preferentially expressed in cTECs and play a role in the selection of the CD4 T cell repertoire. These include the thymus specific serine protease (TSSP) (*Prss16*), and cathepsin L (*CatL*) (13, 14). As MHC II molecules bind to peptides from the endosomal pathway, the function of these genes appears to be to create unique peptides optimized for selecting the CD4 T cell repertoire. Indeed, deficiency in TSSP and CatL impact positive selection of CD4 T cells (13–15).

1.2.2 Cortical Thymic Epithelial Cells and Antigen Presentation

Particularly for MHC II molecules, cTEC utilize a distinct antigen *presentation* pathway in addition to unique antigen *processing* machinery. CD83 is a member of the immunoglobulin superfamily that is expressed by activated dendritic cells and a wide array of other cell types, including B and T cells (16). In dendritic cells, CD83 stabilizes MHC II by preventing ubiquitination and subsequent internalization (17). Importantly, CD83 is constitutively expressed in cTEC and has recently been suggested as a direct target of Foxn1, the lineage defining transcription factor required for thymic epithelial cell growth and differentiation (18).

Mice deficient in CD83 have a substantial defect in CD4 T cell selection (19–21). Because selection of TCR transgenic CD4 T cells was markedly reduced in CD83-deficient bone marrow recipients, this defect in CD4 T cell selection is likely attributed to a failure of positive selection, rather than disproportionate clonal deletion (19). CD83-deficient mice have increased turnover of MHC II at cTEC cell surfaces, suggesting that, like in other APCs, CD83 regulates the stability of MHC II on the surface of cTECs (19, 20). CD83 does so by antagonizing the ubiquitination-dependent lysosomal degradation of MHC II, which is mediated by the ubiquitin ligase, March 8 (19, 22). This mechanism parallels that of MHC II ubiquitination mediated by March 1 in dendritic cells (17). The requirement for stable MHC II surface expression for CD4 T cell selection supports the notion that CD4 T cells may require prolonged interactions with selecting peptides for positive selection, based on the kinetic signaling model for T cell lineage commitment (23, 24).

It is unclear whether March 8 and March 1 evolved simultaneously in distinct cell types to mediate identical functions, or if March 8 plays a more specific role specialized

for cTEC-mediated positive selection. However, March 8 expression does not appear to have a direct impact on the CD4 T cell receptor repertoire (22). One separate function may lie in the ability to target distinct additional substrates, including CD86, which is targeted by March 1 in dendritic cells, but not by March 8 in thymic epithelial cells (17, 22).

Interestingly, Foxn1 controls the expression of both *Cd83* and *Psmb11*, suggesting that Foxn1 may direct positive selection of both CD4 single positive (SP) and CD8SP thymocytes (18, 25). For both MHC I and MHC II restricted thymocytes, positive selection triggers the upregulation of C-C chemokine receptors CCR4 and CCR7 that guide the cells toward the medulla and its dendritic cell (DC)-rich environment (26–31). The APCs here have distinct roles in both clonal deletion and further differentiation of T cells with homeostatic functions.

1.3 Medullary Thymic Epithelial Cells

Medullary thymic epithelial cells (mTEC) play a critical role in mediating tolerance to self- antigens through ectopic expression of tissue restricted antigens (TRAs) (Figure 1.1). TRA expression by mTECs largely depends on AIRE (autoimmune regulator), a transcriptional regulator that controls the expression of antigens normally expressed in certain peripheral tissues (32). Additionally, AIRE plays a role in mTEC development, promoting the expression of CD80 and MHC II on mature mTECs (33, 34). Lineage tracing experiments have revealed that mTECs undergo discrete stages of development, eventually downregulating AIRE. These “post-AIRE” mTECs lose their mature phenotype and express decreased MHC II, CD80/86, and AIRE-dependent TRAs (35, 36). Furthermore, post-AIRE mTECs preferentially migrate toward the center of the

medulla, indicating that localization may dictate how mTECs facilitate central tolerance (35).

Recently, an additional transcription factor that promotes thymic expression of a subset of TRAs via an AIRE-independent mechanism was identified. Fezf2 plays an essential role in mediating immune tolerance to tissue restricted antigens (37). Distinct pathways regulate the expression of Fezf2 and AIRE; Fezf2 is regulated by the lymphotoxin beta receptor (LTβR), whereas AIRE is regulated by receptor activator of nuclear factor-κB (RANK) and CD40, which are members of the tumor necrosis factor receptor superfamily (TNFRSF) (37). Therefore, Fezf2 and AIRE may have emerged at different points in evolution and possibly cooperate by regulating distinct gene sets.

In addition to self-antigen presentation mediated by AIRE and Fezf2, mTECs produce AIRE-independent chemokine ligands, CCL19 and CCL21, which attract CCR7-expressing developing thymocytes to the medulla (29, 31, 38). These ligands may facilitate interactions between these developing thymocytes and mTECs– reviewed in reference 39 – to drive thymocyte selection (39).

1.3.1 Medullary Thymic Epithelial Cells and Clonal Deletion

Classic studies showed that mTECs can facilitate tolerance by inducing clonal deletion of TRA-reactive T cells. In a model in which membrane-bound ovalbumin expression was driven by the rat insulin promoter (RIP-mOVA), and thus specifically expressed in an AIRE-dependent manner, AIRE knockout (KO) and mTEC-depleted mice had a small but significant increase in the number of OT-II transgenic CD4SP thymocytes, suggesting that AIRE plays a role in mediating clonal deletion (40, 41). More recently Malhotra *et al.* used tetramer enrichment to show that rare polyclonal T cells specific for TRA were also modestly increased in AIRE KO mice (42). Clonal

deletion is now assumed to be the mechanism for eliminating a large number of TRA-specific clones as mTEC ablation leads to an increase in the proportion of polyclonal CD4SP thymocytes (35). The role of Fezf2 in mediating clonal deletion is less clear. Fezf2 deficient animals do not have a difference in the CD4SP or CD8SP pool size compared to wild type animals, however differences in TCRVβ usage indicate Fezf2 shapes the CD4 and CD8 TCR repertoire (37).

Because direct MHC II-dependent interactions between thymocytes and mTECs are required for proper medullary architecture and organization (43), assessing the role of mTEC MHC II molecules in tolerance required the development of a method in which the class II transactivator (C2TA) was specifically knocked down (kd) in mTECs via AIRE promoter driven shRNA (44). C2TAkd bone marrow recipients showed a moderate increase in the frequency of CD4SP thymocytes, indicating that mTECs mediate clonal deletion. Interestingly, CD4SP thymocytes further increased when donor bone marrow was also deficient in MHC II, suggesting that mTECs and DCs play non-redundant roles in mediating deletion of the polyclonal T cell repertoire (44). A different group performed high throughput analysis of the TCR repertoire in animals lacking MHC II on bone marrow APCs or in C2TAkd animals. Repertoire analysis revealed fewer unique TCRs enriched in C2TAkd animals compared to animals with MHC II deficient bone marrow, suggesting that while mTECs are capable of mediating clonal deletion, their relative contribution is minimal compared to bone marrow APCs (45).

1.3.2 Medullary Thymic Epithelial Cells and Regulatory T cell Differentiation

A study in which mTECs were shown to induce development of Tregs specific for an AIRE-dependent model antigen gave the first indication that AIRE-expressing mTECs may also impact tolerance through shaping the Treg repertoire (46). Indeed, it was

recently shown that organ-specific Tregs required AIRE-mediated expression of the self-antigen (47, 48). Although polyclonal Treg numbers are not dramatically altered in the absence of AIRE, at least in adult mice (40, 49), AIRE may play a major role in directing specific T cell clones into the Treg lineage. Therefore, strategies to analyze the impact of AIRE and mTECs at the TCR-level have been employed. One approach took advantage of using a fixed TCR-β chain to enable analysis of TCR specificities via sequence analysis of the TCRα chain (45, 50, 51). Perry *et al.* performed high throughput analysis of the TCR Vα2 repertoire in animals lacking MHC II on bone marrow APCs or in C2TAkd animals. Like with clonal deletion, mTECs contributed less to Treg generation compared to bone marrow APCs. However, mTECs contributed substantially more to Treg induction than to clonal deletion at the repertoire level (45). Further TCR analysis in AIRE deficient mice revealed that AIRE plays a major role in selecting the thymic Treg TCR repertoire, particularly on lower frequency TCRs (45).

Similarly, Malchow *et al.* performed deep sequencing of the complete TCRα repertoire in isolated peripheral Treg and conventional T cells in AIRE-sufficient or -deficient animals. This study found a large number of underrepresented Treg TCRs in AIRE-deficient animals. Interestingly, in the absence of AIRE, these clones were identified in the conventional T cell repertoire. A major proportion of the clonotypes mediating autoimmune pathology in AIRE deficient animals are preferentially expressed by Tregs in AIRE-sufficient animals, suggesting that a major mechanism by which AIRE enforces central tolerance is directing autoreactive conventional TCR clones into the regulatory T cell lineage (51).

Recent data also suggest that the AIRE-dependent Treg repertoire is distinct during different points in ontogeny and that these repertoires may be responsible for

protecting separate tissues. Despite similar fractions of MHC II^{hi} mTEC and AIRE expression in perinatal and adult mice, the differences mediating this age-dependent selection of the Treg repertoire seem to lie in distinct antigen processing and presentation machinery capabilities. Perinatal mTECs had a decreased DO to DM ratio compared to adult mTECs. DM aids in the removal of the invariant chain derivative, CLIP, and other peptides from MHC II, while DO is known to inhibit this action. Therefore, perinatal mTECs had a corresponding decrease in the amount of CLIP, suggesting that perinatal mTECs are more efficient at replacing CLIP with other peptides and that the peptide repertoire presented by MHC II may therefore be more broad in perinatal mTECs (49). These data support the notion that AIRE is essential to central tolerance during the neonatal period, but dispensable in adults (52).

Although AIRE's role in mediating Treg differentiation has been more thoroughly investigated, Fezf2 may also play an essential role in Treg lineage commitment. Fezf2 deficient animals have decreased frequencies of thymic Tregs, indicating that Fezf2 may play an even more substantial role in mediating thymic Treg development (37). Further analysis comparing the TCR repertoires of Tregs and conventional T cells in Fezf2 deficient animals will be necessary to determine if Fezf2 similarly directs TCRs from the conventional T cell pool into the Treg lineage.

While the relative importance of the contribution of AIRE-dependent clonal deletion and Treg induction to tolerance in not known, the studies discussed above suggest that AIRE-mediated Treg induction may be the crucial mechanism by which AIRE enforces tolerance. Several studies have recently suggested that clonal deletion of T cells specific for self-antigens and TRAs is incomplete (42, 53–56). T cells specific to an epitope of the AIRE-dependent retina-specific protein interphotoreceptor retinoid

binding protein (IRBP) were incompletely deleted via an AIRE-dependent mechanism (55). Furthermore, through the use of a model utilizing Cre recombinase as a neo-self antigen, Legoux *et al*. were able to track Cre tetramer-specific CD4 T cells in various mouse strains where Cre expression was restricted to specific peripheral tissues. Although efficient deletional tolerance was found in animals which ubiquitously expressed Cre, when the epitope was restricted to peripheral tissues, Cre:I-A^b specific T cell numbers were not decreased in either the thymus or the periphery, suggesting a lack of deletional tolerance (54). Furthermore, tolerance to some tissue specific antigens, such as lung and intestine self-antigens, required antigen-specific Tregs (54). Another study that used a similar model to investigate antigen-specific tolerance to fluorescent proteins expressed by various tissue specific promoters came to similar conclusions. Malhotra *et al*. defined three clusters of self-specific cells. The first cluster is characterized by wild type numbers of cells with relatively few regulatory T cells, suggesting that these cells did not encounter their epitope. Thus, the mechanism mediating tolerance for cluster 1 was likely ignorance. The second cluster resembled that of the lung and intestine-specific cells reported by Legoux *et al*., in which there were relatively large numbers of Treg cells and few effector cells. Finally, the mechanism mediating tolerance to the third cluster was deletion, which also included T cells specific for ubiquitously expressed proteins (42). These data suggest that the mechanism of tolerance for a specific epitope may not be solely mediated by the APC type, but may also depend on its relative expression within the thymus.

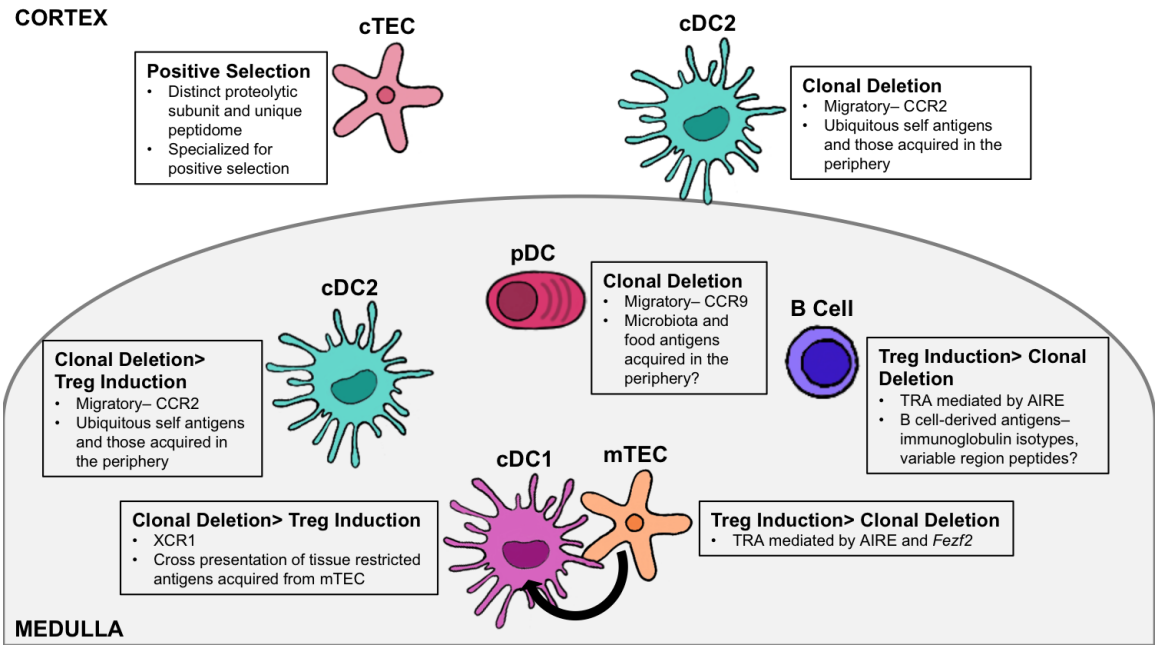

Figure 1.1. Antigen presenting cells encountered in the thymus.

The thymus plays an essential role in mediating self-tolerance by selecting a T cell receptor repertoire based on self-antigens presented by thymic antigen presenting cells (APCs). Thymic APCs include cortical and medullary thymic epithelial cells (cTEC and mTEC), thymic dendritic cells (DC), and B cells. Self-antigens are presented in the thymus via multiple mechanisms. cTEC present antigens specialized for positive selection through their use of the unique proteolytic subunit, β5t. The autoimmune regulator, AIRE, promotes presentation of tissue-restricted self-antigens (TRA) on both mTECs and B cells. Additionally, thymic APCs rely on distinct chemotactic cues for localization within the thymus. These cues, at least in part, govern the unique self-peptides presented by distinct thymic APCs. cDC1 express XCR1, which allows them to localize next to mTEC and acquire mTEC-derived TRAs. cDC2 and plasmacytoid DC (pDC) can acquire antigen in the periphery and present that antigen in the thymus. The chemokine receptors expressed by cDC2 and pDC (CCR2 and CCR9 respectively) may determine the unique self-antigens presented by these two DC subsets. Although a mechanism is yet to be defined, current data suggest that specific medullary APCs favor distinct methods of T cell tolerance– clonal deletion vs. regulatory T cell differentiation.

1.4 Thymic Dendritic Cells

Three universally defined dendritic cell (DC) subsets have been described within the thymus (57). These subsets include plasmacytoid DC (pDC) and two conventional DC (cDC) populations, which are delineated based on their expression of lineage-defining cell surface markers and transcription factors (57, 58) (Figure 1.1). cDC1 are

defined based on their expression of the chemokine receptor, XCR1 (XC-chemokine receptor 1), and require the transcription factor IRF8. Alternatively, cDC2 express SIRPα (signal regulatory protein alpha, CD172a) and require the transcription factor IRF4 (58). These DC subsets are uniquely primed to process and present distinct antigens based on their functional specialization and their ability to respond to different migratory cues.

cDC1 are specialized to cross-present mTEC-derived self-antigens and accumulate in the medulla in an XCR1-dependent manner. XCL1 (XC-chemokine ligand 1 or lymphotactin), the ligand for XCR1, is produced by $mTEC^{hi}$ cells in an AIRE-dependent manner, indicating that XCR1 expression facilitates the transfer of mTEC derived TRAs for cross-presentation (59–61). Recent evidence suggests that these cDC1 undergo constant homeostatic maturation within the thymus; mature cDC1 express CCR7 and upregulate MHC II, CD40, CD83, and CD86. In contrast to immature (CCR7 negative) cDC1, only mature cDC1 are able to cross-present mTEC-derived antigens (62). Therefore, this maturation process is likely essential for efficient self-antigen presentation in the thymus; immature cDC1 may not contribute to or may play a distinct role in driving central tolerance compared to their mature counterparts. The factors that control thymic DC maturation have not yet been defined.

In contrast to cDC1, cDC2 originate in the periphery and are capable of acquiring serum-antigens and/or transporting self-antigens into the thymus (57, 63, 64). C-C chemokine receptor 2 (CCR2) dictates cDC2 migration into the thymus (64). Although both cDC1 and cDC2 localize within the medulla, cDC2 may also accumulate within the perivascular region of the cortex (27, 64). However, the specific site in which this subset accumulates within the thymus remains controversial and the specific chemotactic signals that are required for localization are unknown (1, 64). pDCs also migrate to the

thymus from peripheral sites, however the thymic homing of this subset is CCR9-dependent (65, 66). Like cDC2, pDC are capable of acquiring self-antigens in the periphery and homing to the thymus to present antigens to developing thymocytes (66).

The distinct chemotactic requirements and antigen presenting capabilities of the DC subsets suggests that they may play unique functional roles in facilitating selection of the T cell repertoire.

1.4.1 Thymic Dendritic Cells and Clonal Deletion

Although the relative contribution of bone marrow APCs and mTECs to clonal deletion is unknown, recent studies examining negative selection at the individual TCR level suggest that bone marrow-derived APCs contribute more to clonal deletion than mTECs (45, 67). This makes sense, given that the majority of clonal deletion occurs in the cortex compared to the medulla and that migratory cDC2 can localize in the cortex (64, 67–70).

Recently, a MacNabb *et al.* investigated the role of cDC1 in shaping the $CD8^+$ thymocyte TCR repertoire (71). Through analysis of deep TCR sequencing, this group reported that cDC1 did not impact the $CD8^+$ T cell repertoire. Because cDC1 cross-present TRA acquired from mTEC, this may suggest functional redundancy between cDC1 and mTEC in mediating selection of the $CD8^+$ T cell repertoire. However, using a similar approach, another group demonstrated a BATF3-dependent role for clonal deletion of both conventional $CD4^+$ T cells and Treg (61).

Because cDC2 are capable of acquiring self-antigens in the periphery and transporting them to the thymus, it has been suggested that they mediate tolerance to extrathymic antigens (57, 63, 64). Indeed, OVA-specific thymocytes underwent clonal deletion mediated by circulating DCs in a model in which OVA was expressed

exclusively by cardiomyocytes (63). Interestingly, cDC2 express the highest levels of the CCR4 ligands, CCL17 and CCL22 (72). CCR4 is required for thymocyte migration from the cortex to the medulla (26). Although thymic cellularity in CCR4 deficient animals is mostly unaffected compared to wild type animals, mixed CCR4 deficient and wild type bone marrow chimeras revealed a relative increase in CCR4 deficient $CD69^{+}$ thymocyte populations compared to wild type thymocytes, implying that CCR4-mediated thymocyte–cDC2 interactions are required for efficient clonal deletion (27).

Recent evidence also suggests that there may be variability in the relative contribution of these dendritic cell subsets to clonal deletion over time. The frequency of both cDC2 and pDC populations was increased in 4-week-old non-obese diabetic (NOD) mice compared to their newborn counterparts (73). Additionally, antigen processing and presentation was enhanced in cDC2 from four-week-old mice compared to cDC2 from newborns (73). The frequency of cDC1 in the thymus may also be age-dependent. Perinatal NOD mice had nearly $1/3^{rd}$ of the frequency of cDC1 compared to adults (49). This is in direct contrast to findings reported by Kroger *et al.*, who suggest that newborn NOD mice have a larger proportion of cDC1 compared to 4 week old NOD mice (73). Although the explanation for this discrepancy is unclear, these contradictory findings might be justified by differences in gating strategies, housing conditions, or NOD strains. Additionally, neither group reported cDC1 cell numbers when comparing perinatal to adult mice, which may be more indicative of the temporal changes in this cell population. Overall, the idea of age dependent differences in DC composition is interesting and may consequently result in changes in clonal deletion and Treg cell development, however further studies are needed to more directly define these changes.

As mentioned above, thymic dendritic cells seem to contribute to a large proportion of the deletional tolerance to AIRE-dependent TRAs (42, 55). Thymic DCs mediate AIRE-dependent deletion of T cells specific for IRBP epitope (55). Additionally, in the cluster system described by Malhotra *et al.* (see Section 1.3.2), a major proportion of DCs expressed cluster 3 antigens, in which deletion was the major tolerance mechanism, compared to clusters 1 and 2, in which ignorance or Treg induction were the major mechanisms of tolerance (42).

Because of their capability to produce type I interferons during viral infections (74) and their poor antigen presenting capacity compared to cDC, it was largely believed that pDC assumed an immunomodulatory function within the thymus (75, 76). However, evidence now suggests that pDC may play a role in mediating central tolerance as well. Wild type pDC loaded with OVA peptide and adoptively transferred, migrated to the thymus and promoted deletion of OVA-specific OT-II thymocytes, whereas CCR9-deficient pDC did not (66). Furthermore, because CCR9 is also essential for pDC homing to the small intestine during both homeostatic and inflammatory conditions (77), pDC may mediate tolerance to commensal or food antigens within the thymus, however this hypothesis has not been tested to date.

1.4.2 Thymic Dendritic Cells and Regulatory T Cell Differentiation

Both cDC1 and cDC2 are capable of promoting Treg induction *in vivo* (76, 78, 79), and it has been suggested that cDC2 are more efficient at driving Treg differentiation *in vitro* (79). Interestingly, several recent studies suggest that bone marrow APC play a critical role in promoting selection of AIRE-dependent Treg clones (45, 48, 61, 80). However, there are conflicting reports about whether cDC1 and cDC2 are redundant in their roles for AIRE-dependent Treg selection. Perry *et al.*

demonstrated a non-redundant role with data showing that cDC1 were required for the selection of four AIRE-dependent Treg clones. However, utilizing high throughput TCR analysis comparing cDC1-sufficient and -deficient animals, Leventhal *et al.* concluded that cDC1 did not have an impact on the Treg TCR repertoire. One explanation may be related to the analysis method. Perry *et al.* showed that removal of the three most frequent TCR specificities from analysis was required to determine a difference in Treg TCR repertoires in C2TAkd and WT animals (45). However, Leventhal *et al.* did not utilize this strategy to assess similarity between cDC1-dependent Treg TCRs.

pDC can also promote the development of Treg *in vitro* (81), however their role in mediating Treg differentiation *in vivo* is unclear. pDC did not have an effect on Treg selection of four bone marrow APC-dependent TCRs (45), however the precise role of pDC in mediating Treg selection of the polyclonal repertoire is unknown.

In addition to their role in mediating the TCR-dependent first step of Treg differentiation, DCs may also instruct the second step of Treg development, which requires interleukin (IL)-2 and IL-15 cytokine signals (82). It was previously believed that thymocytes were the major producers of IL-2 in the thymus, however a recent study using thymic tissue slices found that thymic DCs provide a local source of IL-2 to developing Tregs (83). Therefore, distinct APC subsets within the thymus may cooperate to drive thymic Treg differentiation.

The distinct contributions of cDC1 and cDC2 to central tolerance remain to be tested. Unfortunately, no current method exists to specifically deplete cDC2 (84). Therefore, new tools are needed to assess the relative contribution of cDC1 and cDC2 to both clonal deletion and Treg differentiation. Additionally, the relative importance of antigens acquired in the periphery compared to those acquired in the thymus is

unknown. Does the functional specialization of cDC2 change depending on the location of where antigen is acquired? Do intrathymic and extrathymic self-antigens favor different tolerance mechanisms? Is tolerance to commensal and food antigens mediated in the thymus as well as in the periphery?

1.5 Thymic B Cells

Although thymic B cells comprise a similar proportion of total thymic cells compared to DCs and mTECs, relatively little is known about their function in the thymus (85). However, their localization in the medulla and cortico-medullary junction suggests that thymic B cells may play an integral role in mediating Treg development and deletion of autoreactive T cell clones (Figure 1.1) (86, 87). In support of this notion, thymic B cells seem exceptionally primed to present antigens; compared to splenic B cells, thymic B cells have markedly increased expression of MHC II and co-stimulatory molecules, including CD80 and CD86 (85–87).

Whether thymic B cells arise and develop in the thymus or circulate from the periphery and adopt a new phenotype remains unclear, however it is likely that both occur (85, 87, 88). It is evident that the thymic microenvironment is important for driving B cell functions that are distinct from those of the periphery. Notably, licensed thymic B cells express AIRE, whereas peripheral B cells do not (85). Thymocyte interactions with B cells promote B cell licensing much in the way that they orchestrate mTEC maturation, in that in both cases, thymocytes provide TNFRSF stimulation to induce AIRE upregulation. CD40 is critical for the maintenance of thymic B cells and MHC II-restricted cognate interactions drive thymic B cell class switching and AIRE expression, indicating

that cognate interactions between B cells and T cells may be essential for driving central tolerance (85, 89).

Recently, Nuñez *et al.* demonstrated that memory B cells accumulate within the perivascular space of the human thymus in an age-dependent manner (90). However, the expression of molecules associated with antigen presentation decreased in B cells from older thymi, suggesting that B cells may become less integral to T cell selection over time, at least in humans (90). Whether this represents a distinct niche from other thymic B cells is not clear, since a similar phenomenon is not seen in mice (89).

1.5.1 Thymic B Cells and Clonal Deletion

It is evident that thymic B cells can mediate clonal deletion, as B cells have been shown to delete T cells in the context of superantigen and in systems with model antigens (89, 91, 92). More recently, it has been suggested that self-specific B cells present cognate antigen to autoreactive T cells (87). KRN T cells, specific for a peptide from the self-protein glucose-6-phosphate isomerase (GPI), were deleted by B cells with a transgenic B cell receptor (BCR) specific for GPI and by wild-type I-A^{g7} thymic B cells (87). This would suggest that autoreactive B cells within the thymus acquire self-antigen via BCR-mediated endocytosis and mediate tolerance through cognate interactions (87). However, BCR-independent presentation of endogenous self-antigens may also be an important mechanism by which B cells mediate central tolerance. Licensed B cells directly presented an endogenously expressed antigen and mediated clonal deletion of T cells specific for that antigen (85). Interestingly, BCR cross-linking in the presence of CD40 signaling suppressed AIRE induction in thymic B cells, but not MHC II upregulation (85). These findings suggest that both AIRE-expressing and non-expressing B cells in the thymus are capable of mediating clonal deletion. Although more

studies are required to delineate a specific mechanism, this evidence indicates that AIRE-expressing B cells may drive tolerance to endogenous antigens, whereas B cells that do not express AIRE may direct tolerance to BCR-acquired antigens.

B cells may also play a critical role in driving tolerance to B cell-specific antigens; B cells present B cell-specific peptides on MHC II, including variable region peptides (93, 94). Interestingly, recent evidence suggests that thymic B cells undergo class switching, but not somatic hypermutation within the thymus. Class switching is dependent on cognate interactions between B and T cells in the thymus. In the absence of activation induced cytidine deaminase (AID), which is required for class switching, the T cell repertoire is more autoreactive (88). This implies that class switched B cells assist in mediating tolerance of the T cell repertoire. Although the mechanism by which class switching promotes deletion of autoreactive T cells is unclear, class switching may be important for B cells to function as antigen presenting cells, and the class switched B cell may display a distinct MHC II-bound self-peptidome that necessitates T cell tolerance. There is much to be learned in the future about how B cells shape the polyclonal T cell repertoire.

1.5.2 Thymic B Cells and Regulatory T Cell Differentiation

B cells also play a striking role in the development of thymic Tregs. The number and frequency of thymic Tregs is decreased by approximately one third in the absence of B cells (86, 95). Additionally, in BAFF transgenic mice, which have an expansion of extrasplenic B cells, the number and frequency of thymic Treg is increased nearly two-fold (95). This B cell-mediated induction of thymic Tregs is dependent on direct interactions with MHC II and co-stimulatory molecules (86, 95). Additionally, *in vitro* experiments suggest that thymic B cells are capable of directing development of

$CD4^+CD25^+$ Treg precursors, but are not required for the second stage of development into mature Tregs, which requires the cytokines IL-2 or IL-15 (86, 96). Whether AIRE-dependent Tregs arise out of cognate interactions with B cells is unclear (80). However, given the strong expression of TRA transcripts by AIRE-expressing thymic B cells, it will be interesting to see if AIRE expression in B cells contributes distinctly to the Treg TCR repertoire compared to mTECs (45, 85).

1.7 Conclusions and Future Directions

Recent studies evaluating the non-redundant roles by which distinct APC subsets mediate thymocyte selection are providing new insights into how the TCR repertoire is shaped. Although the affinity between TCR and self-peptide–MHC may remain the driving factor in thymocyte selection, the context in which self-peptide is presented is becoming an increasingly important factor in determining thymocyte fate. APC subsets within the thymus are localized based on discrete stromal cues and shape the architecture in which thymocytes are selected. Furthermore, each subset provides a distinct framework in which thymocytes are selected, including chemokines, cytokines, and unique self-peptides (Figure 1.1).

Defining the non-redundant functional capabilities of distinct APC subsets remain major ambitions of future investigations. Until we have a more complete understanding of the various roles of thymic APCs, we will not fully understand if and how the breakdown of central tolerance contributes to human autoimmune diseases. A comprehensive understanding of the thymic APCs required for appropriate selection of the T cell repertoire is also needed as the field seeks to develop methods of stem cell-based T cell production for purposes of therapeutic T cell reconstitution.

1.8 Publication

This chapter has been modified (with permission) from the published article:

Breed, E. R., Lee, S. T., & Hogquist, K. A. (2017, August). Directing T cell fate: how thymic antigen presenting cells coordinate thymocyte selection. In *Seminars in cell & developmental biology*. Academic Press.

Chapter 2

Measuring thymic clonal deletion at the population level

2.1 Introduction

Clonal deletion in the thymus eliminates self-reactive T cells, resulting in a T cell repertoire that is tolerant to self-peptides, but is well equipped to respond to foreign pathogens. The strength of the interaction between the T cell receptor (TCR) and self-peptide–MHC complexes is critical to this process, where strong interactions induce death by apoptosis and weak interactions promote survival and maturation. Importantly, clonal deletion occurs within discrete microenvironments within the thymus: the cortex and the medulla. The medulla is considered a specialized site for negative selection because of AIRE (autoimmune regulator)-mediated expression of tissue-specific antigens and the high concentration of dendritic cells relative to the cortex (1). However, recent studies challenged this conception, suggesting that the majority of clonal deletion occurs at the double positive (DP) stage in the thymus cortex in a process independent of the medulla (67, 68, 70). Nevertheless, the developmental stages at which thymocytes undergo clonal deletion, their corresponding anatomic locations, and the relative proportions at which they undergo clonal deletion at these developmental stages remains controversial.

The reason for this controversy lies primarily in the use of different model systems that have confounded our understanding of clonal deletion in the polyclonal repertoire. Models including the use of endogenous superantigens fail to emulate antigen-specific clonal deletion. TCR transgenics have been used extensively to study clonal deletion and more appropriately model an antigen-specific response to either exogenous peptide injection or endogenous self-peptide. However, the high frequency of a single specificity of antigen-specific T cells results in a number of nonphysiologic effects (97–99). Additionally, TCR transgenics express their TCR early during

development at the double-negative (DN) stage, whereas wild-type (WT) thymocytes do not express surface TCR until the DP stage of development. This results in premature clonal deletion at anatomic locations that are not representative of the polyclonal repertoire (100–102).

More recent studies have attempted to study clonal deletion in settings more representative of the polyclonal environment. BIM deficient mice have an accumulation of self-reactive thymocytes and can therefore be utilized to enumerate T cells that were rescued from clonal deletion (68). This study demonstrated that approximately 75% of thymocytes undergo clonal deletion within the thymus cortex. However, the marked accumulation of thymocytes is not representative of the physiologic conditions in WT mice. A conditional retroviral TCR expression system (retrogenic mice), reported similar conclusions to the BIM knockout studies that approximately 85% of thymocytes undergo clonal deletion in cortex, however only 12 distinct TCRs that were negatively selected were analyzed (67). Finally, peptide–MHC class II tetramers provide a remarkable tool to study tolerance in specific clones within the polyclonal $CD4^+$ T cell repertoire (42, 103), but because of their very small numbers, the anatomic locations at which these clones are deleted are difficult to assess and do not provide a picture at the population level.

Given this, we sought to develop a tool to evaluate clonal deletion in the polyclonal repertoire of WT mice. We designed a cleaved caspase 3-based assay and validated it by a number of different approaches. Using CCR7 to approximate anatomic location in the thymus, we delineate the fraction of thymocytes undergoing clonal deletion in the thymus cortex compared to the medulla. Surprisingly, thymocytes continue to undergo clonal deletion at the most mature stages of development in the thymus medulla. We also report a critical role for CD28-mediated co-stimulation for

clonal deletion both within the thymus cortex and medulla. These findings provide a valuable strategy for studying clonal deletion under normal physiologic and pathologic conditions.

2.2 Results

2.2.1 Identifying clonal deletion in the polyclonal repertoire

We sought to develop a flow cytometry-based assay to identify thymocytes undergoing apoptosis by clonal deletion. Cells activate a cascade of death inducers when undergoing apoptosis, including cleaved caspase 3, which can be detected by intracellular staining. However, in the thymus, caspase 3 is cleaved in cells undergoing apoptosis due either to death by neglect or clonal deletion. To differentiate between these two fates, we used CD5 and T cell receptor (TCR) β, which are upregulated upon T cell receptor signaling (104). Cleaved caspase 3^+ $CD5^+$ $TCR\beta^+$ cells (red gate, Figure 2.1A) potentially represent cells undergoing clonal deletion. To verify this possibility, we utilized $Nur77^{GFP}$ reporter mice, in which GFP expression approximates TCR signal strength (105, 106). GFP expression was high in cells presumed to be undergoing clonal deletion ($CD5^+TCR\beta^+$cleaved caspase 3^+), whereas cells undergoing death by neglect ($CD5^-TCR\beta^-$cleaved caspase 3^+) did not express GFP (Figure 2.1B). Additionally, GFP expression was higher in cells undergoing clonal deletion compared to the total population of signaled cells "auditioning for selection," consistent with the affinity model for selection that proposes that strong TCR–self-peptide–MHC interactions are required to induce clonal deletion (1). In line with this, the frequency of cells undergoing clonal deletion was highest in signaled thymocytes that expressed the most GFP and decreased as GFP expression decreased (Figure 2.1C). We also evaluated mice lacking Bim (BIM KO), which is a proapoptotic molecule required for clonal deletion (68). The frequency of $CD5^+TCR\beta^+$cleaved caspase 3^+ cells was profoundly decreased in Bim KO mice (Figure 2.1E).

To further verify this assay, we examined TCR transgenic thymocytes undergoing either positive or negative selection. We reasoned that T cells with TCRs that do not have an epitope expressed in the thymus would not undergo clonal deletion, whereas TCRs that have an epitope that is over-expressed in the thymus would have an increased proportion of thymocytes that undergo clonal deletion. To do this, we generated 3-way mixed bone marrow chimeras that were 45% SMARTA ($CD4^+$ TCR specific for LCMV GP_{61-80}), 45% OT-II ($CD4^+$ TCR specific for $OVA_{323-339}$), and 10% WT bone marrow (Figure 1F and G). Congenic recipient mice were either WT or RIP-mOVA, which ectopically express OVA peptide under the control of the rat insulin promoter in the thymus. OT-II thymocytes had a high frequency of $CD5^+TCR\beta^+$cleaved caspase 3^+ cells in RIP-mOVA recipients, but not in WT recipients (Figure 2.1G). Likewise, the frequency of such cells amongst SMARTA thymocytes was quite low in either recipient (Figure 2.1G). Altogether, these data support the validity of this approach for identifying thymocytes undergoing clonal deletion within the polyclonal repertoire.

To determine the localization of thymocytes undergoing clonal deletion, we stained for the C-C chemokine receptor CCR7, which is required for migration to the thymus medulla (26–31) (Figure 2.1A). Approximately 22% of the thymocytes undergoing clonal deletion were $CCR7^+$ (Figure 2.1D), which is consistent with previous reports that the majority of clonal deletion occurs in the thymus cortex (67, 68).

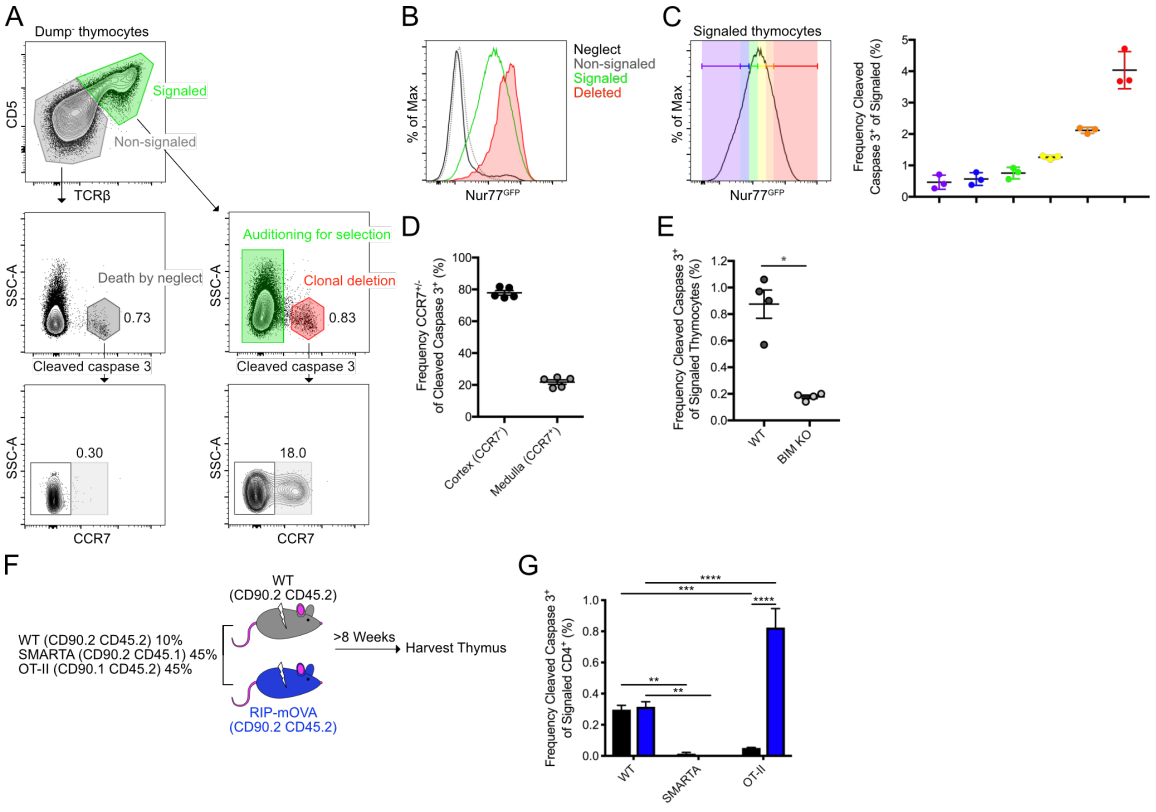

Figure 2.1. Cleaved caspase 3 distinguishes thymocytes undergoing clonal deletion.

(A) Flow cytometry gating strategy for the identification of cells undergoing clonal deletion or death by neglect in the thymus. Signaled and non-signaled thymocytes identified by the expression of CD5 and TCRβ, excluding $CD25^+$, $NK1.1^+$, $CD19^+$, and $TCR\gamma\delta^+$ (Dump) cells (top). Clonal deletion and death by neglect identified by the expression of cleaved caspase 3 (middle) and approximate anatomic location identified by CCR7 (bottom). Numbers adjacent to outlined areas indicate percent cells in each. (B) Flow cytometry from $Nur77^{GFP}$ mice showing GFP expression by $CD5^-TCR\beta^-$cleaved caspase 3^+ (neglect) $CD5^-TCR\beta^-$ (non-signaled), $CD5^+TCR\beta^+$ (signaled), and $CD5^+TCR\beta^+$cleaved caspase 3^+ (deletion) (as demonstrated in A). (C) Flow cytometry from $Nur77^{GFP}$ mice showing gating based on GFP expression (approximately 15% of total $CD5^+TCR\beta^+$ cells per gate) (left) and frequency of cleaved caspase 3 expression among $CD5^+TCR\beta^+$ (signaled) thymocytes in each gate (right). (D) Frequency of $CCR7^-$ or $CCR7^+$ among clonally deleted cells (as shown in A). (E) Frequency of cleaved caspase 3^+ cells among $CD5^+TCR\beta^+$ thymocytes (as gated in A) from BIM WT or BIM KO littermates. (F) Experimental design used to generate bone marrow chimeric mice. (G) Frequency of cleaved caspase 3^+ cells among $CD5^+TCR\beta^+$ (signaled) thymocytes (as gated in A) from bone marrow chimeric mice (as in F). Each symbol (C, D, E) represents an individual mouse. Six- to twelve-week-old male and female mice were used. Small horizontal lines indicate the mean and error bars represent SEM. *P< 0.05,

**P< 0.01, ***P< 0.001, ****P< 0.0001. Statistical significance was determined by Mann-Whitney test (E) or 2way Anova with Dunnett's and Sidak's multiple comparisons tests (G). Data are representative of more than ten experiments (A, B, C, D) or are pooled from two (E, G) independent experiments with at least three mice per group.

2.2.2 Mature thymocytes undergo clonal deletion

Thymocytes in the medulla undergo distinct stages of maturation, during which they become competent to produce cytokines, proliferate, and emigrate (107). A seminal study by Kishimoto and Sprent (108), showed that semi-mature SP thymocytes undergo apoptosis when stimulated with anti-CD3, whereas the most mature SP thymocytes tend to proliferate (108, 109). Thus, we expected most $CCR7^{+}CD5^{+}TCR\beta^{+}$cleaved caspase 3^{+} cells would be of the "semi-mature" phenotype. CD69 and MHCI staining was used to define three distinct stages of SP maturation: $CD69^{+}MHCI^{-}$ semi-mature (SM), $CD69^{+}MHCI^{+}$ mature 1 (M1) and $CD69^{-}MHCI^{+}$ mature 2 (M2) (109). To our surprise, all 3 stages were present amongst $CCR7^{+}$ $CD5^{+}TCR\beta^{+}$cleaved caspase 3^{+} cells—those undergoing deletion in the medulla (Figure 2.2A, top), which suggests that even mature thymocytes can undergo deletion. When examining the frequency of clonal deletion events at each stage, we observed only a modest reduction from the SM to M1 to M2 stages (Figure 2.2B and C). To confirm that the mature phenotype deleted cells truly were later in differentiation, we performed this assay using $RAG2^{GFP}$ mice (where GFP decay acts as a 'molecular timer' from positive selection) (110). GFP decay was equivalent in clonally deleted and non-deleted thymocytes at more mature stages (Figure 2.2A, bottom) confirming that deletion can occur far after positive selection. To verify that these late stage clonal deletion events were due to strong TCR signals (as opposed to failed positive selection), we utilized $Nur77^{GFP}$ reporter mice. GFP expression was higher in thymocytes undergoing clonal deletion in all three stages of maturation

(Figure 2.2D). These data indicate that even the most mature thymocytes can undergo TCR triggered apoptosis.

It was previously established that thymocytes are more susceptible to Treg induction as they mature (81). Given that Treg induction can lead to apoptosis if it falters (111), we considered the possibility that many of the late stage deletion events might be due to failed Treg induction. Consistent with this idea, we observed that the percentage of $FOXP3^{+}/CD25^{+}$ cells amongst deleted thymocytes was increased with maturation (Figure 2.2E).

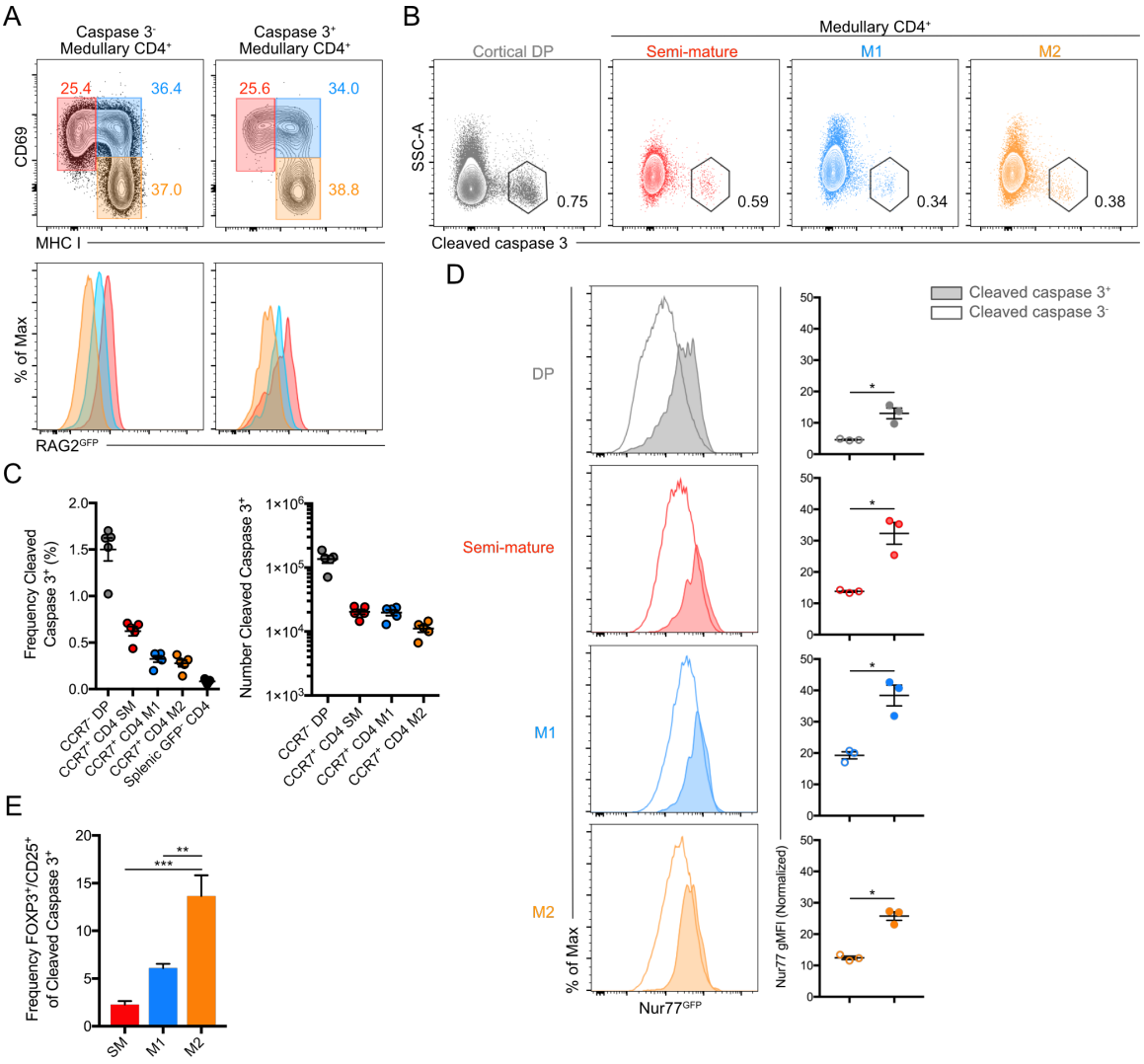

Figure 2.2. Mature thymocytes are susceptible to clonal deletion.

(A) Flow cytometry of total or deleted CD5$^+$TCRβ$^+$ medullary (CCR7$^+$) CD4$^+$ thymocytes from Rag2^{GFP} mice (gated as in Figure 2.1A). Gates of three subsets of medullary thymocytes based on expression of CD69 and MHC I (top), and GFP expression by CD69$^+$MHC I$^-$ (SM), CD69$^+$MHC I$^+$ (M1), and CD69$^-$MHC I$^+$ (M2) cells (bottom). Numbers adjacent to outlined areas indicate percent cells in each. (B) Flow cytometry of deleted thymocytes (as gated in Figure 2.1A) of cortical (CCR7$^-$) DP or medullary (CCR7$^+$) CD4$^+$ subsets. Numbers adjacent to outlined areas indicate percent cleaved caspase 3$^+$ cells in each. (C) Frequency (left) and numbers (right) of cleaved caspase 3$^+$ thymocytes among CD5$^+$TCRβ$^+$ thymocyte subsets or CD4$^+$ splenocytes from Rag2^{GFP} mice (gated as in Figure 2.1A). (D) Flow cytometry of deleted or non-deleted thymocytes (as gated in Figure 2.1A) from Nur77^{GFP} mice (left) and geometric mean fluorescence intensity (gMFI) normalized to controls (right). (E) Frequency of CD25$^+$ or FOXP3$^+$ among CD5$^+$TCRβ$^+$CD4$^+$cleaved caspase 3$^+$ thymocytes negatively enriched for CD4 using

MACS purification from bone marrow chimeric mice that received FOXP3^{GFP} bone marrow. Data are representative of more than 5 independent experiments (A, B, C, D) or 2 independent experiments (E). Each symbol (C, D) represents an individual mouse. Six- to twelve-week-old male and female mice were used. Small horizontal lines indicate the mean and error bars represent SEM. *P< 0.05, **P< 0.01, ***P< 0.001. Statistical significance was determined by one-tailed Mann-Whitney test (D) or ordinary one-way ANOVA with Tukey multiple comparisons test (E).

2.2.3 Contribution of bone marrow APC to clonal deletion in the polyclonal repertoire

Both bone marrow-derived APCs and medullary thymic epithelial cells (mTEC) have been shown to mediate clonal deletion (112). We reasoned that this assay could be used to assess the relative contribution of bone marrow APCs to deletion in the polyclonal repertoire. For this, WT or MHC II-deficient mice (MHC II KO) were used as bone marrow donors into irradiated WT recipient mice (Figure 2.3A, Figure 2.4). We did not assess MHC II-deficient recipients, because lack of MHC II on cortical thymic epithelial cells prevents positive selection of CD4$^+$ T cells. Bone marrow APCs contributed to approximately 43% of clonal deletion events in the thymus cortex (Figure 2.3B) and 41% of clonal deletion events in the thymus medulla (Figure 2.3C). These data show that bone marrow APCs contribute to a substantial proportion of non-redundant clonal deletion events in the polyclonal repertoire.

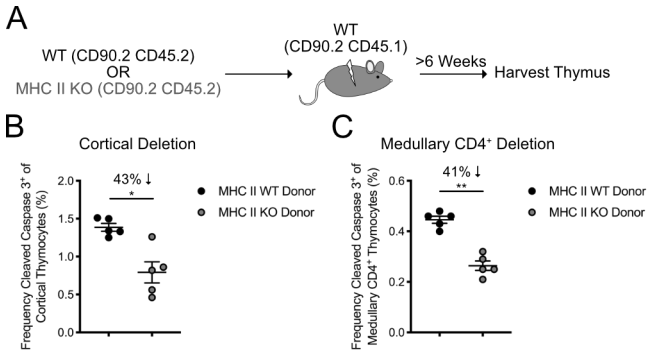

Figure 2.3. Bone marrow derived APC contribute to approximately half of clonal deletion events.

(A) Experimental strategy for generating bone marrow chimeric mice. (B) Frequency of cleaved caspase 3^+ thymocytes among $CD5^+TCR\beta^+$ cortical ($CCR7^-$) thymocytes (as gated in Figure 2.1A). (C) Frequency of cleaved caspase 3^+ thymocytes among $CD5^+TCR\beta^+$ medullary ($CCR7^+$) $CD4^+$ thymocytes (as gated in Figure 2.1A). Each symbol (B, C) represents an individual mouse. Six- to twelve-week-old female mice were used. Small horizontal lines indicate the mean and error bars represent SEM. **P*< 0.05, ***P*< 0.01. Statistical significance was determined by Mann-Whitney test (B, C). Data are pooled from two independent experiments.

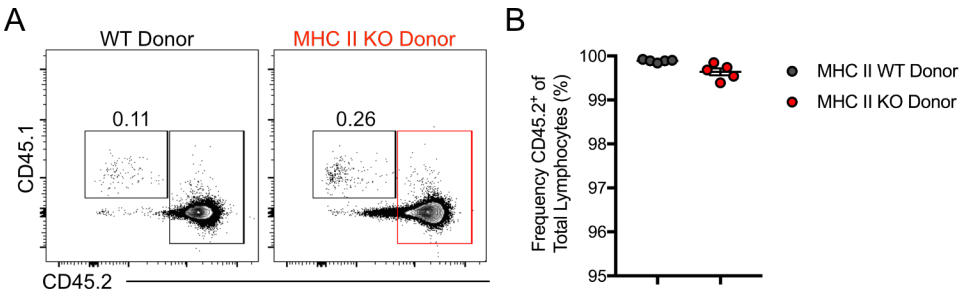

Figure 2.4. MHC II KO bone marrow chimera efficiency.

(A) Flow cytometry of total thymocytes from bone marrow chimeric mice from either WT donor (left) or MHC II KO donor (right) mice (as shown in Figure 2.3A). Numbers adjacent to outlined areas indicate percent $CD45.1^+$ (recipient) cells in each. (B) Frequency $CD45.2^+$ (donor cells) of total thymocytes for each bone marrow chimeric donor. Each symbol represents an individual mouse (B). Six- to twelve-week-old female mice were used. Data are representative of two independent experiments (A) and pooled from two independent experiments (B).

2.2.4 Clonal deletion is dependent on co-stimulatory molecules in both the cortex and medulla

Treg and iNKT cell development and survival in the thymus require CD80 and CD86 co-stimulation via the CD28 receptor (113–117). In contrast, other agonist selected cells– CD8$\alpha\alpha$ intraepithelial lymphocyte precursors (IELp)– need to avoid CD28 co-stimulation for development (118, 119). However, the role of CD28-mediated co-stimulation in clonal deletion has been controversial, primarily because TCR transgenic and superantigen systems were utilized to assess negative selection (120). To address this, we evaluated clonal deletion in CD86 KO, CD80/CD86 KO, and CD28 KO animals (Figure 2.5A). Consistent with previous reports, the frequency of $CD4^+$ and $CD8^+$ thymocytes was increased in CD80/86 KO animals (114, 121) (Figure 2.5B). CD28 co-stimulation contributed to approximately half (56%) of clonal deletion events in the cortex and a third (36%) of clonal deletion events in the medulla (Figure 2.6A and B), indicating that CD28-mediated co-stimulation is required for clonal deletion. Surprisingly, CD86 alone contributed to clonal deletion in the cortex, but not the medulla (Figure 2.6A and B), raising the possibility of a non-redundant role for CD80 and CD86 in mediating clonal deletion.

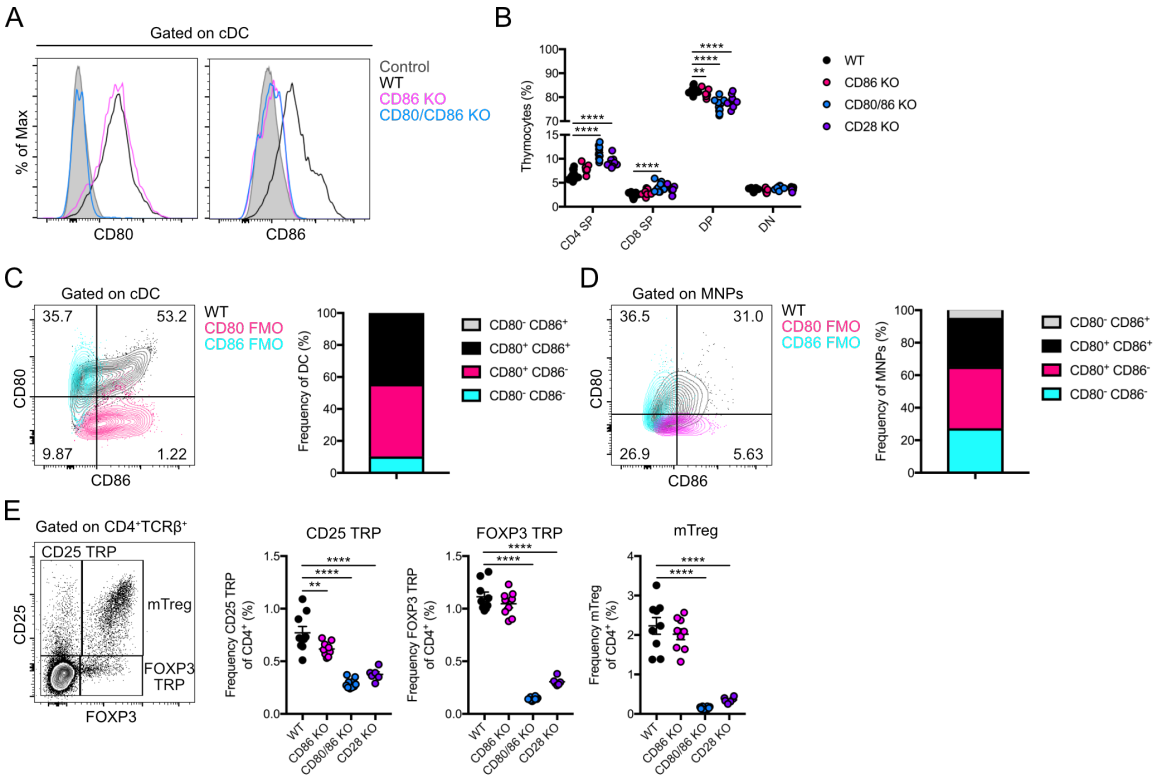

Figure 2.5. Tolerance induction by CD80/CD86.

(A) Flow cytometry of CD11c$^+$ MHC II$^+$ thymic dendritic cells from WT, CD86 KO, or CD80/86 KO mice (key) stained for CD80 (left) and CD86 (right). (B) Frequency of CD4$^+$, CD8$^+$, DP, and DN among total thymocytes from WT, CD86 KO, CD80/86 KO, and CD28 KO mice. (C) Flow cytometry of CD11c$^+$ MHC II$^+$ dendritic cells from WT mice stained for CD80 and CD86 (left) and quantification (right). Numbers indicate percent cells in each quadrant. (D) Flow cytometry of FcγR1$^+$ MNPs from WT mice stained for CD80 and CD86 (left) and quantification (right). (E) Flow cytometric gating strategy for identifying CD25$^+$ Treg progenitors, FOXP3$^+$ Treg progenitors, and mature Treg (left). Frequency of CD25$^+$ (middle, left), FOXP3$^+$ (middle, right), or CD25$^+$FOXP3$^+$ (right) among CD4$^+$ thymocytes from WT, CD86 KO, CD80/CD86 KO, and CD28 KO mice. Each symbol (B, E) represents an individual mouse. Six- to twelve-week-old male and female mice were used. Small horizontal lines indicate the mean and error bars represent SEM. **P< 0.01, ***P< 0.001, ****P< 0.0001. Statistical significance was determined by ordinary one-way ANOVA with Holm-Sidak's multiple comparisons test (B, E). Data are representative of at least three independent experiments (A) or are pooled from at least three independent experiments (B, C, D, E).

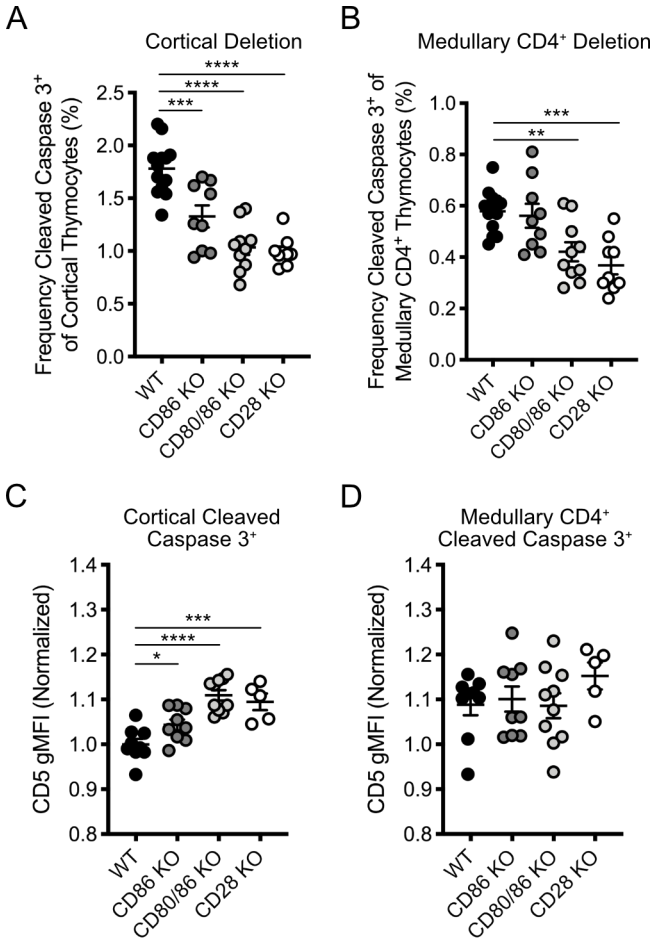

Figure 2.6. Co-stimulatory molecules CD80 and CD86 are required for both cortical and medullary clonal deletion.

(A) Frequency of cleaved caspase 3^+ cells among $CD5^+TCR\beta^+$ cortical ($CCR7^-$) thymocytes (as gated in Figure 2.1A) in WT, CD86 KO, CD80/86 KO, and CD28 KO mice. (B) Frequency of cleaved caspase 3^+ cells among $CD5^+TCR\beta^+$ medullary ($CCR7^+$) $CD4^+$ thymocytes (as gated in Figure 2.1A). (C) CD5 gMFI of cortical deleted thymocytes (normalized to mean of WT CD5 gMFI) (from A). (D) CD5 gMFI of medullary deleted $CD4^+$ thymocytes (normalized to mean of WT CD5 gMFI) (from B). Each symbol (A, B, C, D) represents an individual mouse. Six- to twelve-week-old male and female mice were used. Small horizontal lines indicate the mean and error bars represent SEM. *P< 0.05, **P< 0.01, ***P< 0.001, ****P< 0.0001. Statistical significance was determined by ordinary one-way ANOVA with Holm-Sidak's multiple comparisons test (A, B, C, D). Data are pooled from at least three independent experiments (A, B, C, D).

Given this, we sought to determine if CD86 was expressed in the absence of CD80 by any APC type in the thymus. Using flow cytometry of APC recovered from the thymus after collagenase digestion, we observed a substantial proportion of conventional dendritic cells (cDC) that expressed CD80 alone. However, no cDC expressed only CD86 (Figure 2.5C). Furthermore, no mononuclear phagocytes (MNPs) expressed CD86 alone (Figure 2.5D). To investigate the localization of CD80 and CD86, we utilized immunofluorescence staining and quantitative histo-cytometry to determine which APC subset could be mediating CD86-dependent clonal deletion events in the thymus cortex. In agreement with our findings by flow cytometry, very few cells localized within the thymus cortex or medulla expressed CD86 alone (Figure 2.7A, Figure 2.8A). Within the cortex, CD86 expression was observed on approximately 50% of CD11c-expressing cells and on 70% of F4/80-expressing cells (Figure 2.7B and C, Figure 2.8B and C). Therefore, CD86-mediated clonal deletion in the cortex is likely mediated by both $CD11c^+$ and $F4/80^+$ APC.

Because we could not explain the selective requirement for CD86 in cortical deletion by identifying a cortical APC that only expressed CD86, we reasoned that cortical thymocytes may be more sensitive to and dependent on interactions with $CD80/CD86^+$ APC for clonal deletion. Indeed, in the absence of co-stimulation, the CD5 gMFI was increased on clonally deleted thymocytes in the cortex (Figure 2.6C), indicating that only the most strongly signaled cells could be deleted without co-stimulation. This was not the case of medullary thymocytes (Figure 2.6D). Consistent with this, CD86 alone was not required for Treg development, a process that also occurs in the thymus medulla (Figure 2.5E). Together, these data suggest that cortical

thymocytes have a lower threshold for co-stimulation-dependent negative selection compared to medullary thymocytes.

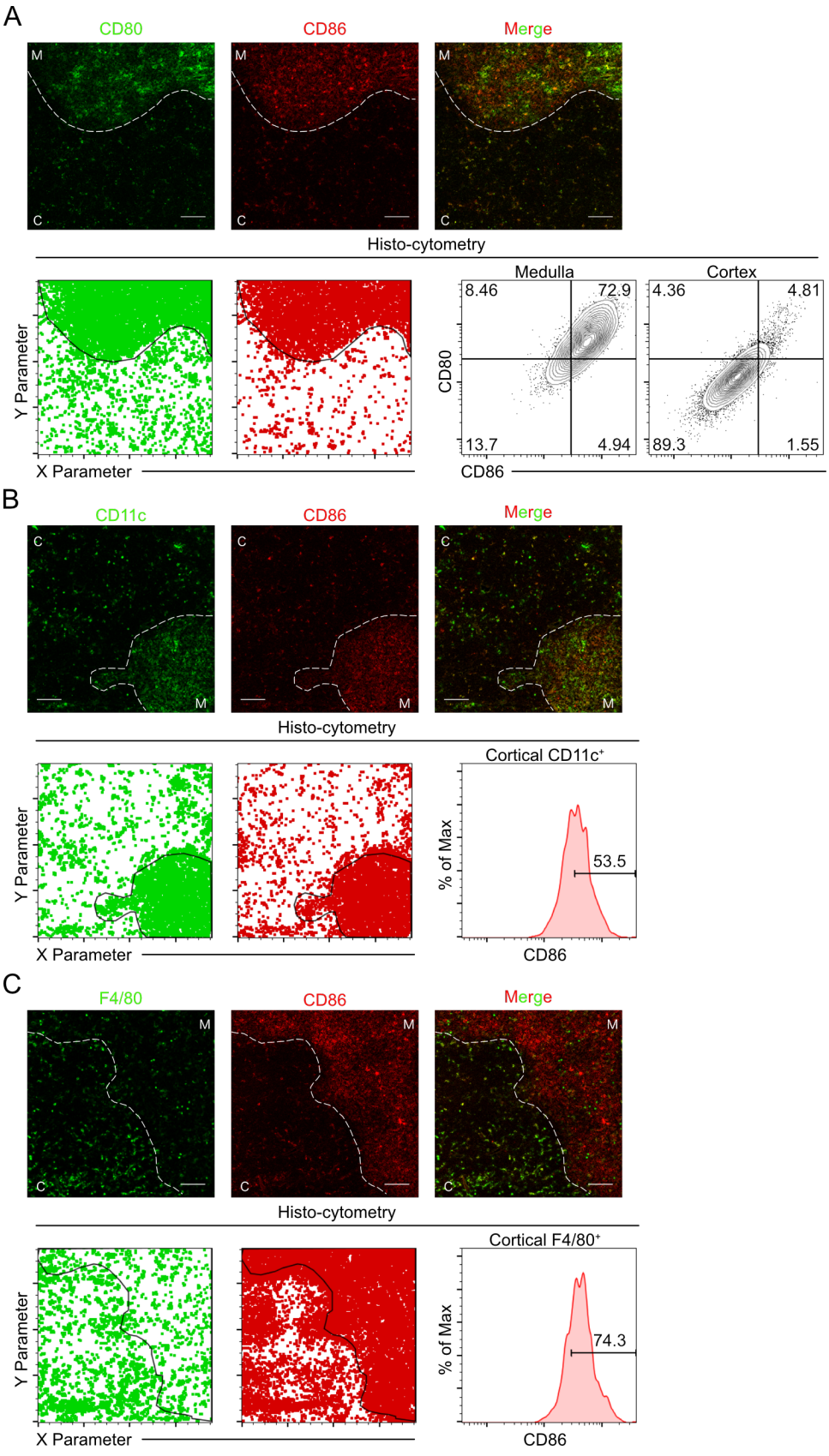
A
CD80
CD86
Merge
M
C
Histo-cytometry
Medulla
Cortex
8.46
72.9
13.7
4.94
4.36
4.81
89.3
1.55
Y Parameter
X Parameter
CD80
CD86
B
CD11c
CD86
Merge
Histo-cytometry
Cortical CD11c+
53.5
% of Max
C
F4/80
CD86
Merge
Histo-cytometry
Cortical F4/80+
74.3

Figure 2.7 CD80 and CD86 are localized in both the thymus cortex and medulla.

(A) Immunofluorescence microscopy (top) of thymic sections from C57BL/6 mice stained for CD80 (green), and CD86 (red). White dashed lines indicate cortical-medullary border based on UEA I staining (not shown). C, cortex; M, medulla. Scale bars 100μm. Analysis of images by histo-cytometry (bottom, left). Dots represent localization of each stain as determined by histo-cytometry. Frequencies of $CD80^+$ and $CD86^+$ cells identified as localized in the cortex by histo-cytometry (bottom, right). Numbers indicate percent cells in each outlined area. (B) Immunofluorescence microscopy (top) of thymic sections from C57BL/6 mice stained for CD11c (green), and CD86 (red). White dashed lines indicate cortical-medullary border based on UEA I staining (not shown). C, cortex; M, medulla. Scale bars 100μm. Analysis of images by histo-cytometry (bottom, left). Dots represent localization of each stain as determined by histo-cytometry. Frequency of $CD86^+$ cells among $CD11c^+$ cells identified as localized in the cortex by histo-cytometry (bottom, right). Number indicates percent cells in gated area. (C) Immunofluorescence microscopy (top) of thymic sections from C57BL/6 mice stained for F4/80 (green), and CD86 (red). White dashed lines indicate cortical-medullary border based on UEA I staining (not shown). C, cortex; M, medulla. Scale bars 100μm. Analysis of images by histo-cytometry (bottom, left). Dots represent localization of each stain as determined by histo-cytometry. Frequency of $CD86^+$ cells among $F4/80^+$ cells identified as localized in the cortex by histo-cytometry (bottom, right). Number indicates percent cells in gated area. Six- to twelve-week-old male and female mice were used. Data are representative of at least three independent experiments.

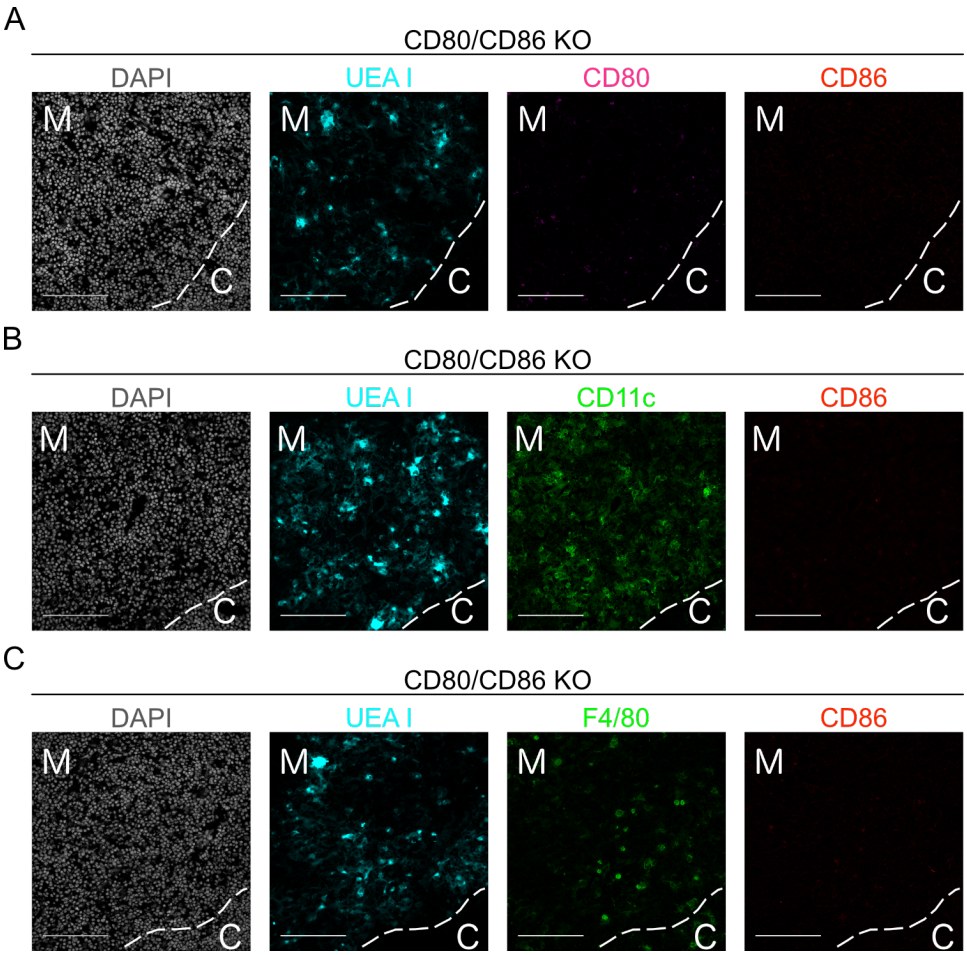

Figure 2.8 Immunofluorescence microscopy of CD80/CD86 KO thymus.

(A) Immunofluorescence microscopy of thymic sections stained for DAPI (gray), UEA I (cyan), CD80 (magenta), and CD86 (red) in CD80/CD86 KO mice. C, cortex; M, medulla. Scale bars 100μm. (B) Immunofluorescence microscopy of thymic sections stained for DAPI (gray), UEA I (cyan), CD11c (green), and CD86 (red) in CD80/CD86 KO mice. C, cortex; M, medulla. Scale bars 100μm. (C) Immunofluorescence microscopy of thymic sections stained for DAPI (gray), UEA I (cyan), F4/80 (green), and CD86 (red) in CD80/CD86 KO mice. C, cortex; M, medulla. Scale bars 100μm. Six- to twelve-week-old male and female mice were used. Data are representative of at least three independent experiments.

2.3 Discussion

Defining the developmental stages and corresponding anatomic locations at which thymocytes undergo clonal deletion within the polyclonal repertoire has been challenging given current approaches. Here, we validated a cleaved caspase 3-based assay that can be used to examine clonal deletion at the population level. We made several observations regarding clonal deletion at distinct maturation stages in the thymus. Consistent with estimates that used other methods (67, 68), we observed that the majority of thymocytes underwent clonal deletion in the thymus cortex. However, thymocytes continued to undergo clonal deletion as they progressed through discrete maturation stages in the thymus medulla. Bone marrow-derived APC contributed to clonal deletion similarly in the thymus cortex and medulla. However, co-stimulatory molecule-mediated clonal deletion decreased as thymocytes emigrated from the cortex to the medulla. Thus, this approach served as a valuable tool to assess clonal deletion throughout thymocyte development.

The degree of clonal deletion that occurs in the thymus cortex (78%) supports previous studies that the majority of clonal deletion occurs within the cortex (67, 68). This likely reflects the high propensity of TCRs to interact with MHC molecules, regardless of the specific peptide (67). Signaled thymocytes that are purged of the most cross-reactive TCRs go on to upregulate CCR7 and migrate to the medulla. Upon further analysis of clonal deletion within the thymus medulla, we observed apoptotic events at each of three distinct stages of maturation (107, 109). These findings are in contrast with a previous study that suggested that only semi-mature thymocytes were susceptible to clonal deletion (122). The discrepancies in these findings may lie in the use of different model systems. Kishimoto and Sprent utilized injection of TCR cross-linking antibodies

to observe thymocyte death *ex vivo*. However, such an approach induces extensive peripheral T cell activation, which can contribute to non-specific thymocyte death through the production of cytokines and glucocorticoid stress hormones (123, 124). To rule out non-specific deletion at these late stages of maturation, we utilized Nur77^{GFP} reporter mice. GFP expression in deleted thymocytes was higher than non-deleted thymocytes at all three stages of maturation. Additionally, we showed that Treg and Treg precursors were enriched in apoptotic thymocytes at the most mature stages of development, supporting the notion that FOXP3 can act as a proapoptotic protein (111). These data therefore suggest that mature thymocytes indeed undergo TCR-induced apoptosis, which can involve FOXP3 induction as thymocytes reach their more mature developmental stage.

We estimate that bone marrow APC contribute to approximately 40-45% of deletion events in both the thymus cortex and medulla. Previous studies estimated that 50-70% of CD4SP thymocytes were deleted by bone marrow APC, based on CD4SP frequencies in MHC II-deficient bone marrow chimeras (44, 125). A more recent study, which based their estimates on high throughput analysis of the TCR repertoire in MHC II-deficient bone marrow chimeras, had a more conservative estimate of 30% of deletion events mediated by bone marrow APC (45). However, this study utilized a fixed TCRβ, which may not fully reflect the WT TCR repertoire. Nonetheless, all of these data support the conception that bone marrow APC play a non-redundant role in mediating clonal deletion.

We also showed a critical role for CD28-mediated co-stimulation in both the thymus cortex and medulla. The extent to which co-stimulation contributed to clonal deletion decreased as thymocytes emigrated from the cortex to the medulla. These

findings are in contrast with multiple studies involving superantigen or TCR-transgenic systems that did not find a requirement for CD28 in mediating clonal deletion (120, 126–129). However, more recent studies did support a requirement for CD28 in superantigen-mediated clonal deletion (119, 130). In one of these studies, Pobezinsky *et al*. showed that autoreactive DN thymocytes are diverted to an alternate CD8$\alpha\alpha$ IELp in the absence of CD28-mediated co-stimulation (118, 119). Conversely, this diversion into agonist subsets was not observed at other stages of thymocyte development. Other agonist-selected cells – iNKT (DP stage) and Treg (CD4SP stage) – require CD28-mediated co-stimulation for their survival and differentiation (113–117). It is unclear what signaling context distinguishes the various roles for CD28 in different thymocyte populations (120, 131).

Surprisingly, our results also establish a non-redundant role for CD86 in mediating clonal deletion in the cortex. We do not yet understand if this is a qualitative role for CD86 in clonal deletion (i.e. CD86 allows the deletion of certain antigen-specific populations) or a quantitative requirement for a certain total level of co-stimulatory ligand. Regarding a qualitative role, we considered the possibility that a distinct $CD80^{-}$ $CD86^{+}$ antigen presenting cell subset was driving cortical clonal deletion. However, neither flow cytometric analysis nor immunofluorescence microscopy supported this hypothesis. Regarding a quantitative role, cortical thymocytes may require a higher total level of CD80/CD86 stimulation to trigger deletion. In this case, one would predict that either CD80 or CD86 deficiency would impact cortical deletion.

In summary, we demonstrated that a cleaved caspase 3-based assay can be used to assess clonal deletion at the polyclonal level. This assay served as a valuable tool to study the location and stages of thymocyte development at which clonal deletion

occurs. We found that thymocytes undergo clonal deletion even at mature stages of development in the thymus medulla and that approximately half of deletion events require co-stimulation. We expect this assay may be useful in understanding the extent to which generalized clonal deletion defects contribute to autoimmunity caused by specific genetic mutations.

2.4 Materials and Methods

2.4.1 Mice

C57BL/6NCrl (B6) and B6.SJL-Ptprc^{a}Pepc^{b}/BoyCrl (B6.SJL) mice were purchased from Charles River Laboratories. C57BL/6Tg(Nr4a1-EGFP/cre)^{820Khog} (Nur77^{GFP}) and C57BL/6Tg(Rag2-EGFP)1Mnz (Rag2^{GFP}) mice were described previously (105, 110). C57BL/6-Tg(Ins2-TFRC/OVA)296Wehi/WehiJ (RIP m-OVA), B6.Cg-Tg(TcraTcrb)425Cbn/J (OT-II), B6.Cg-*Ptprc^{a} Pepc^{b}* Tg(TcrLCMV)1Aox/PpmJ (SMARTA), B6.129S2-*H2$^{dlAb1\text{-}Ea}$*/J (MHC II KO), B6.129S4-*Cd80^{tm1Shr} Cd86^{tm2Shr}*/J (CD80/CD86 KO), and B6.129S2-CD28tm1Mak/J (CD28 KO) were obtained from Jackson Laboratories. C57BL/6Foxp3^{tm2Ayr} (FOXP3^{GFP}) were kindly provided by M. A. Farrar (University of Minnesota) and were described previously (132). *CD80^{flox}BACTg/* B6.129S4-*Cd80^{tm1Shr} Cd86^{tm2Shr}*/J, referred to as CD86 KO mice in this study, were kindly provided by R. J. Hodes (National Institutes of Health) and were described previously (133). Bone marrow chimera mice were generated by reconstituting lethally irradiated (1,000 rads) mice with 10^{7} T cell-depleted donor bone marrow cells. Recipient mice were provided with neomycin and polymyxin B supplemented water for at least 3 weeks following irradiation and bone marrow transplantation. Chimeras were analyzed at a minimum of six weeks after reconstitution. All animal experiments were approved by the Institutional Animal Care and Use Committee of the University of Minnesota. All animals were maintained under specific pathogen-free conditions at the University of Minnesota.

2.4.2 Flow Cytometry and MACS Purification

Single-cell suspensions were stained for 30 minutes at 4º C with the indicated antibodies. Antibodies purchased from BioLegend: CD19 (6D5), CD25 (PC61), CD45.1 (A20), CD45.2 (104), CD64 (X54-5/7.1), CD80 (16-10A1), CD90.1 (OX-7), NK1.1 (PK136), TCRγ/δ (GL3), , TCRβ (H57-597). Antibodies purchased from BD Biosciences: CD4 (GK1.5), CD8α (53-6.7), CD69 (H1.2F3), CD86 (GL1), CD90.2 (30-H12), H-2K^{b} (AF6-88.5), TCRβ (H57-597). Antibodies purchased from Thermo Fischer: CD5 (53-7.3), MHC Class II– I-A/I-E (M5/114.15.2). Antibodies purchased from eBioscience: CD25 (PC61.5), FOXP3 (NRRF-30). Staining for CCR7/CD197 (4B12; eBioscience) was performed for 30 minutes at 37ºC prior to additional surface stains. For cleaved caspase-3 (Asp175) (D3E9; Cell Signaling Technologies) staining: cells were processed as quickly as possible following harvest to avoid non-specific apoptosis. Following surface stain, cells were fixed with cytofix/cytoperm (BD Biosciences) for 30 minutes at 4º C. Cells were then washed with perm/wash buffer (BD Biosciences) twice. Cells were stained with anti-cleaved caspase 3 at a 1:50 dilution for 30 minutes at 20º C. To isolate CD4SP thymocytes, we depleted DP and CD8SP thymocytes via negative enrichment using biotinylated anti-CD8α (53-6.7, eBioscience), Streptavidin MicroBeads (Miltinyi Biotec), and MACS separation columns (Miltinyi Biotec) per manufacturer's protocol. Samples were acquired with BD LSR Fortessa X-20 (BD Biosciences) and analyzed with FlowJo version X (FlowJo LLC).

2.4.3 Immunofluorescence

Thymi were harvested and snap frozen in Optimal Cutting Temperature compound (Sakura Finetek). 7μm sections were fixed and permeabilized in 100% acetone for 20 minutes at 4º C. Samples were then blocked with 5% bovine serum albumin (BSA) and Fc block (anti-CD16/CD32; 2.4G2, Tonbo Biosciences) for one hour at 20ºC prior to staining. Antibodies were purchased from BD Biosciences: CD11c (HL3), BioLegened: F4/80 (BM8), CD86 (GL-1), Tonbo biosciences: CD80 (16-10A1), and Vector Laboratories: Fluorescein labeled Ulex Europaeus Agglutinin I (UEA I). Blocked sections were stained with desired antibodies combined into a cocktail in 0.5% BSA and 0.1% Tween-20 (Sigma Aldrich) overnight at 4ºC prior to DAPI staining. Sections were mounted using Prolong anti-fade mounting medium (Life Technologies). Images were acquired using a Leica DM6000B epifluorescent microscope 16-72 hours later.

2.4.4 Histo-cytometry

Histo-cytometry was performed as described previously, with modifications (134). Briefly, fluorochrome intensities of each region of interest (based on DAPI staining) were quantified using ImageJ. Data were exported into .csv format and imported into FlowJo for two-dimensional plotting. Medulla gates were drawn based on UEA I fluorescence intensity.

2.4.5 Statistical Analysis

Statistical analyses were performed using Prism 7 (GraphPad). Data sets were assessed for normality using D'Agostino & Pearson normality test. For comparison of

two data sets, unpaired Student's *t* test or unpaired Mann-Whitney test were performed. For comparison of three or more data sets, ordinary one-way ANOVA with Holm-Sidak's or Tukey's multiple comparisons test was used. P-values less than 0.05 were considered significant. Sample size, experimental replicates, and additional details are included in the figure legends.

2.5 Publication

This chapter has been modified (with permission) from the published article:

Breed, E. R., Watanabe, M., & Hogquist, K. A. (2019). Measuring Thymic Clonal Deletion at the Population Level. *The Journal of Immunology*, *202*(11), 3226-3233.

Chapter 3

Defining the relative contribution of thymic APC subsets to central tolerance

3.1 Introduction

A variety of antigen presenting cells (APC) in the thymus coordinate the selection of a T cell repertoire that is self-tolerant and effective against foreign pathogens. This selection process is dependent on the affinity of the T cell receptor (TCR) for self-peptide–MHC presented by these APC, where strength of these interactions governs developing T cell fate. Weak interactions generate a naïve TCR repertoire via positive selection, whereas strong interactions can lead to clonal deletion and subsequent cell death by apoptosis. Regulatory T cell differentiation also occurs upon high-affinity TCR–self-peptide–MHC interactions, but requires distinct cytokine and co-stimulatory signals (106, 115, 116).

Thymic APCs include cortical and medullary thymic epithelial cells (cTEC and mTEC), thymic dendritic cells (DC), B cells, and mononuclear phagocytes (MNPs). Self-peptides are presented by these APC subsets via multiple mechanisms. cTEC are specialized to present positively selecting ligands to developing double positive (DP) thymocytes. This is due, in part, to their ability to process and present self-peptides via machinery distinct from other thymic APC (112). mTEC are specialized for negative selection. The autoimmune regulator (AIRE) promotes presentation of tissue-restricted self-antigens (TRA) on both mTECs and B cells (60, 85, 135). These TRAs serve to reflect virtually all of the parenchymal organs within the thymus, thereby preventing dangerous autoreactive interactions after thymic clonal deletion and Treg cell induction (135).

DC represent an exceptionally heterogeneous faction of thymic APC and also play a crucial role in processing and presenting self-peptides. Three major dendritic cell subsets have been described within the thymus. These subsets include plasmacytoid

DC (pDC) and two conventional DC (cDC) populations, which are delineated based on their expression of lineage defining cell surface markers and transcription factors (57, 58). The two cDC subsets are comprised of XCR1$^+$ (X-C chemokine receptor 1) cDC1, which cross-present TRAs acquired from mTEC, and SIRPα^+ (signal regulatory protein alpha) cDC2, which are capable of circulating to the thymus and displaying self-antigen acquired from the periphery (1, 57, 59, 63, 136). Plasmacytoid DC (pDC) are also capable of acquiring self-peptide in the periphery for presentation in the thymus (65).

The heterogeneity and distinct functional capabilities of these APC subsets suggest that there are non-redundant roles by which they mediate central tolerance. While each of these thymic APC subsets has been shown to be capable of mediating clonal deletion or Treg differentiation, many of these studies relied on model systems that are not representative of thymocyte selection in the polyclonal repertoire (137). These models include the use of endogenous superantigens, which do not imitate antigen-specific clonal deletion, and TCR transgenics, which due to the abundance of a single TCR and the timing at which the TCR is expressed during development, have a number of nonphysiologic consequences (97–102). Importantly, because of the strategies employed to study whether APC subsets mediate clonal deletion or Treg differentiation, their relative contribution to these processes is unknown.

Given this, we sought to determine the extent to which different APC subsets in the thymus contribute to clonal deletion and nascent Treg differentiation in the polyclonal repertoire. Using a cleaved caspase-3 based assay to quantify clonal deletion in mice with APC-specific ablation or deficiency, we found that clonal deletion was not altered in the absence of B cells, pDC, XCR1$^+$ cDC1, or MNPs. However, in an effort to eliminate SIRPα^+ cDC2, we discovered that a fraction of this subset expresses the surface lectin,

CD301b. This subset required IL-4/IL-13 and was localized primarily within the thymus medulla. Mice lacking these DC had a measurable reduction in clonal deletion events, suggesting a non-redundant role for this subset in mediating clonal deletion.

3.2 Results

3.2.1 Enumeration of thymic APC subsets

As a whole, bone marrow APCs play a non-redundant role in mediating both clonal deletion and Treg selection (44, 45, 125, 137). To examine the relative contribution of distinct APC subsets to negative selection, we first sought to fully characterize and enumerate bone marrow APCs in adult (8-week-old) C57BL/6 mice (Figure 3.1A, Figure 3.2A and B). To determine the antigen presenting capability of these subsets, we assessed the expression of MHC II and the co-stimulatory molecules, CD80 and CD86 (Figure 3.1B and C). The conventional dendritic cell (cDC) subsets and B cells had the highest MHC II and cDC had the highest co-stimulatory molecule expression (Figure 3.1 B and C). Eosinophils, which are surprisingly abundant in the thymus, and neutrophils, which are more rare, expressed very little MCH II or CD86 (Figure 3.1 B and C). In light of the relative MHC II and co-stimulatory molecule expression by these different APC subsets, we devised strategies to selectively deplete the APC subsets with the best antigen presenting potential (Figure 3.2C). There is currently no way to test a specific role for SIRPα^+ cDC2s in mediating thymocyte negative selection due to lack of available depletion models. We therefore sought an alternative strategy by selectively targeting a subset of SIRPα^+ cDC2s, which express the surface lectin, CD301b (macrophage galactose N-acetyl-galactosamine specific lectin 2; MGL2$^{DTR\text{-}eGFP}$) (138).

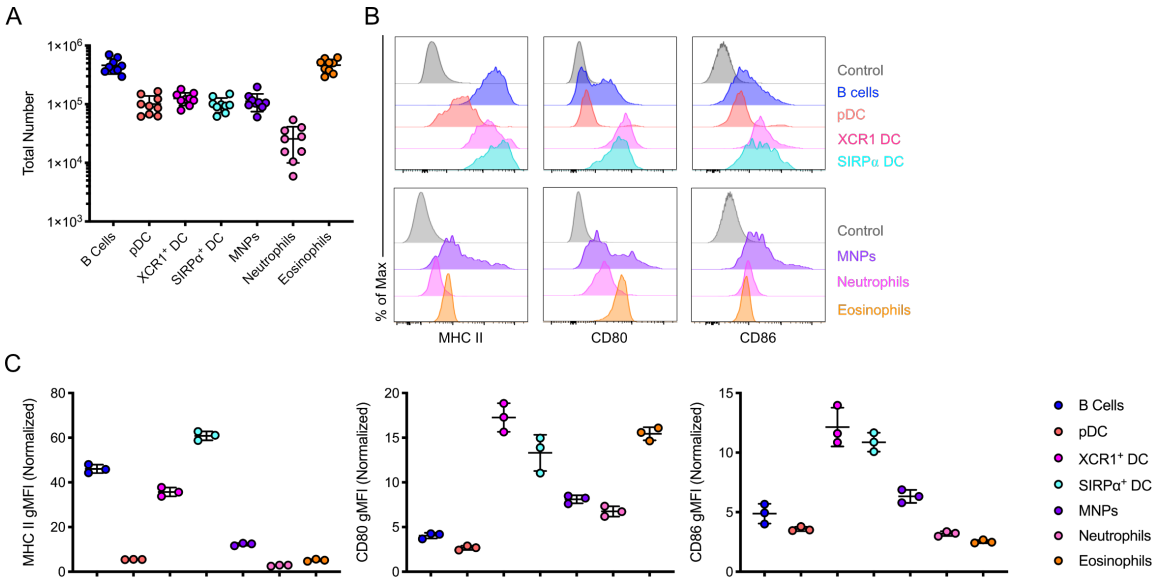

Figure 3.1. Enumeration of thymic APC subsets.

(A) Numbers of antigen presenting cell subsets (gated as in Supplementary Figure 1A, B) in 8-week-old mice. (B) Representative flow cytometry histograms showing expression of MHC II (left), CD80 (middle), and CD86 (right) by the indicated antigen presenting cell subset (gated as in Figure 3.2 A, B). (C) MHC II (left), CD80 (middle), and CD86 (right) gMFI (normalized to controls) of antigen presenting cell subsets. Each symbol (A, C) represents an individual mouse. Eight to nine-week-old female mice were used. Small horizontal lines indicate the mean, and error bars represent SEM. Data are pooled from three (A) or one (C) independent experiments or are representative of at least three independent experiments (B).

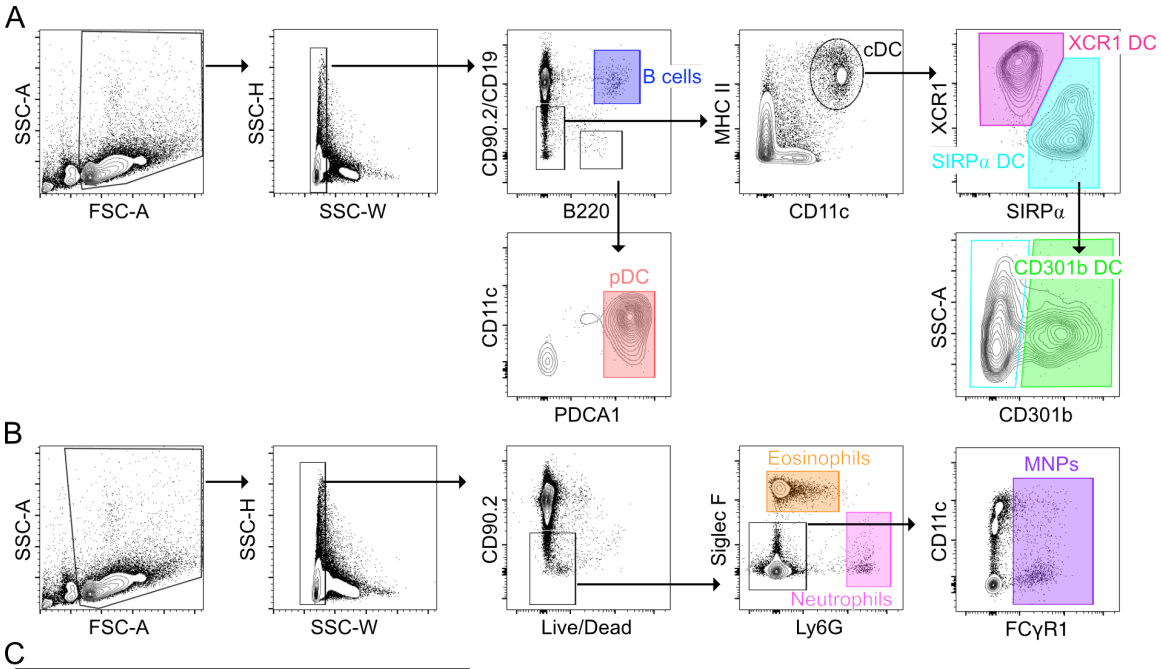

C

Strategy for targeting APC subsets

APC subset	Mouse strain
B cells	$Mb1^{Cre+/+}$
pDC	$BDCA2^{DTR}$
XCR1 DC	$BATF3^{-/-}$
SIRPα DC	$MGL2^{DTR\text{-}eGFP}$
MNPs	$LysM^{Cre+/-}$ x $IAb^{fl/fl}$

Figure 3.2. Comprehensive gating strategy to identify thymic APC subsets.

(A) Flow cytometry gating strategy for identifying B cells and dendritic cell subsets. B cells were identified by the expression of CD19 and B220 (blue; top, middle). Plasmacytoid DC were identified by the expression of B220, CD11c, and PDCA-1 (CD317) (salmon; bottom, middle). Conventional dendritic cells were identified by the expression of MHC II and CD11c (top, middle right). cDC1 were identified by the expression of XCR1 (magenta) and cDC2 identified by the expression of SIRPα (teal; top, right). $CD301b^{+}$ cDC2 were identified by the expression of CD301b (green; bottom, right). (B) Flow cytometry gating strategy for identifying eosinophils, neutrophils, and MNPs. Eosinophils were identified by the expression of Siglec F (orange) and neutrophils were identified by the expression of Ly6G (1A8) (pink; middle right). MNPs were identified by the expression of FcγR1 (CD64) (purple; right). (C) Mouse strains utilized to target each APC subset. Data are representative of more than 10 independent experiments (A, B).

3.2.2 CD301b is expressed by a large proportion of SIRPα cDC in the thymus

To determine if MGL2$^{DTR\text{-}eGFP}$ mice could be used as a model to selectively deplete a proportion of thymic SIRPα^+ cDC2, we first evaluated the expression of CD301b on SIRPα^+ cDC2. As previously reported, CD301b was expressed by a subset of SIRPα^+ cDC2 in the skin draining lymph nodes (sdLN), but not the spleen (Figure 3.3A and B) (138, 139). Surprisingly, an even larger proportion (~45%) of SIRPα^+ cDC2 expressed CD301b in the thymus (Figure 3.3A and B). It has been shown that CD301b$^+$ dermal dendritic cells mediate type 2 immune responses (138, 140–142). To determine if thymic CD301b$^+$ cDC2 were responsive to type 2 cytokines, we analyzed the expression of CD301b on SIRPα^+ cDC2 in mice lacking IL-4 (IL-4 KO) or the shared receptor for IL-4 and IL-13 (IL-4Rα KO). In the absence of IL-4, the frequency of CD301b$^+$ SIRPα^+ cDC2 decreased by half (Figure 3.3C and D). And in the absence of IL-4R, they were completely absent, suggesting that thymic CD301b cDC2 require type 2 cytokines (Figure 3.3C and D). Because thymic invariant natural killer T (iNKT) cells are the primary source of thymic IL-4 in the steady state, we sought to determine if CD301b expression was dependent, at least in part, on IL-4 provided by iNKT cells. We therefore examined CD301b expression in mice lacking iNKT cells (CD1d KO). As expected, similar to IL-4 KO mice, the expression of CD301b on SIRPα^+ cDC2 was decreased by nearly half (Figure 3.3C and D).

Previous work from our lab demonstrated that there is an age-dependent skewing of iNKT subsets, in which NKT2 cells represent a higher proportion of iNKT subsets early in life, but decline in adulthood (143). This suggests that steady state IL-4

production in the thymus is highest early in life. It has also been shown that the proportion of SIRPα^+ cDC2 increases from birth to 4 weeks of age in NOD mice (73). To test if this temporal fluctuation in IL-4 production impacted CD301b expression by SIRPα^+ cDC2, we examined thymic APC in C57BL/6 mice at various ages (Figure 3.3E, Figure 3.4). CD301b on SIRPα^+ cDC2 was similar at all ages (Figure 3.3E). Consistent with previous reports, there was a modest increase in SIRPα^+ cDC2 with age (Figure 3.4C) (73). Accordingly, the frequency of CD301b$^+$ SIRPα^+ cDC2 increased with age as well (Figure 3.3D).

Because IL-4-producing NKT2 are concentrated within the thymus medulla (12; data not shown), we sought to determine the localization of CD301b-expressing cells. Indeed, CD301b expression in the thymus was localized primarily within the thymus medulla (Figure 3.3F), further supporting the notion that thymic NKT2 support this subset of cDC.

Previous studies suggested that XCR1$^+$ cDC1 are tissue resident, whereas SIRPα^+ cDC2 can circulate (57). To gain insight into what fraction of CD301b$^+$ SIRPα^+ cDC2 circulate, we generated parabiotic mice, which through the joining of vasculature share blood circulation (Figure 3.3G). Congenically distinct CD45.1$^+$ and CD45.2$^+$ mice were surgically conjoined for 30 days. Consistent with known circulation patterns, naïve CD8 T cells equilibrated in parabiotic pairs (Figure 3.3H). >95% of XCR1$^+$ cDC1 were of host origin, verifying that this subset does not circulate (Figure 3.3H). However, ~90% of SIRPα^+ cDC2 were also of host origin, indicating that while this subset may be more migratory than XCR1$^+$ cDC1, SIRPα^+ cDC2 are predominately tissue resident (Figure 3.3H). There was no difference in circulation between CD301b$^-$ and CD301b$^+$ SIRPα^+ cDC2, suggesting that these subsets have similar migratory patterns (Figure 3.3H).

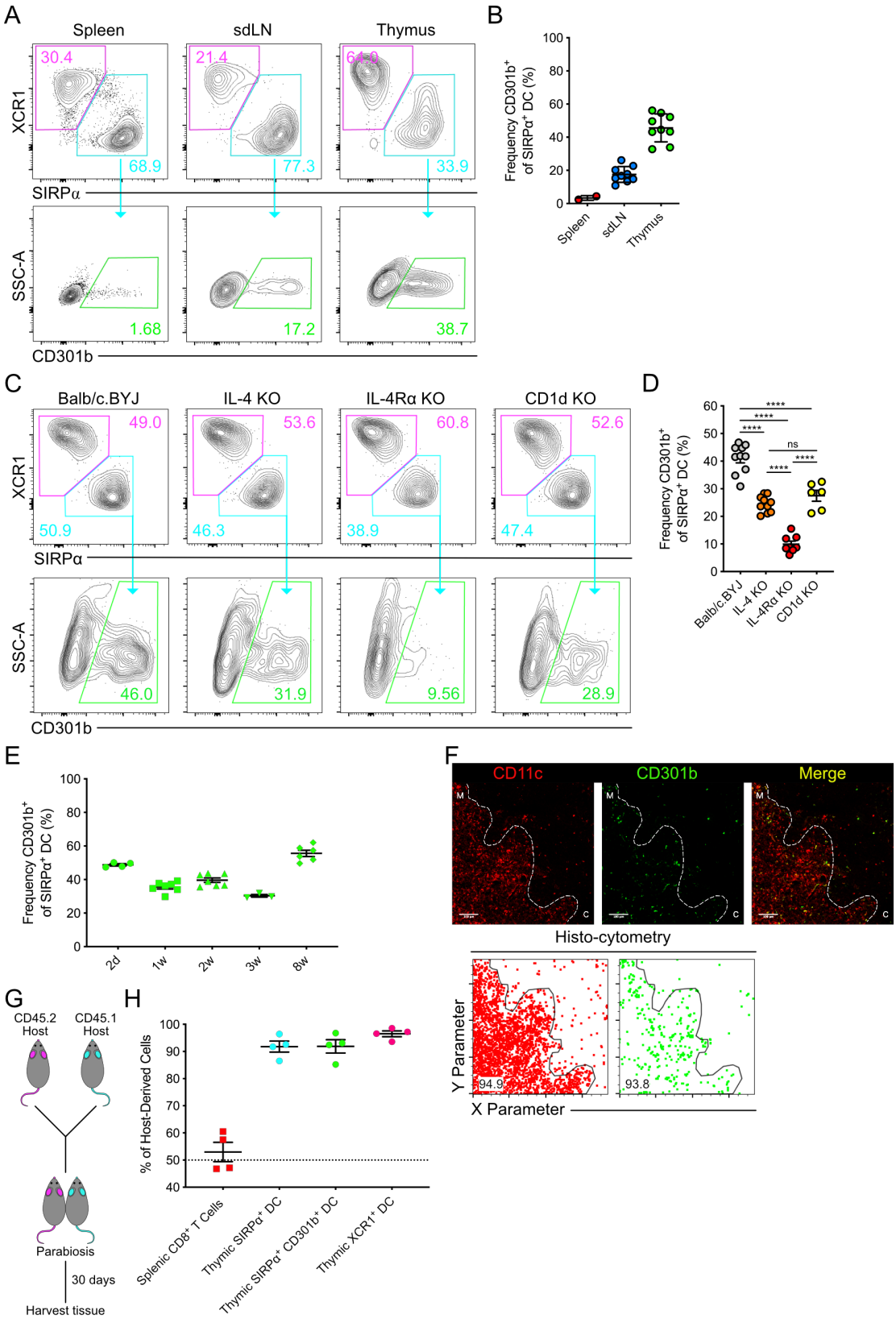
A
Spleen
sdLN
Thymus
30.4
21.4
64.9
68.9
77.3
33.9
XCR1
SIRPα
SSC-A
1.68
17.2
38.7
CD301b
B
Frequency CD301b+ of SIRPα+ DC (%)
Spleen
sdLN
Thymus
C
Balb/c.BYJ
IL-4 KO
IL-4Rα KO
CD1d KO
49.0
53.6
60.8
52.6
50.9
46.3
38.9
47.4
46.0
31.9
9.56
28.9
D
****
ns
Balb/c.BYJ
IL-4 KO
IL-4Rα KO
CD1d KO
E
Frequency CD301b+ of SIRPα+ DC (%)
2d
1w
2w
3w
8w
F
CD11c
CD301b
Merge
Histo-cytometry
Y Parameter
X Parameter
94.9
93.8
G
CD45.2 Host
CD45.1 Host
Parabiosis
30 days
Harvest tissue
H
% of Host-Derived Cells
Splenic CD8+ T Cells
Thymic SIRPα+ DC
Thymic SIRPα+ CD301b+ DC
Thymic XCR1+ DC

Figure 3.3. CD301b+ SIRPα+ DC were enriched in the thymus compared to peripheral SLO and localized in the thymus medulla.

(A) Representative flow cytometry of XCR1$^+$ and SIRPα$^+$ cDC (top) and CD301b$^+$ DC (bottom) from spleen (bottom), pooled sdLN (middle), and thymus (right) from C57BL/6 mice. Numbers adjacent to outlined areas represent percent cells in each. (B) Frequency of CD301b$^+$ among SIRPα$^+$ DC in spleen, sdLN, and thymus from C57BL/6 mice. (C) Representative flow cytometry of XCR1$^+$ and SIRPα$^+$ cDC (top) and CD301b$^+$ DC (bottom) from Balb/c.BYJ (left), IL-4 KO (middle left), IL-4Rα KO (middle right), and CD1d KO (right) mice. Numbers adjacent to outlined areas represent percent cells in each. (D) Frequency of thymic CD301b$^+$ among SIRPα$^+$ cDC2 in Balb/c.BYJ, IL-4 KO, IL-4Rα KO, and CD1d KO mice. (E) Frequency of thymic CD301b$^+$ among SIRPα$^+$ DC in 2d, 1w, 2w, 3w, and 8w-old C57BL/6 mice. (F) Immunofluorescence microscopy (top) of thymic sections from C57BL/6 mice stained for CD11c (red) and CD301b (green). White dashed lines indicate cortical-medullary border based on UEA I staining (not shown). C, cortex; M, medulla. Scale bars 100μm. Analysis of images by histo-cytometry (bottom, left). Dots represent localization of each stain as determined by histo-cytometry. Frequency of CD301b$^+$ cells identified as localized in the cortex by histo-cytometry (bottom, right). Numbers indicate percent cells in each outlined area. (G) Experimental strategy for generating parabiotic mice. (H) Frequency of cells derived from the host parabiont amongst splenic CD8 T cells, thymic SIRPα$^+$ cDC2, thymic CD301b$^+$ cDC2, or thymic XCR1$^+$ cDC1. Each symbol (B, D, E, H) represents an individual mouse. Six to twelve-week-old male and female mice were used. Small horizontal lines indicate the mean and error bars represent SEM. Data are representative of at least three independent experiments (A, C, F), pooled from at least three independent experiments (B, D), pooled from one or two independent experiments (E), or are from one experiment (H).

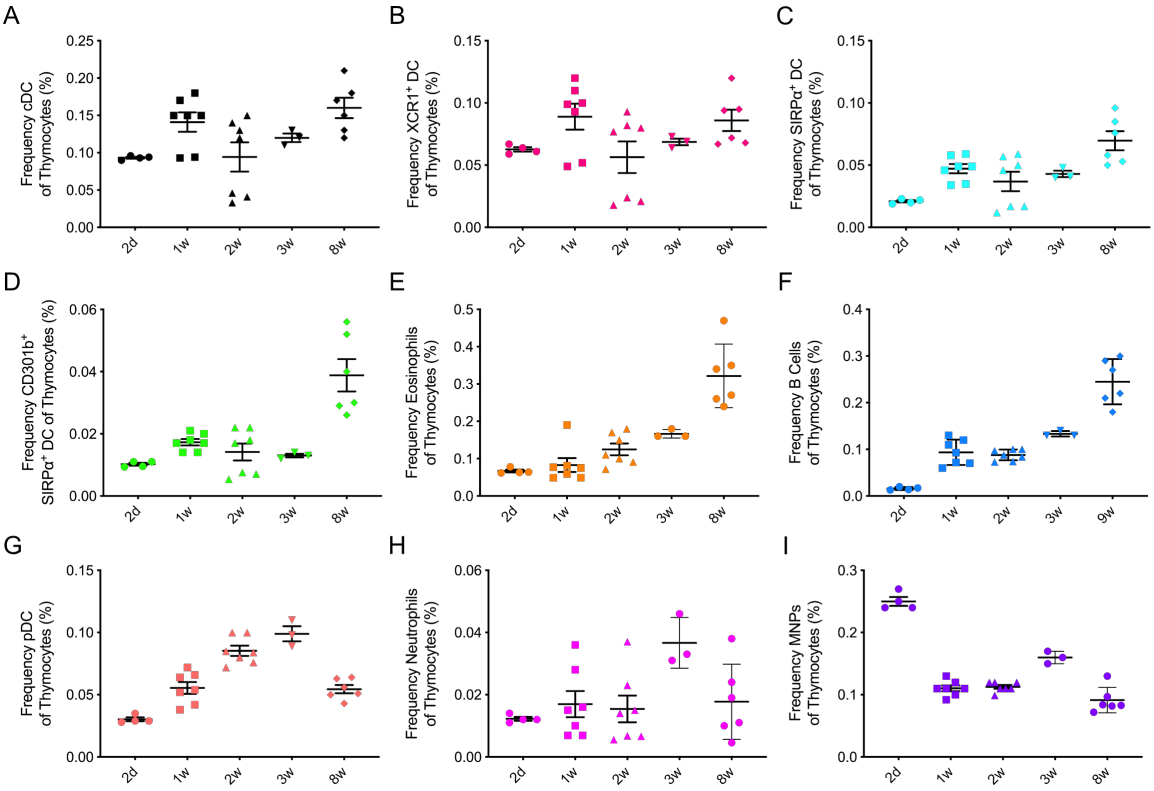

Figure 3.4. Ontogeny of thymic APC subsets.

(A-I) Frequency of thymic APC subsets (as indicated) among total lymphocytes in 2d, 1w, 2w, 3w, and 8w-old C57BL/6 mice (as in Supplementary Figure 1A, B). Each symbol represents an individual mouse. Male and female mice were used. Small horizontal lines indicate the mean and error bars represent SEM. Data are pooled from one, two, or three independent experiments.

3.2.3 Distinguishing APC influence on nascent Treg generation

Previous studies have suggested distinct roles for various APC subsets in mediating the differentiation of Treg (112), however these studies did not distinguish between nascent Treg undergoing selection in the thymus and recirculating Treg. Because about half of $CD25^{+}FOXP3^{+}$ mature Treg (mTreg) (Figure 3.5A) represent recirculating cells (110) (Figure 3.5B), we sought to identify cell surface markers to distinguish nascent from recirculating mTreg. To differentiate nascent and recirculating cells, we first utilized $RAG2^{GFP}$ mice, in which GFP decay acts as a "molecular timer" from positive selection (110). In line with a recent study, CD73 in combination with various markers (CD44, CCR7, and neuropilin 1 (NRP1)) could distinguish between nascent and recirculating mTreg (Figure 3.5C) (144, 145). Over 90% of $CD73^{-}$ mTreg were $RAG2^{GFP+}$ and over 85% of $CD73^{+}$ mTreg were $RAG2^{GFP-}$ (Figure 3.6A). Further analysis revealed that CD73 in combination with CD44, CCR7, or NRP1 could ideally distinguish between nascent and recirculating $CD4^{+}$ T cells in the thymus (Figure 3.6B and C).

To determine the individual contribution of distinct APC subsets to the generation of mTreg, we evaluated the thymic development of mTreg in mice with selective APC deficiencies (Figure 3.2C). These strategies showed >85% depletion efficiency (Figure 3.7). We also examined AIRE-deficient (AIRE KO) animals, which had a 50% reduction in mTreg (Figure 3.5 D), as previously reported. Also consistent with previous reports, animals lacking B cells had a reduction in mTreg (Figure 3. 5 D) (86, 95). The mTreg pool was not affected in the absence of any of the three individual DC subsets or in mice lacking MHC II on MNPs (Figure 3.5 D). We chose to selectively knockout MHC II on MNPs in contrast to selective depletion because the thymus atrophies acutely in mice

after diphtheria toxin depletion in LysM^{Cre}-*Csf1r*$^{LsL\text{-}DTR}$ mice (data not shown) (146). To broaden our analysis, we evaluated nascent and recirculating mTreg in these animals. AIRE KO animals had a reduction in both nascent and recirculating mTreg (Figure 3.5E), suggesting that AIRE directly influences the size of the mTreg pool selected. However, B cell KO mice only had a reduction in recirculating mTreg, indicating that B cells do not affect the size of the selected Treg pool in the thymus, but that B cells may be important for the maintenance or trafficking of mTreg in the periphery (Figure 3.5F) (147). Neither the DC subsets nor MNPs impacted the size of the nascent or recirculating mTreg pool (Figure 3.8).

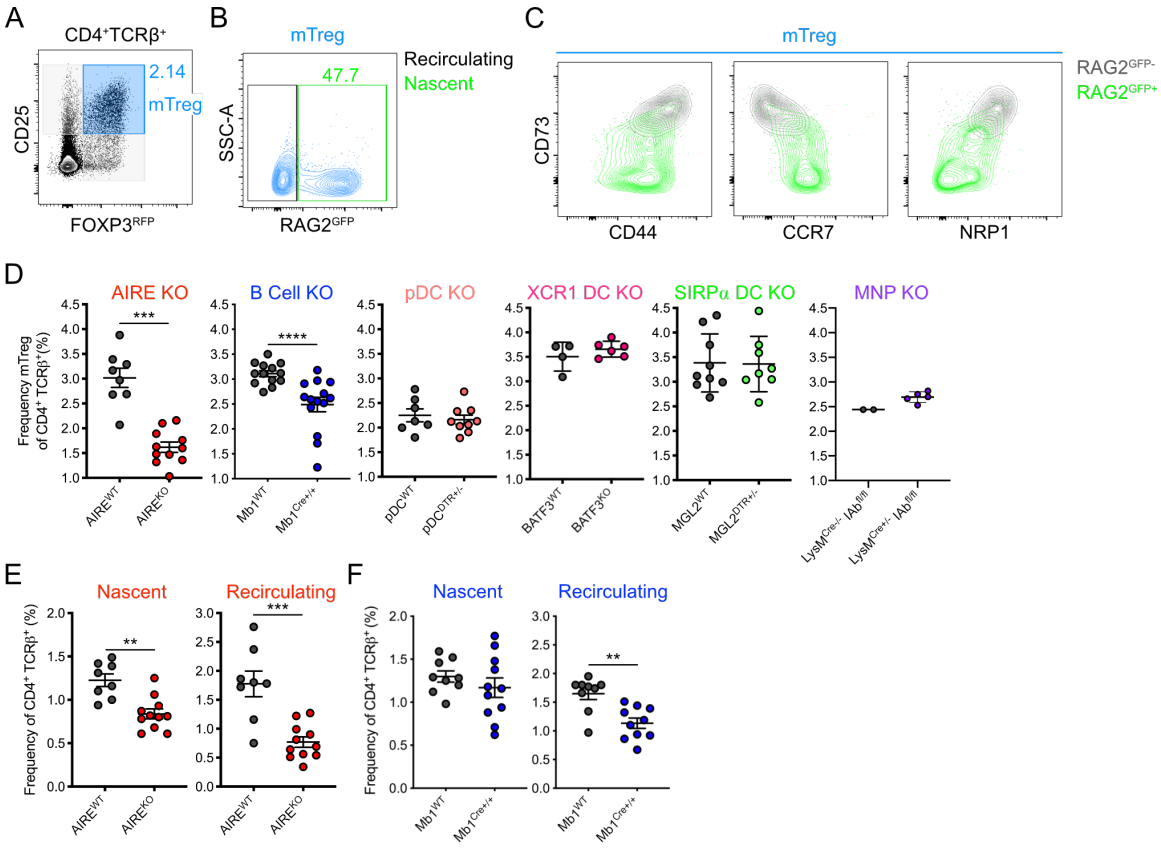

Figure 3.5. Individual APC subset deficiency did not impact the size of the nascent mTreg pool.

(A) Flow cytometry gating strategy for identifying mature Treg. (B) Flow cytometry of mature Treg from RAG2^{GFP} mice. Recirculating mTreg were identified as GFP^{-} (black outline) and nascent mTreg are GFP^{+} (green outline). Numbers adjacent to outlined areas indicate percent cells in each. (C) Surface staining of CD73, CD44, CCR7, and NRP1 on RAG2^{GFP-} (recirculating; gray) or RAG2^{GFP+} (nascent; green) mTreg (as gated in Figure 3.5A). (D) Frequency of mTreg among TCRβ^{+} CD4 T cells (as gated in Figure 2A) in mice with selective APC deficiencies (as labeled). (E) Frequency of nascent (left) or recirculating (right) mTreg among TCRβ^{+} CD4 T cells in AIRE^{WT} or AIRE^{KO} mice, based on expression of CD73 and CD44 (as in Figure 3.6A; top left). (F) Frequency of nascent (left) or recirculating (right) mTreg among TCRβ^{+} CD4 T cells in Mb1^{WT} or Mb1$^{Cre+/+}$ mice, based on expression of CD73 and CD44 (as in Figure 3.6A; top left). Each symbol (D, E, F) represents an individual mouse. Six to twelve-week-old male and female mice were used. Small horizontal lines indicate the mean and error bars represent SEM. **P< 0.01, ***P< 0.001, ****P< 0.0001. Statistical significance was determined by Mann-Whitney test (D, E, F). Data were pooled from at least three independent experiments (D, E, F) or are representative of at least three independent experiments (A, B, C).

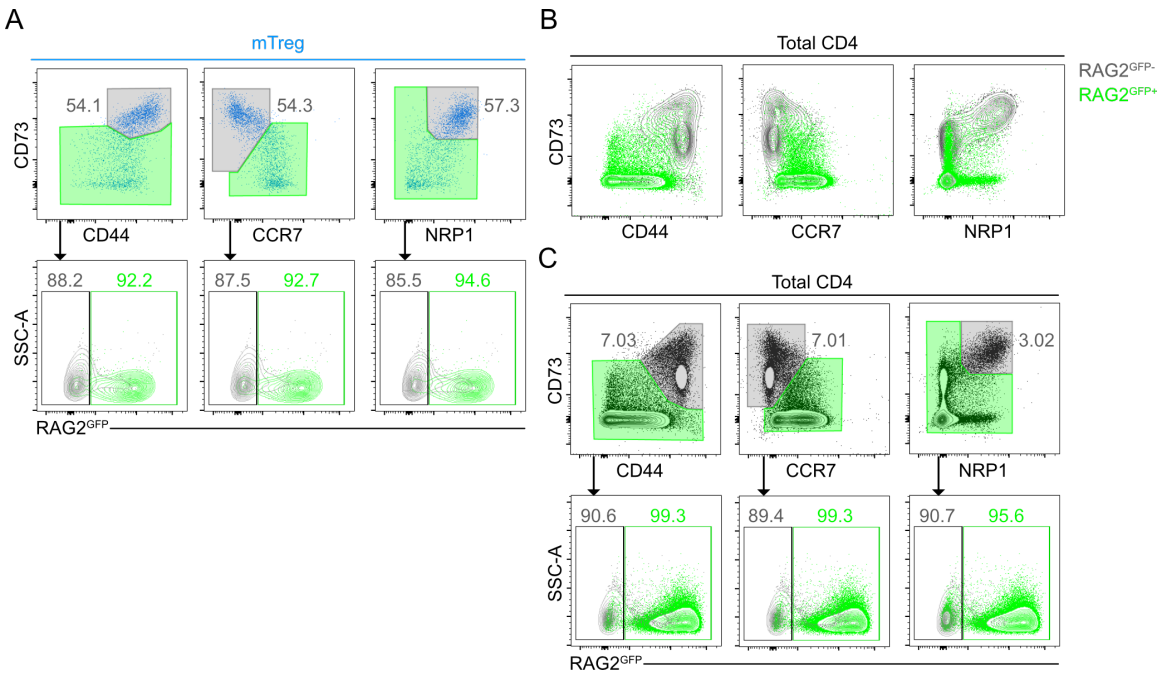

Figure 3.6. Identifying nascent and recirculating CD4 T cells.

(A) Gating strategy for identifying recirculating (gray) and nascent (green) mTreg based on CD73, CD44, CCR7, and NRP1 expression (top) and GFP expression ($RAG2^{GFP}$) of the indicated gate (bottom). Numbers adjacent to the outlined areas represent percent cells that are GFP^- (gray) or GFP^+ (green) from the correlating gates (top). (B) Surface staining of CD73, CD44, CCR7, and NRP1 on $RAG2^{GFP-}$ (recirculating; black) or $RAG2^{GFP+}$ (nascent; green) $TCR\beta^+$ CD4 T cells. (C) Gating strategy for identifying recirculating (gray) and nascent (green) $TCR\beta^+$ CD4 T cells based on CD73, CD44, CCR7, and NRP1 expression (top) and GFP expression ($RAG2^{GFP}$) of the indicated gate (bottom). Numbers adjacent to the outlined areas represent percent cells that are GFP^- (gray) or GFP^+ (green) from the correlating gates (top). Six to twelve-week-old male and female mice were used. Data are representative of at least three independent experiments.

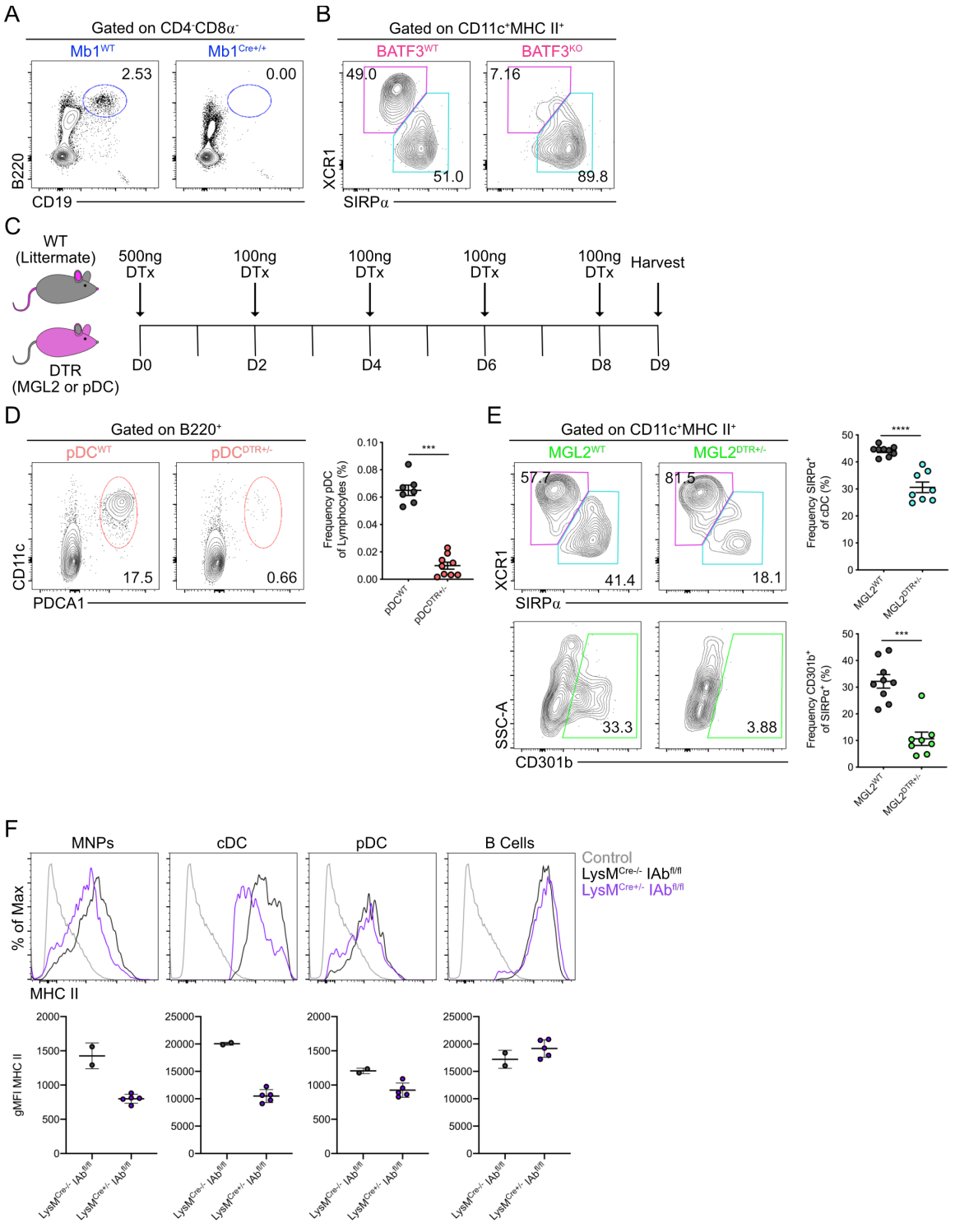
A
Gated on CD4-CD8α-
Mb1WT
Mb1Cre+/+
2.53
0.00
B220
CD19
B
Gated on CD11c+MHC II+
BATF3WT
BATF3KO
49.0
51.0
7.16
89.8
XCR1
SIRPα
C
WT
(Littermate)
DTR
(MGL2 or pDC)
500ng DTx
100ng DTx
100ng DTx
100ng DTx
100ng DTx
Harvest
D0
D2
D4
D6
D8
D9
D
Gated on B220+
pDCWT
pDCDTR+/-
17.5
0.66
CD11c
PDCA1
Frequency pDC of Lymphocytes (%)
***
pDCWT
pDCDTR+/-
E
Gated on CD11c+MHC II+
MGL2WT
MGL2DTR+/-
57.7
41.4
81.5
18.1
XCR1
SIRPα
Frequency SIRPα+ of cDC (%)
****
MGL2WT
MGL2DTR+/-
33.3
3.88
SSC-A
CD301b
Frequency CD301b+ of SIRPα+ (%)
***
MGL2WT
MGL2DTR+/-
F
MNPs
cDC
pDC
B Cells
Control
LysMCre-/- IAbfl/fl
LysMCre+/- IAbfl/fl
% of Max
MHC II
gMFI MHC II
LysMCre-/- IAbfl/fl
LysMCre+/- IAbfl/fl

Figure 3.7. APC subset depletion efficiency.

(A) Representative flow cytometry plots of $B220^{+}CD19^{+}$ B cells from $Mb1^{WT}$ (left) and $Mb1^{Cre+/+}$ (right) mice. Numbers adjacent to outlined areas represent percent cells in each. (B) Representative flow cytometry plots of $XCR1^{+}$ and $SIRP\alpha^{+}$ DC from $BATF3^{WT}$ (left) and $BATF3^{KO}$ (right) mice. Numbers adjacent to outlined areas represent percent cells in each. (C) Experimental strategy for selective depletion of $CD301b^{+}$ DC ($MGL2^{DTR}$) or pDC ($BDCA2^{DTR}$). (D) Representative flow cytometry plots of $CD11c^{+}PDCA1^{+}$ pDC from diphtheria toxin treated pDC^{WT} (left) or $pDC^{DTR+/-}$ (middle) mice (Figure 3.7C), and frequency of pDC among lymphocytes after diphtheria toxin treatment (right). Numbers adjacent to outlined areas represent percent cells in each. (E) Representative flow cytometry plots of $XCR1^{+}$ and $SIRP\alpha^{+}$ DC from $MGL2^{WT}$ (top left) or $MGL2^{DTR+/-}$ (top middle) mice (as in Figure 3.2A) and frequency of $SIRP\alpha^{+}$ DC among cDC after diphtheria toxin treatment (top right). Representative flow cytometry plots of $CD301b^{+}$ $SIRP\alpha^{+}$ DC from $MGL2^{WT}$ (bottom left) or $MGL2^{DTR+/-}$ (bottom middle) mice (as in Figure 3.7C), and frequency of $CD301b^{+}$ among $SIRP\alpha^{+}$ DC after diphtheria toxin treatment (bottom right). Numbers adjacent to outlined areas represent percent cells in each. (F) Representative flow cytometry histograms showing expression of MHC II on thymic APC subsets (top) and MHC II gMFI (bottom) from littermate control or $LysM^{Cre+/-}$ $IAb^{fl/fl}$ mice. Each symbol (D, E, F) represents an individual mouse. Six to twelve-week-old male and female mice were used. Small horizontal lines indicate the mean and error bars represent SEM. ***$P< 0.001$, ****$P< 0.0001$. Statistical significance was determined by Mann-Whitney test (D, E). Data are representative of at least three independent experiments (A, B), or are pooled from three independent experiments (D, E), or one experiment (F).

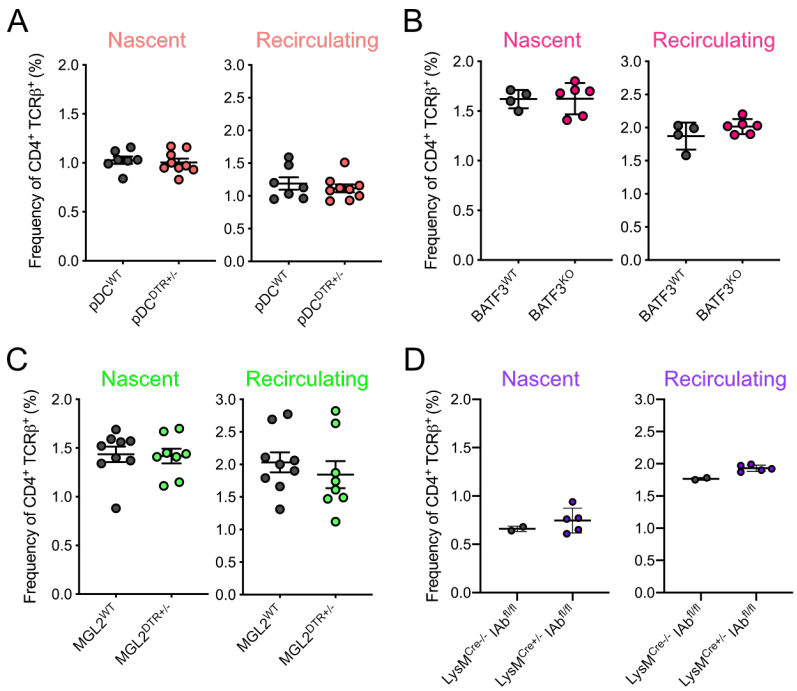

Figure 3.8. Nascent and recirculating Treg in APC deficient mice.

(A-D) Frequency of nascent (left) or recirculating (right) mTreg among TCRβ$^+$ CD4 T cells based on expression of CD73 and CD44 (as in Figure 3.6A; top left) in (A) pDC^{WT} or pDC$^{DTR+/-}$ mice (as in Supplementary Figure 5C, D), (B) BATF3^{WT} or BATF3^{KO} mice, (C) MGL2^{WT} or MGL2$^{DTR+/-}$ mice (as in Figure 3.7C, E), or (D) littermate control or LysM$^{Cre+/-}$IAb$^{fl/fl}$ mice. Each symbol represents an individual mouse. Six to twelve-week-old male and female mice were used. Small horizontal lines indicate the mean and error bars represent SEM. Statistical significance was determined by Mann-Whitney test. Data are pooled from two (A, B), three (C), or one independent experiments (D).

3.2.4 CD301b$^+$ SIRPα^+ cDC play a non-redundant role in mediating clonal deletion

While several APC subsets, including XCR1$^+$ cDC1, pDC, and B cells, have been shown to be capable of mediating clonal deletion, most of these studies utilized TCR transgenic models (112). To address this, we examined clonal deletion at the population level using a cleaved caspase 3-based assay in each APC-deficient strain (Figure 3.2C) (148). Total CD4 numbers in these strains were the same as their wild-type controls (Figure 3.9A). As expected, AIRE KO animals had a reduction (~33%) in clonal deletion of medullary CD4 T cells (Figure 3.10A; left). These animals also had a modest reduction in clonal deletion of cortical thymocytes (Figure 3.9B). We did not observe a distinct role for B cells, pDC, XCR1$^+$ cDC, or MNPs in mediating clonal deletion at the population level (Figure 3.10A). However, after a 10-day depletion of CD301b$^+$ SIRPα^+ cDC2 (Figure 3.7C), clonal deletion of medullary CD4 T cells was reduced by approximately 20%, suggesting a non-redundant role for CD301b$^+$ SIRPα^+ cDC2 in facilitating clonal deletion (Figure 3.10A; middle right). In line with the medullary localization of this CD301b$^+$ cDC2 subset, cortical clonal deletion was not affected (Figure 3.9B).

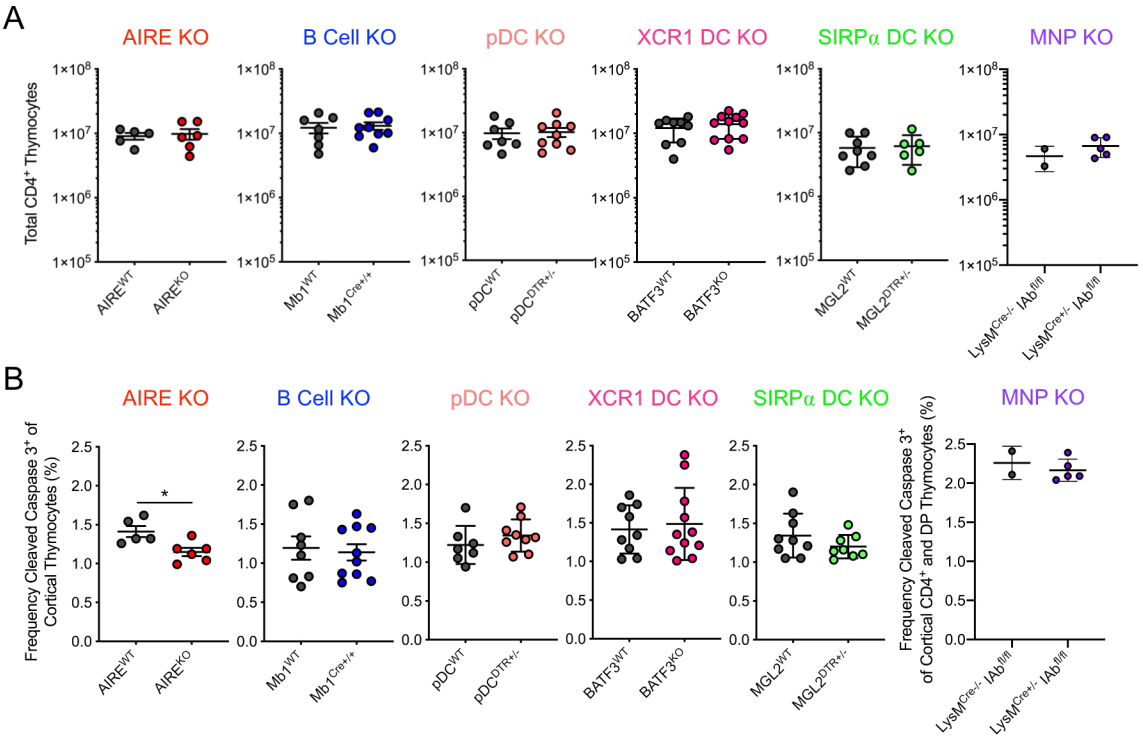

Figure 3.9. Enumeration of thymocytes and cortical clonal deletion in mice with selective APC deficiency.

(A) Total CD4 T cells in mice with selective APC deficiencies (as labeled). (B) Frequency of $CD5^+$ $TCR\beta^+$ cleaved caspase 3^+ thymocytes among DP T cells in mice with selective APC deficiencies (as labeled). Each symbol represents an individual mouse. Six to twelve-week-old male and female mice were used. Small horizontal lines indicate the mean and error bars represent SEM. *P< 0.05. Statistical significance was determined by Mann-Whitney test. Data are pooled from at least three independent experiments.

To further confirm that CD301b^{+} SIRPα^{+} cDC2 were capable of mediating clonal deletion, we utilized an eGFPp–I-A^{b} tetramer to detect CD4 T cells specific for the model self-antigen, eGFP (42). To test tolerance to eGFP, we immunized MGL2$^{DTR\text{-}eGFP}$ mice or WT littermate controls with eGFPp in complete freunds adjuvant (CFA). Magnetic enrichment for tetramer-bound cells from pooled secondary lymphoid organs was employed to directly measure total numbers of eGFPp–I-A^{b}–specific CD4 T cells. Immunized MGL2$^{DTR\text{-}eGFP}$ mice had fewer than 100 eGFPp–I-A^{b}–specific CD4 T cells (50-fold fewer than WT controls) (Figure 3.10B and C). Additionally, very few FOXP3^{+} Treg (Figure 3.10D and E) or CXCR5^{+} T follicular helper cells (Tfh) (Figure 3.10F and G) were observed in these mice. These numbers are suggestive of intrathymic deletion or "cluster 3 tolerance" proposed by Malhotra *et al.* (42). This is in contrast to the alternative tolerance mechanisms– ignorance (cluster 1) or partial clonal deletion with enhanced Treg potential (cluster 2) put forward by this group (42). Interestingly, only 8% of cDC were I-Ab^{+} eGFP^{+} in MGL2$^{DTR\text{-}eGFP}$ mice (Figure 3.11). This percentage was lower than those observed in other cluster 3 mouse strains (Itgax^{eYFP} and ACTB^{eGFP}) by Malhotra *et al.*, indicating that while the total number of APC presenting cell expressing a particular self-antigen may be important, the APC subset presenting the self-antigen may also play an critical role in determining the tolerance mechanism enforced (42).

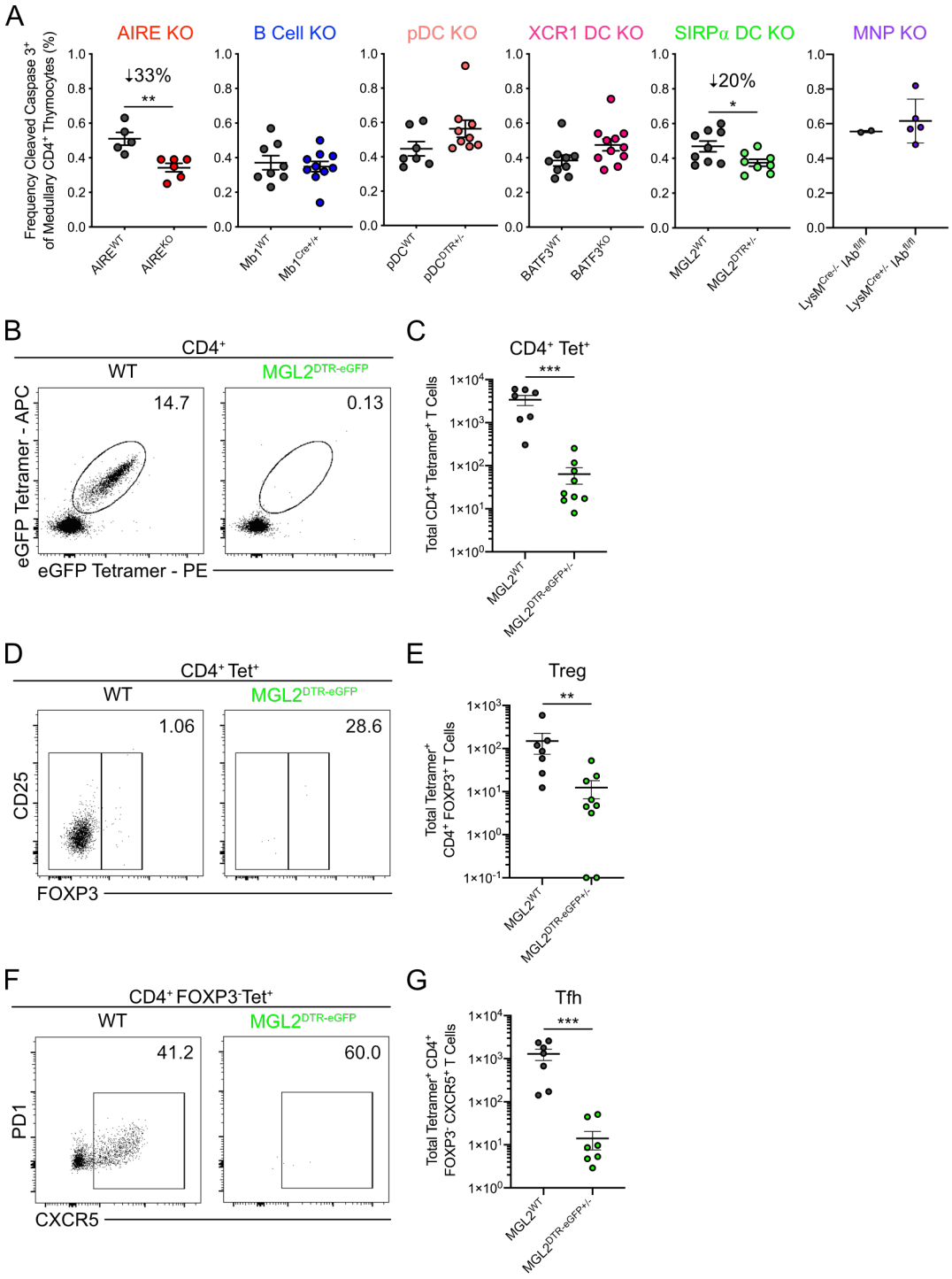
A
AIRE KO
B Cell KO
pDC KO
XCR1 DC KO
SIRPα DC KO
MNP KO
Frequency Cleaved Caspase 3+ of Medullary CD4+ Thymocytes (%)
↓33%
**
↓20%
*
AIRE^WT
AIRE^KO
Mb1^WT
Mb1^Cre+/+
pDC^WT
pDC^DTR+/-
BATF3^WT
BATF3^KO
MGL2^WT
MGL2^DTR+/-
LysM^Cre-/- IAb^fl/fl
LysM^Cre+/- IAb^fl/fl
B
CD4+
WT
MGL2^DTR-eGFP
14.7
0.13
eGFP Tetramer - APC
eGFP Tetramer - PE
C
CD4+ Tet+
***
Total CD4+ Tetramer+ T Cells
MGL2^WT
MGL2^DTR-eGFP+/-
D
CD4+ Tet+
WT
MGL2^DTR-eGFP
1.06
28.6
CD25
FOXP3
E
Treg
**
Total Tetramer+ CD4+ FOXP3+ T Cells
MGL2^WT
MGL2^DTR-eGFP+/-
F
CD4+ FOXP3- Tet+
WT
MGL2^DTR-eGFP
41.2
60.0
PD1
CXCR5
G
Tfh
***
Total Tetramer+ CD4+ FOXP3- CXCR5+ T Cells
MGL2^WT
MGL2^DTR-eGFP+/-

Figure 3.10. CD301b+ SIRPα+ cDC play a non-redundant role in clonal deletion.

(A) Frequency of $CD5^+$ $TCR\beta^+$ cleaved caspase 3^+ thymocytes among $CCR7^+$ CD4 T cells in mice with selective APC deficiencies (as labeled). (B) Representative flow cytometry analyzing eGFPp–IA^b–PE and eGFPp–IA^b–APC staining of tetramer-enriched CD4 T cells from pooled spleens and lymph nodes of $MGL2^{WT}$ and $MGL2^{DTR}$ 10 days after immunization with 100μg eGFPp emulsified with CFA. (C) Total eGFPp–IA^b–tetramer-binding CD4 T cells (as in Figure 3B). (D) Representative flow cytometry of CD25 and FOXP3 expression among eGFPp–IA^b–tetramer-binding CD4 T cells identified in B. (E) Total $FOXP3^+$ cells among eGFPp–IA^b–tetramer-binding CD4 T cells. (F) Representative flow cytometry of PD1 and CXCR5 expression among eGFPp–IA^b–tetramer-binding CD4 T cells identified in B. (E) Total $CXCR5^+$ cells among eGFPp–IA^b–tetramer-binding CD4 T cells. Each symbol (A, C, E, G) represents an individual mouse. Six to twelve-week-old male and female mice were used. Small horizontal lines indicate the mean and error bars represent SEM. **P*< 0.05, ***P*< 0.01, ****P*< 0.001. Statistical significance was determined by Mann-Whitney test (A, C, E, G). Data are pooled from at least three independent experiments.

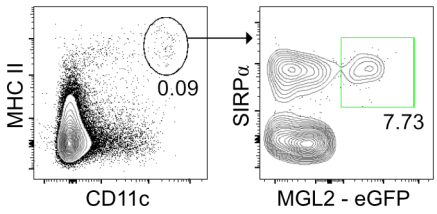

Figure 3.11. eGFP expression by cDC in MGL2DTR-eGFP mice.

(A) Representative flow cytometry of MHC II^+ $CD11c^+$ cDC (left) and MGL2-eGFP expression on $SIRP\alpha^+$ cDC (right). Numbers adjacent to outlined areas represent percent cells in each. Six to twelve-week-old male and female mice were used. Data are representative of at least three independent experiments.

3.3 Discussion

Developing thymocytes encounter self-peptide–MHC on an assortment of APCs with distinct functional capabilities in order to generate self-tolerance. Although a number of previous studies demonstrated contributions of each subset to clonal deletion or Treg cell differentiation, the relative extent to which each APC enforces these self-tolerance mechanisms remained unclear. Here, we took a comprehensive approach to investigate the role of distinct APC subsets to clonal deletion or Treg cell generation at the population level.

While no studies collectively enumerated the different bone marrow-derived APC in the thymus, our analysis is in line with previous estimates of the relative proportion of these subsets. The three DC subsets– XCR1$^+$ cDC1, SIRPα^+ cDC2, and pDC– were equally represented in the thymus (1, 57, 65), each constituting approximately 1x10^5 cells in an adult C57BL/6 mouse. B cells were similarly proportionate compared to the combined DC subsets (1), totaling 4x10^5 cells. The other myeloid subsets are less well described in the thymus. Surprisingly, eosinophils were quite abundant, comprising 5x10^5 cells, a proportion equal to that of B cells. MNPs represented a fraction similar to that of the individual DC subsets (1x10^5 cells), while neutrophils constituted only one-sixth of these populations.

Previous work from our group and others demonstrated that both MHC II and co-stimulatory molecule expression are critical for Treg development and clonal deletion (44, 45, 113, 115–117, 125, 137). Here, we showed that the cDC subsets and B cells in the thymus are particularly well equipped to promote tolerance via these mechanisms because of their high MHC II and co-stimulatory molecule expression. In contrast, eosinophils, while abundant did not express MHCII or co-stimulatory molecules.

Combined, the relative proportion and antigen presenting capabilities of particular subsets suggests that they could be superior at enforcing central tolerance when compared to other thymic APC.

The role of AIRE in mediating Treg cell differentiation at the population level has been somewhat controversial. It was initially reported that there is no defect in Treg cell development in adult AIRE-deficient mice (32, 40, 149), however others have demonstrated a nearly 50% defect in adult and particularly in neonatal mice (49, 59). Additionally, analysis of the Treg cell TCRα repertoire in AIRE-deficient mice showed clear differences, revealing that AIRE plays a critical role in selecting the Treg cell repertoire (45, 51). Here, we report a 50% reduction in the frequency of both nascent and recirculating mTreg cells in the thymus of AIRE deficient adult mice. While the reasons for these conflicting reports are unclear, the defect that we observed may be due to our analysis of collectively younger adult mice (49, 52).

It is assumed that clonal deletion is a major mechanism by which AIRE enforces central tolerance. Several landmark studies showed that mTECs can facilitate clonal deletion of TRA-specific TCR transgenic thymocytes (40, 41). More recently, through the use of tetramer enrichment, it was shown that polyclonal TRA-specific T cells were modestly increased in the absence of AIRE (42). Indeed, we observed a 33% reduction in medullary $CD4^+$ thymocytes undergoing clonal deletion in AIRE-deficient mice compared to their WT counterparts. Surprisingly, we also noted a mild defect in cortical ($CCR7^-$ thymocyte) clonal deletion in mice lacking AIRE. This suggests that some thymocytes may contact $MHCII^+$ mTEC, cDC1, or B cells (the major APC that present AIRE dependent self-antigens) prior to expression of CCR7, although further work would be required to test this definitively.

We showed that while B cell deficiency certainly impacts the size of the mTreg cell pool, B cells may not have as great an impact on nascent mTreg cell development as previously thought (86, 95). Using CD73 in combination with CD44 to identify recirculating mTreg cells, we demonstrated that systemic B cell deficiency primarily impacted the recirculating mTreg cell pool in the thymus. Because recirculating mTreg cells represent nearly 50% of the total thymic mTreg cells (110), this population may have skewed the findings in previous studies (86, 95). Interestingly, Ray *et al.* found that GITR-GITRL signaling in between T and B cells in peripheral lymphoid organs was required for peripheral Treg cell maintenance (147), which may explain our findings here. While several studies showed that B cells are capable of mediating clonal deletion either using endogenous superantigens or TCR transgenic models (85, 87, 89, 91, 92), we did not identify a non-redundant role for B cells in mediating clonal deletion at the population size level. However, this does not rule out that thymic B cell deficiency may have altered the Treg cell TCR repertoire.

pDC, XCR1$^+$ cDC1, and MNPs were dispensable for both mTreg cell development and clonal deletion at the population size level as well. pDC are capable of promoting Treg cell differentiation *in vitro* (81), however their role in Treg cell development *in vivo* was unclear. OVA-loaded pDC were shown to mediate clonal deletion, but not Treg cell development, of OT-II thymocytes. However, this model system may reflect the high-affinity TCR–pMHC interaction more than a physiologic role for pDC in mediating central tolerance. Our findings that XCR1$^+$ cDC1 do not impact Treg cell differentiation or clonal deletion are in line with previous work that demonstrated that BATF3-deficient mice had a modest increase in the proportion of thymic Treg cells and no difference in the Treg cell TCR repertoire (80). This group also

used deep TCR sequencing to determine that XCR1$^+$ cDC1 do not mediate clonal deletion of CD8$^+$ thymocytes (71). Thymic MNPs are critical for clearing apoptotic debris (150, 151), however whether they contribute to thymocyte negative selection remained unclear. Here, we did not find a non-redundant role for MNPs in mediating either clonal deletion or mTreg cell differentiation. More work will be necessary to determine how thymic MNPs impact the TCR repertoire. Collectively, our findings suggest functional redundancy for pDC, XCR1$^+$ cDC1, and MNPs in mediating central tolerance at least at the population size level.

Alternatively, our results did establish a non-redundant role for SIRPα^+ cDC2 in clonal deletion at the population size level. Although there is currently no method to selectively target all SIRPα^+ cDC2, we found that nearly half of thymic SIRPα^+ cDC2 express CD301b, which could be depleted using MGL2$^{DTR\text{-}eGFP}$ mice (138). Depletion of CD301b$^+$ SIRPα^+ cDC2 led to a 20% reduction in the size of the clonal deleted population. Why depleting this DC subset had a detectable effect, while depleting any other APC subset did not, is currently unclear. Interestingly, CD301b expression was enriched on thymic SIRPα^+ cDC2 compared to SIRPα^+ cDC2 in secondary lymphoid organs. We demonstrated that these CD301b-expressing SIRPα^+ cDC2 were dependent on the type 2 cytokine-enriched thymic environment that our group has shown is largely established by thymus tissue resident NKT2 cells that produce IL-4 at steady state (143). How these type 2 cytokine-dependent SIRPα^+ cDC2 differentially impact tolerance induction compared to other SIRPα^+ cDC2 will require development of additional tools (84). However, DC have been shown to be capable of mediating Treg cell selection in TCR transgenic models and *in vitro* (76, 78, 79), leaving the possibility that the remaining SIRPα^+ cDC2 in our system could promote Treg cell differentiation.

In summary, our comprehensive analysis of thymic APC and their ability to induce either clonal deletion or Treg cell differentiation provides insight into the differential tolerance mechanisms promoted by these subsets. AIRE unequivocally had the greatest relative impact on both Treg cell development and clonal deletion. However, we identified a subset of SIRPα^+ cDC2 that was dependent on type 2 cytokine signaling and played a non-redundant role in mediating clonal deletion. Given the profound impact of type 2 cytokines on this CD301b$^+$ SIRPα^+ cDC2 subset and the effect that this subset had enforcing central tolerance, it is interesting to consider the influence that a type 2 cytokine-enriched environment has on generating a self-tolerant TCR repertoire. Perhaps IL-4 and IL-13 impact the thymic APC peptidome to induce tolerance to type 2 cytokine-dependent processes in the periphery, such as wound healing and the inflammatory response to helminth infections (152). Whether the functional preference of this CD301b$^+$ SIRPα^+ cDC2 for clonal deletion is due to superior antigen presenting capability via increased MHC II and co-stimulatory molecule expression or a unique peptidome will be the work of future studies.

3.4 Materials and Methods

Mice

C57BL/6NCrl (B6) and B6.SJL-Ptprc^{a}Pepc^{b}/BoyCrl (B6.SJL) mice were purchased from Charles River Laboratories. C57BL/6Tg(Rag2-EGFP)1Mnz (Rag2^{GFP}) mice were described previously (110). B6.129S2-*Aire*$^{tm1.1Doi}$/J (AIRE KO), B6.C(Cg)-*Cd79a*$^{tm1(cre)Reth}$/EhobJ (Mb1^{Cre}), C57BL/6-Tg(CLEC4C-HBEGF)956Cln/J (pDC^{DTR}), B6.129S(C)-*Batf3*^{tm1Kmm}/J (BATF3 KO), B6(FVB)-*Mgl2*$^{tm1.1(HBEGF/EGFP)Aiwsk}$/J (MGL2^{DTR}), B6.129P2-*Lyz2*$^{tm1(cre)Ifo}$/J (LysM^{Cre}), B6.129X1-*H2-Ab1*^{tm1Koni}/J (IAb$^{fl/fl}$), BALB/cByJ, and C.129S2-*Cd1*^{tm1Gru}/J (CD1d KO) were purchased from Jackson Laboratories. BALB/c Il4tm1(CD2)Mmrs (IL-4 KO) and BALB/c Il4ratm1Fbb (IL-4Rα KO) were described previously (143). All animal experiments were approved by the Institutional Animal Care and Use Committee of the University of Minnesota. All animals were maintained under specific pathogen-free conditions at the University of Minnesota.

Parabiosis Surgery

Parabiosis surgeries were performed as previously described (153). Briefly, mice were anesthetized with ketamine. Flank hair was shaved and then further removed using Nair. Lateral incisions were made and mice were joined with interrupted horizontal mattress sutures with 5–0 NOVAFIL. Additional sutures were placed through the olecranon and knee joints to secure the legs. Parabiotic pairs were analyzed 30 days after surgeries.

Diphtheria Toxin Treatment

pDC^{DTR}, MGL2^{DTR}, and littermate control mice were injected intraperitoneally with diphtheria toxin every 48 hours for 9 days (5 injections in total). The first injection contained 500ng diphtheria toxin in 100μL PBS; the following injections contained 100ng diphtheria toxin in 100μL PBS. Mice were analyzed the day after the final injection.

Immunization

Mice were given subcutaneous and intraperitoneal injection of 100μL CFA emulsion (Sigma-Aldrich) containing 100μg peptide (described below) in DMSO split over two sites.

Tetramers and Cell Enrichment and Flow Cytometry

Biotin-labeled I-A^b monomers containing eGFP peptide (HDFFKSAMPEGYVQE) covalently linked to the I-A^b β-chain were purified and combined with streptavidin- PE or streptavidin- APC (Prozyme) to produce fluorescence-labeled I-A^b tetramers as described previously (42).

Single cell suspensions were prepared from pooled spleen and lymph nodes (inguinal, axillary, brachial, cervical, para-aortic, and mesenteric). Cells were stained for 1h at room temperature with PE- and APC-conjugated tetramers and anti-CXCR5 (2G8, BD). PE and APC MicroBeads (Miltinyi Biotec) and MACS separation columns (Miltinyi Biotec) were utilized for enrichment as previously described (154).

Single-cell suspensions were stained for 30 minutes at 4º C with the indicated antibodies (below). Staining for CCR7/CD197 (4B12; eBioscience) was performed for 30

minutes at 37ºC prior to additional surface stains. Cleaved caspase-3 (D3E9; Cell Signaling Technologies) staining was described previously (148).

For thymic APC populations, thymi were first injected with 500μL Collagenase D (1mg/mL; Roche), then finely chopped in 1mL Collagenase D, and incubated for 30 minutes at 37ºC. Single cell suspensions were then prepared and stained as indicated.

Samples were acquired with BD LSR Fortessa X-20 (BD Biosciences) and analyzed with FlowJo version X (FlowJo LLC).

Antibodies

Antibodies purchased from BioLegend: NK1.1 (PK136), CD11c (N418), CD19 (6D5), CD25 (PC61), TCRγ/δ (GL3), CD80 (16-10A1), CD64 (X54-5/7.1), CD45.1 (A20), CD45.2 (104), CD45R (B220; RA3-6B2), CD90.1 (OX-7), CD172a (SIRPα; P84), CD301b (MGL2; URA-1), CD317 (PDCA-1, BST2; 129C1), F4/80 (BM8), TCRβ (H57-597), XCR1 (ZET).

Antibodies purchased from BD Biosciences: CD4 (GK1.5), CD8a (53-6.7), CD69 (H1.2F3), H-2K^{b} (AF6-88.5), TCRβ (H57-597), CD86 (GL1), CD90.2 (30-H12), Siglec F (E50-2440).

Antibodies purchased from Thermo Fischer: CD5 (53-7.3), MHC Class II– I-A/I-E (M5/114.15.2), Ly6C (HK1.4).

Antibodies purchased from eBioscience: CD25 (PC61.5), FOXP3 (NRRF-30), Ly6C (HK1.4).

Immunofluorescence

Thymi were harvested and snap frozen in Optimal Cutting Temperature compound (Sakura Finetek). Tissue samples were sectioned into 7μm at -20ºC. Sections were then fixed and permeabilized in 100% acetone for 20 minutes at 4º C. Fixed sections were blocked with 5% bovine serum albumin (BSA) and Fc block (anti-CD16/CD32 (2.4G2, Tonbo Biosciences) for one hour at 20ºC. Antibodies were purchased from BD Biosciences: CD8α (53-6.7), CD11c (HL3), BioLegened: CD301b (MGL2; URA-1), and Vector Laboratories: Fluorescein labaled Ulex Europaeus Agglutinin I (UEAI). Sections were stained with an antibody cocktail in 0.5% BSA and 0.1% Tween-20 (Sigma Aldrich) overnight at 4º C. Following wash steps and DAPI staining, sections were mounted using Prolong anti-fade mounting medium (Life Technologies). Images were acquired using a Leica DM6000B epifluorescent microscope 16-72 hours later.

Histo-cytometry

Histo-cytometry was performed as previously described (134, 148). Briefly, fluorochrome intensities based on region of interest defined by DAPI staining were quantified and exported as .csv files using ImageJ. FlowJo version X (FlowJo LLC) was used for analysis.

Statistical Analysis

Statistical analyses were performed using Prism 8 (GraphPad). D'Agostino & Pearson test was used to assess normality. For comparison of two data sets, unpaired Student's *t* test or unpaired Mann-Whitney test were performed (based on normality results). For

comparison of three or more data sets, ordinary one-way ANOVA with Holm-Sidak's or Tukey's multiple comparisons test was used. P-values less than 0.05 were considered significant. Sample size, experimental replicates, and additional details are provided in the figure legends.

Chapter 4

Conclusions

The immune system is balanced between self-antigen-driven tolerance and pathogen-driven immunity. Thymic selection of the T cell repertoire (central tolerance) and deletion and anergy in lymphoid and non-lymphoid organs (peripheral tolerance) serve as mechanisms to maintain this balance. The importance that central tolerance plays in upholding this balance is highlighted by the transcriptional regulator, AIRE. AIRE functions by promoting promiscuous gene expression of tissue restricted antigens by B cells and mTECs in the thymus in order to generate a T cell repertoire that is tolerant to peripheral organs (40, 85, 135). Mutations in AIRE result in APECED (autoimmune polyendocrinopathy-candidiasis-ectodermal dystrophy; also known as autoimmune polyendocrine syndrome type 1, APS1), which is characterized by autoantibody production and lymphocytic infiltration in multiple organs (155, 156). While the role of AIRE underscores the importance of the self-tolerance generated in the thymus, there are numerous APCs that coordinate to enact this process as well. Many studies gained insight into how central tolerance is directed within the thymus, however the use of different model systems obscured our understanding of how this occurs within the polyclonal thymocyte pool. The aim of this thesis work was to gain better insight into how central tolerance, particularly clonal deletion and Treg cell differentiation, is orchestrated within the polyclonal population.

To better understand the developmental stages and corresponding anatomic locations at which thymocytes undergo clonal deletion within the polyclonal pool, we developed and validated a cleaved caspase-3 based assay to identify thymocytes undergoing clonal deletion. Because cleaved caspase-3 is expressed by all cells undergoing apoptosis, we utilized the activation markers, CD5 and TCRβ, to distinguish between thymocytes undergoing death by neglect and clonal deletion. Using CCR7 to

approximate the anatomic location at which thymocytes were undergoing clonal deletion, we verified previous estimates that the majority of clonal deletion occurs within the thymus cortex (67, 68, 70). In contrast to seminal work which suggested that only the least mature thymocytes undergo clonal deletion (108), we found that developing thymocytes continue to undergo clonal deletion even at their most mature stages of development in the thymus medulla (Figure 4.1). This suggests a model by which not all self-reactive thymocytes encounter their deleting antigen before thymic egress and supports previous studies which propose that central tolerance is an imperfect process (42, 55, 56, 103). It is interesting to consider that the time developing thymocytes spend navigating the thymus prior to egress may correlate to the efficiency of central tolerance. For example, one might predict that mice treated with FTY720, a functional agonist of S1PR1 (Sphingosine-1-phosphate receptor 1), to temporarily prevent thymocyte egress would have a less autoreactive TCR repertoire compared to untreated animals.

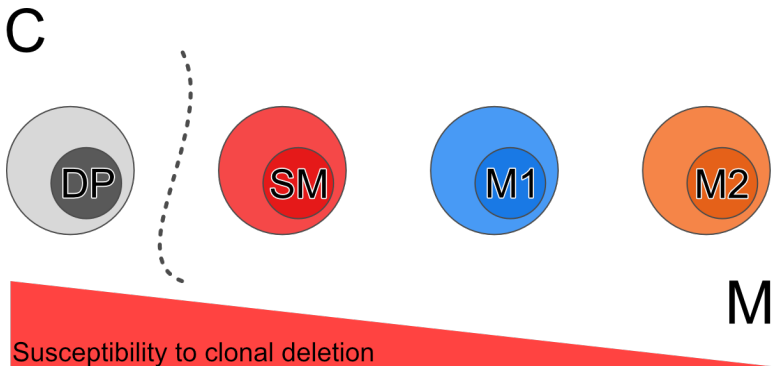

Figure 4.1. Model for susceptibility to clonal deletion during thymocyte maturation.

Double positive (DP) thymocytes localized in the thymus cortex (C) undergo clonal deletion at the greatest frequency. Thymocytes continue to undergo clonal deletion in the medulla (M) at each stage of development (semi-mature (SM); mature 1 (M1); and mature 2 (M2)), but become less susceptible as they mature.

We also examined how antigen presentation capability, namely MHC II and the co-stimulatory molecules, CD80 and CD86, impacted clonal deletion using this cleaved caspase-3 based assay. Our findings supported previous work that demonstrated a non-redundant role for MHC II on bone marrow-derived APCs in mediating clonal deletion (45). Importantly, we also found that CD28-mediated co-stimulation, the significance of which had been controversial (119, 126–128, 157), is critical for clonal deletion in both the thymus cortex and medulla. We further established a non-redundant role for CD86 in mediating clonal deletion in the thymus cortex, suggesting that cortical thymocytes may be more sensitive to co-stimulation-driven clonal deletion than those in the medulla. Future work examining the dose-dependent effect of co-stimulatory molecule expression on thymocyte differentiation and clonal deletion will be necessary to support this hypothesis.

We further explored these findings by more thoroughly examining the distinct APC subsets within the thymus. Given the different proportional representation, antigen-presenting capabilities, and distinct functional properties of these various thymic APCs, we hypothesized that APCs may have non-redundant roles in mediating central tolerance. B cells and the two cDC subsets (XCR1$^+$ cDC1 and SIRPα^+ cDC2) were the most highly represented bone marrow-derived APCs within the thymus and also expressed the highest levels of MHC II and co-stimulatory molecules. Using mice with cell-specific deficiencies, we examined the relative role that these APCs play in generating nascent mTreg cells and mediating clonal deletion.

Because nearly half of the mature Treg cells in the thymus are recirculating (110), we sought to identify makers to distinguish nascent from recirculating mTreg cells. We identified that CD73 in combination with CD44 could accurately identify both

recirculating mTreg and CD4 T cells. AIRE-deficient mice had a reduction in both nascent and recirculating mTreg cells, indicating that AIRE is critical to thymic mTreg cell differentiation. In contrast to previous studies that identified B cells as essential for mTreg cell development (86, 95), we found that nascent mTreg cell development in the absence of B cells was similar to WT mice. However, the recirculating mTreg cell pool was decreased in B cell-deficient animals, suggesting that previous findings may have been skewed by this recirculating population.

Since there is currently no tool to efficiently target SIRPα^+ cDC2, we sought an alternative method to deplete a substantial proportion of this population. We discovered that the thymus harbors a large fraction of CD301b-expressing SIRPα^+ cDC2. The proportion of these CD301b$^+$ SIRPα^+ cDC2 was much greater than that in the skin draining lymph nodes, where this population was originally described. Further investigation of this population revealed that the type 2 cytokine enriched environment in the thymus was required for this population. Without IL-4 and IL-13 signaling, CD301b-expressing SIRPα^+ cDC2 were absent from the thymus. Because thymic tissue resident NKT2 are the major source of IL-4 in the thymus, we hypothesized that NKT cells are required for a major proportion of CD301b-expessing SIRPα^+ cDC2. Indeed, the population of CD301b$^+$ SIRPα^+ cDC2 was reduced by half in the absence of NKT cells. Further enforcing the notion that the IL-4 produced by NKT2 cells supports this population, we determined that CD301b$^+$ SIRPα^+ cDC2 are localized primarily within the thymus medulla, where NKT2 are concentrated (Figure 4.2).

Using the cleaved caspase-3 assay we developed to quantify clonal deletion at the population level, we assessed the relative contribution of different APC subsets to clonal deletion. As expected, AIRE-deficient animals had a reduction in medullary clonal

deletion events. Interestingly, depletion of CD301b-expessing SIRPα^+ cDC2, also resulted in a modest reduction in medullary clonal deletion (Figure 4.2). We confirmed the findings of our cleaved caspase-3 assay by using tetramers to identify eGFP-specific CD4 T cells. Following immunization with eGFP peptide and CFA, we found that there were very few eGFP-specific CD4 T cells in MGL2$^{DTR\text{-}eGFP}$ mice compared to WT littermate controls. The total number of eGFP-specific CD4 T cells in MGL2$^{DTR\text{-}eGFP}$ was consistent with numbers proposed by Malhotra *et al.* that categorize clonal deletion as the major tolerance mechanism (42).

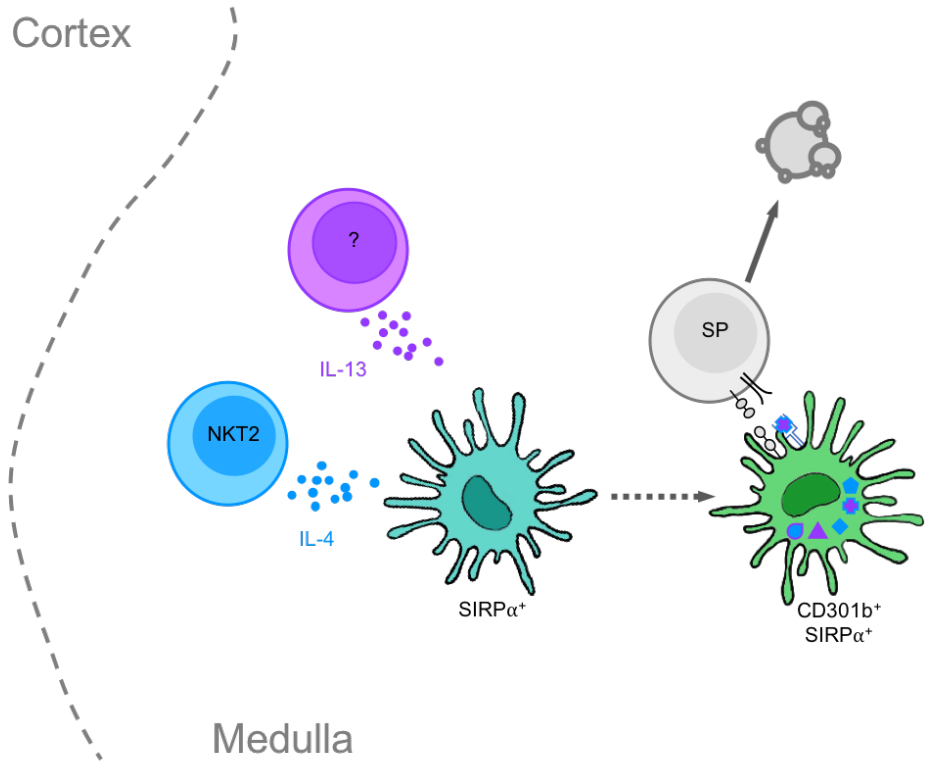

Figure 4.2. CD301b+ SIRPα+ cDC2 mediate clonal deletion.

CD301b$^+$ SIRPα^+ cDC2 require IL-4, produced by thymic resident NKT2 cells localized in the medulla, and IL-13, the source of which is currently unknown. Blue and purple shapes represent unique peptides induced by IL-4 and IL-13, including CD301b. These IL-4 and IL-13 dependent cDC2 mediate clonal deletion of medullary SP thymocytes in a non-redundant manner.

The studies outlined here implicate AIRE is the major enforcer of central tolerance, both by mTreg cell differentiation and clonal deletion, at the population level. A subset of type 2 cytokine-dependent SIRPα^+ cDC2 were also critical for mediating clonal deletion. While we did not identify non-redundant roles for B cells, pDC, XCR1$^+$ cDC1, or MNPs for mediating clonal deletion or mTreg cell selection, this does not rule out the possibility that these APC subsets facilitate central tolerance at the TCR repertoire level. To date, only XCR1$^+$ cDC1 have been studied for their role in shaping the TCR repertoire, and the findings by two different groups remain controversial (45, 61, 71, 80). Because XCR1$^+$ cDC1 are well known to cross-present TRA acquired from mTEC (and therefore likely have overlapping peptidomes) (59–62), data that did not identify differences in Treg or CD8$^+$ thymocyte repertoires suggested functional overlap between this cDC subset and mTEC in mediating central tolerance (71, 80). However, another group's findings are more nuanced. Perry *et al.* demonstrated that XCR1$^+$ cDC1 affect both clonal deletion and Treg cell selection within the TCR repertoire (45, 61). This group showed that CD36, a scavenger receptor, mediates the transfer of AIRE-dependent cell-surface (but not cytoplasmic) antigens to XCR1$^+$ cDC1 (61). Through TCRα sequencing, this group showed that XCR1$^+$ cDC1 facilitate Treg cell selection and clonal deletion and that they also contribute to a proportion of AIRE-dependent thymocyte selection. These findings support previous work that suggests a unique role for bone marrow-derived APC in mediating tolerance via indirect presentation (158). The different conclusions drawn by these two groups lies primarily within the analysis methods employed. In addition to the lack of consensus on data set analysis, other limitations exist; both groups restricted TCR diversity by using a transgenic fixed TCRβ chain to facilitate data analysis (45, 80). It will be interesting to see how other APC

subsets impact development of the TCR repertoire once these complications are addressed.

Although we did not examine the impact of distinct APCs on thymocyte selection at different ages, we did show that the proportion of APC subsets is different during neonatal development compared to adults. It is reasonable to hypothesize that the roles that these APC play in mediating clonal deletion or Treg cell selection would be unique in neonates compared to adults. In support of this hypothesis, it was recently shown that distinct Treg cell populations develop during the perinatal window and that these develop due to age-dependent differences in antigen processing in mTEC (49).

Given that type 2 cytokines were essential for CD301b-expessing SIRPα^+ cDC2, it is interesting to contemplate what other effects the type 2 cytokine-enriched environment of the thymus has on other thymic APC subsets. It also raises the question of whether the individual APC is more important for mediating tolerance or if a unique peptidome (in this case induced by IL-4 and IL-13) has an overall greater impact on the T cell repertoire selected. One might expect that IL-4Rα-deficient mice would have a more substantially altered TCR repertoire compared to mice lacking a specific APC subset. In addition to IL-4-producing NKT2, NKT1 and NKT17 effector populations also produce cytokines (IFN-γ and IL-17 respectively) in the steady state (143). Additionally, IFN-β is produced by mTEC in the steady state and impacts T cell maturation in the thymus (109, 159, 160). Understanding how intrathymic cytokine production impacts APC antigen processing and presentation, the consequent peptidomes, and the resulting TCR repertoires will be the work of future studies.

References

1. Klein, L., B. Kyewski, P. M. Allen, and K. A. Hogquist. 2014. Positive and negative selection of the T cell repertoire: what thymocytes see (and don't see). *Nat Rev Immunol* 14: 377–391.

2. Coux, O., K. Tanaka, and A. L. Goldberg. 1996. Structure and functions of the 20S and 26S proteasomes. *Annu. Rev. Biochem.* 65: 801–847.

3. Murata, S., K. Sasaki, T. Kishimoto, S. Niwa, H. Hayashi, Y. Takahama, and K. Tanaka. 2007. Regulation of CD8+ T cell development by thymus-specific proteasomes. *Science (80-.).* 316: 1349–1353.

4. Florea, B. I., M. Verdoes, N. Li, W. A. van der Linden, P. P. Geurink, H. van den Elst, T. Hofmann, A. de Ru, P. A. van Veelen, and K. Tanaka. 2010. Activity-based profiling reveals reactivity of the murine thymoproteasome-specific subunit β5t. *Chem. Biol.* 17: 795–801.

5. Nitta, T., S. Murata, K. Sasaki, H. Fujii, A. M. Ripen, N. Ishimaru, S. Koyasu, K. Tanaka, and Y. Takahama. 2010. Thymoproteasome shapes immunocompetent repertoire of CD8+ T cells. *Immunity* 32: 29–40.

6. Takada, K., F. Van Laethem, Y. Xing, K. Akane, H. Suzuki, S. Murata, K. Tanaka, S. C. Jameson, A. Singer, and Y. Takahama. 2015. TCR affinity for thymoproteasome-dependent positively selecting peptides conditions antigen responsiveness in CD8+ T cells. *Nat. Immunol.* .

7. Sasaki, K., Y. Ohte, S. Murata, K. Takada, H. Kondo, Y. Takahama, H. Sorimachi, and K. Tanaka. 2015. Thymoproteasomes produce unique peptide motifs for positive selection of $CD8^+$ T cells. *Nat. Commun.* 6.

8. Kincaid, E. Z., S. Murata, K. Tanaka, and K. L. Rock. 2016. Specialized proteasome subunits have an essential role in the thymic selection of CD8+ T cells. *Nat. Immunol.* 17: 938–945.

9. Xing, Y., S. C. Jameson, and K. A. Hogquist. 2013. Thymoproteasome subunit-β5T generates peptide-MHC complexes specialized for positive selection. *Proc. Natl. Acad. Sci.* 110: 6979–6984.

10. Vigneron, N., V. Stroobant, J. Chapiro, A. Ooms, G. Degiovanni, S. Morel, P. van der Bruggen, T. Boon, and B. J. Van den Eynde. 2004. An antigenic peptide produced by peptide splicing in the proteasome. *Science (80-.).* 304: 587–590.

11. Dalet, A., P. F. Robbins, V. Stroobant, N. Vigneron, Y. F. Li, M. El-Gamil, K. Hanada, J. C. Yang, S. A. Rosenberg, and B. J. Van den Eynde. 2011. An antigenic peptide produced by reverse splicing and double asparagine deamidation. *Proc. Natl. Acad. Sci.* 108: E323–E331.

12. Liepe, J., F. Marino, J. Sidney, A. Jeko, D. E. Bunting, A. Sette, P. M. Kloetzel, M. P. H. Stumpf, A. J. R. Heck, and M. Mishto. 2016. A large fraction of HLA class I ligands are proteasome-generated spliced peptides. *Science (80-.).* 354: 354–358.

13. Gommeaux, J., C. Gregoire, P. Nguessan, M. Richelme, M. Malissen, S. Guerder, B. Malissen, and A. Carrier. 2009. Thymus-specific serine protease regulates positive selection of a subset of CD4+ thymocytes. *Eur J Immunol* 39: 956–964.

14. Nakagawa, T., W. Roth, P. Wong, A. Nelson, A. Farr, J. Deussing, J. A. Villadangos, H. Ploegh, C. Peters, and A. Y. Rudensky. 1998. Cathepsin L: critical role in Ii degradation and CD4 T cell selection in the thymus. *Science (80-.).* 280: 450–453.

15. Honey, K., T. Nakagawa, C. Peters, and A. Rudensky. 2002. Cathepsin L regulates CD4+ T cell selection independently of its effect on invariant chain: a role in the generation of positively selecting peptide ligands. *J Exp Med* 195: 1349–1358.

16. Breloer, M., and B. Fleischer. 2008. CD83 regulates lymphocyte maturation, activation and homeostasis. *Trends Immunol.* 29: 186–194.

17. Tze, L. E., K. Horikawa, H. Domaschenz, D. R. Howard, C. M. Roots, R. J. Rigby, D. A. Way, M. Ohmura-Hoshino, S. Ishido, and C. E. Andoniou. 2011. CD83 increases MHC II and CD86 on dendritic cells by opposing IL-10–driven MARCH1-mediated ubiquitination and degradation. *J. Exp. Med.* 208: 149–165.

18. Žuklys, S., A. Handel, S. Zhanybekova, F. Govani, M. Keller, S. Maio, C. E. Mayer, H. Y. Teh, K. Hafen, and G. Gallone. 2016. Foxn1 regulates key target genes essential for T cell development in postnatal thymic epithelial cells. *Nat. Immunol.* 17: 1206–1215.

19. von Rohrscheidt, J., E. Petrozziello, J. Nedjic, C. Federle, L. Krzyzak, H. L. Ploegh, S. Ishido, A. Steinkasserer, and L. Klein. 2016. Thymic CD4 T cell selection requires attenuation of March8-mediated MHCII turnover in cortical epithelial cells through CD83. *J. Exp. Med.* 213: 1685–1694.

20. Kuwano, Y., C. M. Prazma, N. Yazawa, R. Watanabe, N. Ishiura, A. Kumanogoh, H. Okochi, K. Tamaki, M. Fujimoto, and T. F. Tedder. 2007. CD83 influences cell-surface MHC class II expression on B cells and other antigen-presenting cells. *Int. Immunol.* 19: 977–992.

21. Fujimoto, Y., L. Tu, A. S. Miller, C. Bock, M. Fujimoto, C. Doyle, D. A. Steeber, and T. F. Tedder. 2002. CD83 expression influences CD4+ T cell development in the thymus. *Cell* 108: 755–767.

22. Liu, H., R. Jain, J. Guan, V. Vuong, S. Ishido, N. L. La Gruta, D. H. Gray, J. A. Villadangos, and J. D. Mintern. 2016. Ubiquitin ligase MARCH 8 cooperates with CD83 to control surface MHC II expression in thymic epithelium and CD4 T cell selection. *J. Exp. Med.* 213: 1695–1703.

23. Kimura, M. Y., J. Thomas, X. Tai, T. I. Guinter, M. Shinzawa, R. Etzensperger, Z. Li, P. Love, T. Nakayama, and A. Singer. 2016. Timing and duration of MHC I positive selection signals are adjusted in the thymus to prevent lineage errors. *Nat Immunol* .

24. Singer, A., S. Adoro, and J.-H. Park. 2008. Lineage fate and intense debate: myths, models and mechanisms of CD4-versus CD8-lineage choice. *Nat. Rev. Immunol.* 8: 788–801.

25. Uddin, M. M., I. Ohigashi, R. Motosugi, T. Nakayama, M. Sakata, J. Hamazaki, Y. Nishito, I. Rode, K. Tanaka, T. Takemoto, S. Murata, and Y. Takahama. 2017. Foxn1-beta5t transcriptional axis controls CD8+ T-cell production in the thymus. *Nat Commun* 8: 14419.

26. Cowan, J. E., N. I. McCarthy, S. M. Parnell, A. J. White, A. Bacon, A. Serge, M. Irla, P. J. L. Lane, E. J. Jenkinson, and W. E. Jenkinson. 2014. Differential requirement for CCR4 and CCR7 during the development of innate and adaptive αβT cells in the adult thymus. *J. Immunol.* 193: 1204–1212.

27. Hu, Z., J. N. Lancaster, C. Sasiponganan, and L. I. R. Ehrlich. 2015. CCR4 promotes medullary entry and thymocyte–dendritic cell interactions required for central tolerance. *J. Exp. Med.* 212: 1947–1965.

28. Kurobe, H., C. Liu, T. Ueno, F. Saito, I. Ohigashi, N. Seach, R. Arakaki, Y. Hayashi, T. Kitagawa, and M. Lipp. 2006. CCR7-dependent cortex-to-medulla migration of positively selected thymocytes is essential for establishing central tolerance. *Immunity* 24: 165–177.

29. Kwan, J., and N. Killeen. 2004. CCR7 directs the migration of thymocytes into the thymic medulla. *J Immunol* 172: 3999–4007.

30. Nitta, T., S. Nitta, Y. Lei, M. Lipp, and Y. Takahama. 2009. CCR7-mediated migration of developing thymocytes to the medulla is essential for negative selection to tissue-restricted antigens. *Proc. Natl. Acad. Sci.* 106: 17129–17133.

31. Ueno, T., F. Saito, D. H. D. Gray, S. Kuse, K. Hieshima, H. Nakano, T. Kakiuchi, M. Lipp, R. L. Boyd, and Y. Takahama. 2004. CCR7 signals are essential for cortex–medulla migration of developing thymocytes. *J. Exp. Med.* 200: 493–505.

32. Anderson, M. S., E. S. Venanzi, L. Klein, Z. Chen, S. P. Berzins, S. J. Turley, H. von Boehmer, R. Bronson, A. Dierich, and C. Benoist. 2002. Projection of an immunological self shadow within the thymus by the aire protein. *Science (80-.).* 298: 1395–1401.

33. Gray, D., J. Abramson, C. Benoist, and D. Mathis. 2007. Proliferative arrest and rapid turnover of thymic epithelial cells expressing Aire. *J. Exp. Med.* 204: 2521–2528.

34. Gäbler, J., J. Arnold, and B. Kyewski. 2007. Promiscuous gene expression and the developmental dynamics of medullary thymic epithelial cells. *Eur. J. Immunol.* 37: 3363–3372.

35. Metzger, T. C., I. S. Khan, J. M. Gardner, M. L. Mouchess, K. P. Johannes, A. K. Krawisz, K. M. Skrzypczynska, and M. S. Anderson. 2013. Lineage tracing and cell ablation identify a post-Aire-expressing thymic epithelial cell population. *Cell Rep.* 5: 166–179.

36. Nishikawa, Y., H. Nishijima, M. Matsumoto, J. Morimoto, F. Hirota, S. Takahashi, H. Luche, H. J. Fehling, Y. Mouri, and M. Matsumoto. 2014. Temporal lineage tracing of Aire-expressing cells reveals a requirement for Aire in their maturation program. *J. Immunol.* 192: 2585–2592.

37. Takaba, H., Y. Morishita, Y. Tomofuji, L. Danks, T. Nitta, N. Komatsu, T. Kodama, and H. Takayanagi. 2015. Fezf2 Orchestrates a Thymic Program of Self-Antigen Expression for Immune Tolerance. *Cell* 163: 975–987.

38. Lkhagvasuren, E., M. Sakata, I. Ohigashi, and Y. Takahama. 2013. Lymphotoxin β receptor regulates the development of CCL21-expressing subset of postnatal medullary thymic epithelial cells. *J. Immunol.* 190: 5110–5117.

39. Hu, Z., J. N. Lancaster, and L. I. R. Ehrlich. 2015. The contribution of chemokines and migration to the induction of central tolerance in the thymus. *Front. Immunol.* 6.

40. Anderson, M. S., E. S. Venanzi, Z. Chen, S. P. Berzins, C. Benoist, and D. Mathis. 2005. The cellular mechanism of Aire control of T cell tolerance. *Immunity* 23: 227–239.

41. Anderson, M. S., and M. A. Su. 2016. AIRE expands: new roles in immune tolerance and beyond. *Nat Rev Immunol* 16: 247–258.

42. Malhotra, D., J. L. Linehan, T. Dileepan, Y. J. Lee, W. E. Purtha, J. V Lu, R. W. Nelson, B. T. Fife, H. T. Orr, and M. S. Anderson. 2016. Tolerance is established in polyclonal CD4+ T cells by distinct mechanisms, according to self-peptide expression patterns. *Nat. Immunol.* 17: 187–195.

43. Irla, M., S. Hugues, J. Gill, T. Nitta, Y. Hikosaka, I. R. Williams, F. X. Hubert, H. S. Scott, Y. Takahama, G. A. Hollander, and W. Reith. 2008. Autoantigen-specific interactions with CD4+ thymocytes control mature medullary thymic epithelial cell cellularity. *Immunity* 29: 451–463.

44. Hinterberger, M., M. Aichinger, O. P. da Costa, D. Voehringer, R. Hoffmann, and L. Klein. 2010. Autonomous role of medullary thymic epithelial cells in central CD4+ T cell tolerance. *Nat. Immunol.* 11: 512–519.

45. Perry, J. S. A., C.-W. J. Lio, A. L. Kau, K. Nutsch, Z. Yang, J. I. Gordon, K. M. Murphy, and C.-S. Hsieh. 2014. Distinct contributions of Aire and antigen-presenting-cell subsets to the generation of self-tolerance in the thymus. *Immunity* 41: 414–426.

46. Aschenbrenner, K., L. M. D'Cruz, E. H. Vollmann, M. Hinterberger, J. Emmerich, L. K. Swee, A. Rolink, and L. Klein. 2007. Selection of Foxp3+ regulatory T cells specific for

self antigen expressed and presented by Aire+ medullary thymic epithelial cells. *Nat. Immunol.* 8: 351–358.

47. Malchow, S., D. S. Leventhal, S. Nishi, B. I. Fischer, L. Shen, G. P. Paner, A. S. Amit, C. Kang, J. E. Geddes, J. P. Allison, N. D. Socci, and P. A. Savage. 2013. Aire-dependent thymic development of tumor-associated regulatory T cells. *Science (80-.).* 339: 1219–1224.

48. Lin, J., L. Yang, H. M. Silva, A. Trzeciak, Y. Choi, S. R. Schwab, M. L. Dustin, and J. J. Lafaille. 2016. Increased generation of Foxp3+ regulatory T cells by manipulating antigen presentation in the thymus. *Nat. Commun.* 7.

49. Yang, S., N. Fujikado, D. Kolodin, C. Benoist, and D. Mathis. 2015. Regulatory T cells generated early in life play a distinct role in maintaining self-tolerance. *Science (80-.).* 348: 589–594.

50. Hsieh, C.-S., Y. Liang, A. J. Tyznik, S. G. Self, D. Liggitt, and A. Y. Rudensky. 2004. Recognition of the peripheral self by naturally arising CD25+ CD4+ T cell receptors. *Immunity* 21: 267–277.

51. Malchow, S., D. S. Leventhal, V. Lee, S. Nishi, N. D. Socci, and P. A. Savage. 2016. Aire Enforces Immune Tolerance by Directing Autoreactive T Cells into the Regulatory T Cell Lineage. *Immunity* 44: 1102–1113.

52. Guerau-de-Arellano, M., M. Martinic, C. Benoist, and D. Mathis. 2009. Neonatal tolerance revisited: a perinatal window for Aire control of autoimmunity. *J. Exp. Med.* 206: 1245–1252.

53. Moon, J. J., P. Dash, T. H. Oguin, J. L. McClaren, H. H. Chu, P. G. Thomas, and M. K. Jenkins. 2011. Quantitative impact of thymic selection on Foxp3+ and Foxp3− subsets of self-peptide/MHC class II-specific CD4+ T cells. *Proc. Natl. Acad. Sci.* 108: 14602–14607.

54. Legoux, F. P., J.-B. Lim, A. W. Cauley, S. Dikiy, J. Ertelt, T. J. Mariani, T. Sparwasser, S. S. Way, and J. J. Moon. 2015. CD4+ T Cell Tolerance to Tissue-Restricted Self Antigens Is Mediated by Antigen-Specific Regulatory T Cells Rather Than Deletion. *Immunity* 43: 896–908.

55. Taniguchi, R. T., J. J. DeVoss, J. J. Moon, J. Sidney, A. Sette, M. K. Jenkins, and M. S. Anderson. 2012. Detection of an autoreactive T-cell population within the polyclonal repertoire that undergoes distinct autoimmune regulator (Aire)-mediated selection. *Proc Natl Acad Sci U S A* 109: 7847–7852.

56. Yu, W., N. Jiang, P. J. Ebert, B. A. Kidd, S. Muller, P. J. Lund, J. Juang, K. Adachi, T. Tse, M. E. Birnbaum, E. W. Newell, D. M. Wilson, G. M. Grotenbreg, S. Valitutti, S. R. Quake, and M. M. Davis. 2015. Clonal Deletion Prunes but Does Not Eliminate Self-Specific alphabeta CD8(+) T Lymphocytes. *Immunity* 42: 929–941.

57. Li, J., J. Park, D. Foss, and I. Goldschneider. 2009. Thymus-homing peripheral dendritic cells constitute two of the three major subsets of dendritic cells in the steady-state thymus. *J. Exp. Med.* 206: 607–622.

58. Guilliams, M., C.-A. Dutertre, C. L. Scott, N. McGovern, D. Sichien, S. Chakarov, S. Van Gassen, J. Chen, M. Poidinger, and S. De Prijck. 2016. Unsupervised high-dimensional analysis aligns dendritic cells across tissues and species. *Immunity* 45: 669–684.

59. Lei, Y., A. M. Ripen, N. Ishimaru, I. Ohigashi, T. Nagasawa, L. T. Jeker, M. R. Bösl, G. A. Holländer, Y. Hayashi, and R. de Waal Malefyt. 2011. Aire-dependent production of XCL1 mediates medullary accumulation of thymic dendritic cells and contributes to regulatory T cell development. *J. Exp. Med.* 208: 383–394.

60. Gallegos, A. M., and M. J. Bevan. 2004. Central tolerance to tissue-specific antigens mediated by direct and indirect antigen presentation. *J. Exp. Med.* 200: 1039–1049.

61. Perry, J. S. A., E. V Russler-Germain, Y. W. Zhou, W. Purtha, M. L. Cooper, J. Choi, M. A. Schroeder, V. Salazar, T. Egawa, B.-C. Lee, N. A. Abumrad, B. S. Kim, M. S. Anderson, J. F. DiPersio, and C.-S. Hsieh. 2018. Transfer of Cell-Surface Antigens by Scavenger Receptor CD36 Promotes Thymic Regulatory T Cell Receptor Repertoire Development and Allo-tolerance. *Immunity* 48: 923-936.e4.

62. Ardouin, L., H. Luche, R. Chelbi, S. Carpentier, A. Shawket, F. M. Sanchis, C. Santa Maria, P. Grenot, Y. Alexandre, and C. Grégoire. 2016. Broad and Largely Concordant Molecular Changes Characterize Tolerogenic and Immunogenic Dendritic Cell Maturation in Thymus and Periphery. *Immunity* 45: 305–318.

63. Bonasio, R., M. L. Scimone, P. Schaerli, N. Grabie, A. H. Lichtman, and U. H. von Andrian. 2006. Clonal deletion of thymocytes by circulating dendritic cells homing to the thymus. *Nat Immunol* 7: 1092–1100.

64. Baba, T., Y. Nakamoto, and N. Mukaida. 2009. Crucial contribution of thymic Sirpα+ conventional dendritic cells to central tolerance against blood-borne antigens in a CCR2-dependent manner. *J. Immunol.* 183: 3053–3063.

65. Hadeiba, H., T. Sato, A. Habtezion, C. Oderup, J. Pan, and E. C. Butcher. 2008. CCR9 expression defines tolerogenic plasmacytoid dendritic cells able to suppress acute graft-versus-host disease. *Nat Immunol* 9: 1253–1260.

66. Hadeiba, H., K. Lahl, A. Edalati, C. Oderup, A. Habtezion, R. Pachynski, L. Nguyen, A. Ghodsi, S. Adler, and E. C. Butcher. 2012. Plasmacytoid dendritic cells transport peripheral antigens to the thymus to promote central tolerance. *Immunity* 36: 438–450.

67. McDonald, B. D., J. J. Bunker, S. A. Erickson, M. Oh-Hora, and A. Bendelac. 2015. Crossreactive αβ T Cell Receptors Are the Predominant Targets of Thymocyte Negative Selection. *Immunity* .

68. Stritesky, G. L., Y. Xing, J. R. Erickson, L. A. Kalekar, X. Wang, D. L. Mueller, S. C. Jameson, and K. A. Hogquist. 2013. Murine thymic selection quantified using a unique method to capture deleted T cells. *Proc Natl Acad Sci U S A* 110: 4679–4684.

69. Daley, S. R., D. Y. Hu, and C. C. Goodnow. 2013. Helios marks strongly autoreactive CD4+ T cells in two major waves of thymic deletion distinguished by induction of PD-1 or NF-kappaB. *J Exp Med* 210: 269–285.

70. McCaughtry, T. M., T. A. Baldwin, M. S. Wilken, and K. A. Hogquist. 2008. Clonal deletion of thymocytes can occur in the cortex with no involvement of the medulla. *J Exp Med* 205: 2575–2584.

71. MacNabb, B. W., D. E. Kline, A. R. Albright, X. Chen, D. S. Leventhal, P. A. Savage, and J. Kline. 2019. Negligible Role for Deletion Mediated by cDC1 in CD8 $^{+}$ T Cell Tolerance. *J. Immunol.* 202: 2628–2635.

72. Ehrlich, L. I. R., D. Y. Oh, I. L. Weissman, and R. S. Lewis. 2009. Differential contribution of chemotaxis and substrate restriction to segregation of immature and mature thymocytes. *Immunity* 31: 986–998.

73. Kroger, C. J., B. Wang, and R. Tisch. 2016. Temporal increase in thymocyte negative selection parallels enhanced thymic SIRPalpha+ DC function. *Eur J Immunol* 46: 2352–2362.

74. Reizis, B., M. Colonna, G. Trinchieri, F. Barrat, and M. Gilliet. 2011. Plasmacytoid dendritic cells: one-trick ponies or workhorses of the immune system? *Nat. Rev. Immunol.* 11: 558–565.

75. Villadangos, J. A., and L. Young. 2008. Antigen-presentation properties of plasmacytoid dendritic cells. *Immunity* 29: 352–361.

76. Atibalentja, D. F., K. M. Murphy, and E. R. Unanue. 2011. Functional redundancy between thymic CD8alpha+ and Sirpalpha+ conventional dendritic cells in presentation of blood-derived lysozyme by MHC class II proteins. *J Immunol* 186: 1421–1431.

77. Wendland, M., N. Czeloth, N. Mach, B. Malissen, E. Kremmer, O. Pabst, and R. Förster. 2007. CCR9 is a homing receptor for plasmacytoid dendritic cells to the small intestine. *Proc. Natl. Acad. Sci.* 104: 6347–6352.

78. Atibalentja, D. F., C. A. Byersdorfer, and E. R. Unanue. 2009. Thymus-blood protein interactions are highly effective in negative selection and regulatory T cell induction. *J Immunol* 183: 7909–7918.

79. Proietto, A. I., S. van Dommelen, P. Zhou, A. Rizzitelli, A. D'Amico, R. J. Steptoe, S. H. Naik, M. H. Lahoud, Y. Liu, and P. Zheng. 2008. Dendritic cells in the thymus contribute to T-regulatory cell induction. *Proc. Natl. Acad. Sci.* 105: 19869–19874.

80. Leventhal, D. S., D. C. Gilmore, J. M. Berger, S. Nishi, V. Lee, S. Malchow, D. E.

Kline, J. Kline, D. J. Vander Griend, and H. Huang. 2016. Dendritic Cells Coordinate the Development and Homeostasis of Organ-Specific Regulatory T Cells. *Immunity* 44: 847–859.

81. Wirnsberger, G., F. Mair, and L. Klein. 2009. Regulatory T cell differentiation of thymocytes does not require a dedicated antigen-presenting cell but is under T cell-intrinsic developmental control. *Proc. Natl. Acad. Sci.* 106: 10278–10283.

82. Lio, C. W., and C. S. Hsieh. 2008. A two-step process for thymic regulatory T cell development. *Immunity* 28: 100–111.

83. Weist, B. M., N. Kurd, J. Boussier, S. W. Chan, and E. A. Robey. 2015. Thymic regulatory T cell niche size is dictated by limiting IL-2 from antigen-bearing dendritic cells and feedback competition. *Nat Immunol* 16: 635–641.

84. Loschko, J., G. J. Rieke, H. A. Schreiber, M. M. Meredith, K.-H. Yao, P. Guermonprez, and M. C. Nussenzweig. 2016. Inducible targeting of cDCs and their subsets in vivo. *J. Immunol. Methods* 434: 32–38.

85. Yamano, T., J. Nedjic, M. Hinterberger, M. Steinert, S. Koser, S. Pinto, N. Gerdes, E. Lutgens, N. Ishimaru, and M. Busslinger. 2015. Thymic B cells are licensed to present self antigens for central T cell tolerance induction. *Immunity* 42: 1048–1061.

86. Lu, F.-T., W. Yang, Y.-H. Wang, H.-D. Ma, W. Tang, J.-B. Yang, L. Li, A. A. Ansari, and Z.-X. Lian. 2015. Thymic B cells promote thymus-derived regulatory T cell development and proliferation. *J. Autoimmun.* 61: 62–72.

87. Perera, J., L. Meng, F. Meng, and H. Huang. 2013. Autoreactive thymic B cells are efficient antigen-presenting cells of cognate self-antigens for T cell negative selection. *Proc. Natl. Acad. Sci.* 110: 17011–17016.

88. Perera, J., Z. Zheng, S. Li, H. Gudjonson, O. Kalinina, J. I. C. Benichou, K. E. Block, Y. Louzoun, D. Yin, and A. S. Chong. 2016. Self-Antigen-Driven Thymic B Cell Class Switching Promotes T Cell Central Tolerance. *Cell Rep.* 17: 387–398.

89. Fujihara, C., J. A. Williams, M. Watanabe, H. Jeon, S. O. Sharrow, and R. J. Hodes. 2014. T cell–B cell thymic cross-talk: maintenance and function of thymic B cells requires cognate CD40–CD40 ligand interaction. *J. Immunol.* 193: 5534–5544.

90. Nuñez, S., C. Moore, B. Gao, K. Rogers, Y. Hidalgo, J. Pedro, S. Restaino, Y. Naka, G. Bhagat, and J. C. Madsen. 2016. The human thymus perivascular space is a functional niche for viral-specific plasma cells. *Sci. Immunol.* 1: eaah4447.

91. Frommer, F., and A. Waisman. 2010. B cells participate in thymic negative selection of murine auto-reactive CD4+ T cells. *PLoS One* 5: e15372–e15372.

92. Kleindienst, P., I. Chretien, T. Winkler, and T. Brocker. 2000. Functional comparison of thymic B cells and dendritic cells in vivo. *Blood* 95: 2610–2616.

93. Munthe, L. A., A. Corthay, A. Os, M. Zangani, and B. Bogen. 2005. Systemic autoimmune disease caused by autoreactive B cells that receive chronic help from Ig V region-specific T cells. *J. Immunol.* 175: 2391–2400.

94. Detanico, T., R. A. Heiser, K. Aviszus, C. Bonorino, and L. J. Wysocki. 2011. Self-tolerance checkpoints in CD4 T cells specific for a peptide derived from the B cell antigen receptor. *J. Immunol.* 187: 82–91.

95. Walters, S. N., K. E. Webster, S. Daley, and S. T. Grey. 2014. A role for intrathymic B cells in the generation of natural regulatory T cells. *J. Immunol.* 193: 170–176.
96. Hsieh, C. S., H. M. Lee, and C. W. Lio. 2012. Selection of regulatory T cells in the thymus. *Nat Rev Immunol* 12: 157–167.

97. Marzo, A. L., K. D. Klonowski, A. Le Bon, P. Borrow, D. F. Tough, and L. Lefrançois. 2005. Initial T cell frequency dictates memory CD8+ T cell lineage commitment. *Nat. Immunol.* 6: 793–9.

98. Hataye, J., J. J. Moon, A. Khoruts, C. Reilly, and M. K. Jenkins. 2006. Naive and memory CD4+ T cell survival controlled by clonal abundance. *Science* 312: 114–6.

99. Bautista, J. L., C.-W. J. Lio, S. K. Lathrop, K. Forbush, Y. Liang, J. Luo, A. Y. Rudensky, and C.-S. Hsieh. 2009. Intraclonal competition limits the fate determination of regulatory T cells in the thymus. *Nat. Immunol.* 10: 610–7.

100. Takahama, Y., E. W. Shores, and A. Singer. 1992. Negative selection of precursor thymocytes before their differentiation into CD4+CD8+ cells. *Science* 258: 653–6.

101. Lacorazza, H. D., C. Tucek-Szabo, L. V Vasović, K. Remus, and J. Nikolich-Zugich. 2001. Premature TCR alpha beta expression and signaling in early thymocytes impair thymocyte expansion and partially block their development. *J. Immunol.* 166: 3184–93.

102. Erman, B., L. Feigenbaum, J. E. Coligan, and A. Singer. 2002. Early TCRalpha expression generates TCRalphagamma complexes that signal the DN-to-DP transition and impair development. *Nat. Immunol.* 3: 564–9.

103. Legoux, F. P., J.-B. Lim, A. W. Cauley, S. Dikiy, J. Ertelt, T. J. Mariani, T. Sparwasser, S. S. Way, and J. J. Moon. 2015. CD4+ T cell tolerance to tissue-restricted self antigens is mediated by antigen-specific regulatory T cells rather than deletion. *Immunity* 43: 896–908.

104. Dutz, J. P., C. J. Ong, J. Marth, and H. S. Teh. 1995. Distinct differentiative stages of CD4+CD8+ thymocyte development defined by the lack of coreceptor binding in positive selection. *J. Immunol.* 154: 2588–99.

105. Moran, A. E., K. L. Holzapfel, Y. Xing, N. R. Cunningham, J. S. Maltzman, J. Punt, and K. A. Hogquist. 2011. T cell receptor signal strength in Treg and iNKT cell development demonstrated by a novel fluorescent reporter mouse. *J Exp Med* 208:

1279–1289.

106. Stritesky, G. L., S. C. Jameson, and K. A. Hogquist. 2012. Selection of Self-Reactive T Cells in the Thymus. *Annu. Rev. Immunol.* 30: 95–114.

107. Hogquist, K. A., Y. Xing, F.-C. Hsu, and V. S. Shapiro. 2015. T Cell Adolescence: Maturation Events Beyond Positive Selection. *J. Immunol.* 195: 1351–7.

108. Kishimoto, H., and J. Sprent. 1997. Negative selection in the thymus includes semimature T cells. *J. Exp. Med.* 185: 263–71.

109. Xing, Y., X. Wang, S. C. Jameson, and K. A. Hogquist. 2016. Late stages of T cell maturation in the thymus involve NF-[kappa] B and tonic type I interferon signaling. *Nat. Immunol.* 17: 565–573.

110. McCaughtry, T. M., M. S. Wilken, and K. A. Hogquist. 2007. Thymic emigration revisited. *J. Exp. Med.* 204: 2513–2520.

111. Tai, X., B. Erman, A. Alag, J. Mu, M. Kimura, G. Katz, T. Guinter, T. McCaughtry, R. Etzensperger, and L. Feigenbaum. 2013. Foxp3 transcription factor is proapoptotic and lethal to developing regulatory T cells unless counterbalanced by cytokine survival signals. *Immunity* 38: 1116–1128.

112. Breed, E. R., S. T. Lee, and K. A. Hogquist. 2018. Directing T cell fate: How thymic antigen presenting cells coordinate thymocyte selection. *Semin. Cell Dev. Biol.* 84: 2–10.

113. Williams, J. A., J. Zhang, H. Jeon, T. Nitta, I. Ohigashi, D. Klug, M. J. Kruhlak, B. Choudhury, S. O. Sharrow, L. Granger, A. Adams, M. A. Eckhaus, S. R. Jenkinson, E. R. Richie, R. E. Gress, Y. Takahama, and R. J. Hodes. 2014. Thymic Medullary Epithelium and Thymocyte Self-Tolerance Require Cooperation between CD28-CD80/86 and CD40-CD40L Costimulatory Pathways. *J. Immunol.* 192: 630–640.

114. Williams, J. A., J. M. Lumsden, X. Yu, L. Feigenbaum, J. Zhang, S. M. Steinberg, and R. J. Hodes. 2008. Regulation of thymic NKT cell development by the B7-CD28 costimulatory pathway. *J. Immunol.* 181: 907–17.

115. Lio, C.-W. J., L. F. Dodson, C. M. Deppong, C.-S. Hsieh, and J. M. Green. 2010. CD28 facilitates the generation of Foxp3(-) cytokine responsive regulatory T cell precursors. *J. Immunol.* 184: 6007–13.

116. Vang, K. B., J. Yang, A. J. Pagán, L.-X. Li, J. Wang, J. M. Green, A. A. Beg, and M. A. Farrar. 2010. Cutting edge: CD28 and c-Rel-dependent pathways initiate regulatory T cell development. *J. Immunol.* 184: 4074–7.

117. Strom, J. A. B., J. Tooley, S. K. Ye, X. X. Subudhi, T. B. Q. Zheng, K. J. Tang, E. K. Henriksen, and A. J. Boden. 2003. Regulatory T Cells + CD25 + Homeostasis of CD4 Cutting Edge: CD28 Controls Peripheral. *J Immunol Ref.* 171: 3348–3352.

118. Ruscher, R., R. L. Kummer, Y. J. Lee, S. C. Jameson, and K. A. Hogquist. 2017. CD8αα intraepithelial lymphocytes arise from two main thymic precursors. *Nat. Immunol.* 18: 771–779.

119. Pobezinsky, L. A., G. S. Angelov, X. Tai, S. Jeurling, F. Van Laethem, L. Feigenbaum, J.-H. Park, and A. Singer. 2012. Clonal deletion and the fate of autoreactive thymocytes that survive negative selection. *Nat. Immunol.* 13: 569–578.

120. Klein, L., E. A. Robey, and C.-S. Hsieh. 2019. Central CD4+ T cell tolerance: deletion versus regulatory T cell differentiation. *Nat. Rev. Immunol.* 19: 7–18.

121. Vacchio, M., J. Williams, and R. Hodes. 2005. A novel role for CD28 in thymic selection: elimination of CD28/B7 interactions increases positive selection. *Eur. J. Immunol.* 35: 418–427.

122. Kishimoto, H., Z. Cai, A. Brunmark, M. R. Jackson, P. A. Peterson, and J. Sprent. 1996. Differing roles for B7 and intercellular adhesion molecule-1 in negative selection of thymocytes. *J. Exp. Med.* 184: 531–537.

123. Hogquist, K. A., T. A. Baldwin, and S. C. Jameson. 2005. Central tolerance: learning self-control in the thymus. *Nat. Rev. Immunol.* 5: 772–82.

124. Brewer, J. A., O. Kanagawa, B. P. Sleckman, and L. J. Muglia. 2002. Thymocyte apoptosis induced by T cell activation is mediated by glucocorticoids in vivo. *J. Immunol.* 169: 1837–43.

125. van Meerwijk, J. P. M., S. Marguerat, R. K. Lees, R. N. Germain, B. J. Fowlkes, and H. R. MacDonald. 1997. Quantitative impact of thymic clonal deletion on the T cell repertoire. *J. Exp. Med.* 185: 377–384.

126. Tan, R., S. J. Teh, J. A. Ledbetter, P. S. Linsley, and H. S. Teh. 1992. B7 costimulates proliferation of CD4-8+ T lymphocytes but is not required for the deletion of immature CD4+8+ thymocytes. *J. Immunol.* 149: 3217–24.

127. Page, D. M., L. P. Kane, J. P. Allison, and S. M. Hedrick. 1993. Two signals are required for negative selection of CD4+CD8+ thymocytes. *J. Immunol.* 151: 1868–80.

128. Walunas, T. L., A. I. Sperling, R. Khattri, C. B. Thompson, and J. A. Bluestone. 1996. CD28 expression is not essential for positive and negative selection of thymocytes or peripheral T cell tolerance. *J. Immunol.* 156: 1006–13.

129. Dautigny, N., A. Le Campion, and B. Lucas. 1999. Timing and casting for actors of thymic negative selection. *J. Immunol.* 162: 1294–302.

130. Buhlmann, J. E., S. K. Elkin, and A. H. Sharpe. 2003. A role for the B7-1/B7-2:CD28/CTLA-4 pathway during negative selection. *J. Immunol.* 170: 5421–8.

131. Collette, Y., A. Benziane, D. Razanajaona, and D. Olive. 1998. Distinct regulation of

T-cell death by CD28 depending on both its aggregation and T-cell receptor triggering: a role for Fas-FasL. *Blood* 92: 1350–63.

132. Fontenot, J. D., J. P. Rasmussen, L. M. Williams, J. L. Dooley, A. G. Farr, and A. Y. Rudensky. 2005. Regulatory T Cell Lineage Specification by the Forkhead Transcription Factor Foxp3. *Immunity* 22: 329–341.

133. Watanabe, M., C. Fujihara, A. J. Radtke, Y. J. Chiang, S. Bhatia, R. N. Germain, and R. J. Hodes. 2017. Co-stimulatory function in primary germinal center responses: CD40 and B7 are required on distinct antigen-presenting cells. *J. Exp. Med.* 214: 2795–2810.

134. Lee, Y. J., H. Wang, G. J. Starrett, V. Phuong, S. C. Jameson, and K. A. Hogquist. 2015. Tissue-Specific Distribution of iNKT Cells Impacts Their Cytokine Response. *Immunity* 43: 566–578.

135. Derbinski, J., A. Schulte, B. Kyewski, and L. Klein. 2001. Promiscuous gene expression in medullary thymic epithelial cells mirrors the peripheral self. *Nat. Immunol.* 2: 1032–1039.

136. Steinman, R. M., D. Hawiger, and M. C. Nussenzweig. 2003. Tolerogenic dendritic cells*. *Annu. Rev. Immunol.* 21: 685–711.

137. Breed, E. R., M. Watanabe, and K. A. Hogquist. 2019. Measuring Thymic Clonal Deletion at the Population Level. *J. Immunol.* 202: 3226–3233.

138. Kumamoto, Y., M. Linehan, J. S. Weinstein, B. J. Laidlaw, J. E. Craft, and A. Iwasaki. 2013. CD301b+ Dermal Dendritic Cells Drive T Helper 2 Cell-Mediated Immunity. *Immunity* 39: 733–743.

139. Kumamoto, Y., K. Denda-Nagai, S. Aida, N. Higashi, and T. Irimura. 2009. MGL2 Dermal dendritic cells are sufficient to initiate contact hypersensitivity in vivo. *PLoS One* 4: e5619.

140. Gao, Y., S. A. Nish, R. Jiang, L. Hou, P. Licona-Limón, J. S. Weinstein, H. Zhao, and R. Medzhitov. 2013. Control of T helper 2 responses by transcription factor IRF4-dependent dendritic cells. *Immunity* 39: 722–32.

141. Murakami, R., K. Denda-Nagai, S. Hashimoto, S. Nagai, M. Hattori, and T. Irimura. 2013. A Unique Dermal Dendritic Cell Subset That Skews the Immune Response toward Th2. *PLoS One* 8: e73270.

142. Connor, L. M., S.-C. Tang, M. Camberis, G. Le Gros, and F. Ronchese. 2014. Helminth-conditioned dendritic cells prime CD4+ T cells to IL-4 production in vivo. *J. Immunol.* 193: 2709–17.

143. Lee, Y. J., K. L. Holzapfel, J. Zhu, S. C. Jameson, and K. A. Hogquist. 2013. Steady-state production of IL-4 modulates immunity in mouse strains and is determined

by lineage diversity of iNKT cells. *Nat. Immunol.* 14: 1146–1154.

144. Owen, D. L., S. A. Mahmud, L. E. Sjaastad, J. B. Williams, J. A. Spanier, D. R. Simeonov, R. Ruscher, W. Huang, I. Proekt, C. N. Miller, C. Hekim, J. C. Jeschke, P. Aggarwal, U. Broeckel, R. S. LaRue, C. M. Henzler, M.-L. Alegre, M. S. Anderson, A. August, A. Marson, Y. Zheng, C. B. Williams, and M. A. Farrar. 2019. Thymic regulatory T cells arise via two distinct developmental programs. *Nat. Immunol.* 20: 195–205.

145. Cowan, J. E., N. I. McCarthy, and G. Anderson. 2016. CCR7 Controls Thymus Recirculation, but Not Production and Emigration, of Foxp3+ T Cells. *Cell Rep.* 14: 1041–1048.

146. Schreiber, H. A., J. Loschko, R. A. Karssemeijer, A. Escolano, M. M. Meredith, D. Mucida, P. Guermonprez, and M. C. Nussenzweig. 2013. Intestinal monocytes and macrophages are required for T cell polarization in response to Citrobacter rodentium. *J. Exp. Med.* 210: 2025–39.

147. Dittel Avijit Ray, B. N., S. Basu, and C. B. Williams. 2019. Ligand Maintenance of Regulatory T Cells via GITR for B Cells in Suppressing Autoimmunity by Independent Regulatory Role − A Novel IL-10. .

148. Breed, E. R., M. Watanabe, and K. A. Hogquist. 2019. Measuring Thymic Clonal Deletion at the Population Level. *J. Immunol.* 202: 3226–3233.

149. Kuroda, N., T. Mitani, N. Takeda, N. Ishimaru, R. Arakaki, Y. Hayashi, Y. Bando, K. Izumi, T. Takahashi, T. Nomura, S. Sakaguchi, T. Ueno, Y. Takahama, D. Uchida, S. Sun, F. Kajiura, Y. Mouri, H. Han, A. Matsushima, G. Yamada, and M. Matsumoto. 2005. Development of Autoimmunity against Transcriptionally Unrepressed Target Antigen in the Thymus of Aire-Deficient Mice. *J. Immunol.* 174: 1862–1870.

150. Surh, C. D., and J. Sprent. 1994. T-cell apoptosis detected in situ during positive and negative selection in the thymus. *Nature* 372: 100–103.

151. Dzhagalov, I. L., K. G. Chen, P. Herzmark, and E. A. Robey. 2013. Elimination of self-reactive T cells in the thymus: a timeline for negative selection. *PLoS Biol.* 11: e1001566.

152. Gause, W. C., T. A. Wynn, and J. E. Allen. 2013. Type 2 immunity and wound healing: evolutionary refinement of adaptive immunity by helminths. *Nat. Rev. Immunol.* 13: 607–614.

153. Skon, C. N., J.-Y. Lee, K. G. Anderson, D. Masopust, K. A. Hogquist, and S. C. Jameson. 2013. Transcriptional downregulation of S1pr1 is required for the establishment of resident memory CD8+ T cells. *Nat. Immunol.* 14: 1285–1293.

154. Moon, J. J., H. H. Chu, M. Pepper, S. J. McSorley, S. C. Jameson, R. M. Kedl, and M. K. Jenkins. 2007. Naive CD4+ T Cell Frequency Varies for Different Epitopes and Predicts Repertoire Diversity and Response Magnitude. *Immunity* 27: 203–213.

155. Mathis, D., and C. Benoist. 2009. Aire. *Annu. Rev. Immunol.* 27: 287–312.

156. Peterson, P., T. Org, and A. Rebane. 2008. Transcriptional regulation by AIRE: molecular mechanisms of central tolerance. *Nat. Rev. Immunol.* 8: 948–57.

157. Jones, L. A., D. J. Izon, J. D. Nieland, P. S. Linsley, and A. M. Kruisbeek. 1993. CD28-B7 interactions are not required for intrathymic clonal deletion. *Int. Immunol.* 5: 503–12.

158. Yap, J. Y., R. C. Wirasinha, A. Chan, D. R. Howard, C. C. Goodnow, and S. R. Daley. 2018. Indirect presentation in the thymus limits naive and regulatory T-cell differentiation by promoting deletion of self-reactive thymocytes. *Immunology* 154: 522–532.

159. Lienenklaus, S., M. Cornitescu, N. Zietara, M. Łyszkiewicz, N. Gekara, J. Jabłónska, F. Edenhofer, K. Rajewsky, D. Bruder, M. Hafner, P. Staeheli, and S. Weiss. 2009. Novel reporter mouse reveals constitutive and inflammatory expression of IFN-beta in vivo. *J. Immunol.* 183: 3229–36.

160. Otero, D. C., D. P. Baker, and M. David. 2013. IRF7-dependent IFN-β production in response to RANKL promotes medullary thymic epithelial cell development. *J. Immunol.* 190: 3289–98.